The Salcombe metal cargoes: New light on the provenance and circulation of tin and copper in Later Bronze Age Europe provided by trace elements and isotopes

Article *in* Journal of Archaeological Science · February 2022

DOI: 10.1016/j.jas.2022.105543

CITATIONS
13

READS
736

6 authors, including:

Daniel Berger
Curt Engelhorn Zentrum Archäometrie
71 PUBLICATIONS **380** CITATIONS
SEE PROFILE

Quanyu Wang
Shandong University
19 PUBLICATIONS **99** CITATIONS
SEE PROFILE

Gerhard Brügmann
Curt Engelhorn Zentrum Archäometrie
139 PUBLICATIONS **3,679** CITATIONS
SEE PROFILE

Ben Roberts
Durham University
50 PUBLICATIONS **1,110** CITATIONS
SEE PROFILE

The Salcombe metal cargoes: New light on the provenance and circulation of tin and copper in Later Bronze Age Europe provided by trace elements and isotopes

Daniel Berger[a]*, Quanyu Wang[b]*, Gerhard Brügmann[a], Nicole Lockhoff[a], Benjamin W. Roberts[c], and Ernst Pernicka[a, d]

[a] Curt-Engelhorn-Zentrum Archäometrie gGmbH, D6, 3, D-68159 Mannheim, Germany

[b] Joint International Research Laboratory of Environmental and Social Archaeology, Shandong University, Qingdao, Shandong, 266237, China

[c] Department of Archaeology, Durham University, South Road, Durham, DH1 3LE, UK

[d] Institut für Geowissenschaften, Ruprecht-Karls-Universität Heidelberg, Im Neuenheimer Feld 234–236, D-69120 Heidelberg, Germany

* corresponding authors

daniel.berger@ceza.de; q.wang@sdu.edu.cn

Highlights

- Sn, Cu and bronze artefacts from alleged shipwrecks near Salcombe are investigated
- Relationships between artefacts revealed based on trace elements and isotopes
- Correlations of trace elements and isotopes indicate bronze recycling
- Cu ingots probably used for the production of bronzes from the site
- Sn most likely mined in Britain and resembling Late Bronze Age Sn from Israel

Abstract

Since the mid-1970s a Bronze Age assemblage of metal objects has been recovered from the seabed off the south Devon coast at Salcombe, southwest England. The assemblage spans two suspected shipwreck events and comprises nearly 400 pieces of raw materials and finished artefacts, primarily in copper, tin, bronze and gold. Among these are 280 copper and 40 tin ingots, by far the largest discovery of Bronze Age ingots in either metal from northwestern Europe. Research in recent years revealed the microstructural and chemical nature of the ingots and enabled some preliminary conclusions on the metals trade in Europe in the Later Bronze Age. The present study aims to extend this knowledge by determining the tin, copper and lead isotopic compositions of the ingots using HR-MC-ICP-MS. In addition, bronze artefacts (swords, rapiers, palstaves and weights) from the Salcombe site are included in the multi-proxy approach in order to investigate their history and the possible relationships between finished products and ingots. In combination with the available chemical data of previous studies, the current results of the tin metal show that most likely two tin sources in southwest Britain supplied the ore for their production. This also sheds light on Late Bronze Age tin ingots from Israel that share the same geochemical characteristics with one group of the finds from Salcombe. Although the tin in the bronzes is similar to the tin in the ingots, it is not certain that the latter were used to make the bronzes. Correlations of copper and tin isotopes and trace elements of the bronzes point to a mixing or even recycling of copper-tin alloys rather than the alloying of individual components of copper and tin. However, the copper ingots from the assemblage could have been an additional component in the mixing process given their impurity pattern and isotopic composition. At the same time, a close relationship between swords of the Rosnoën type and palstaves from the cargo is disclosed. Lead isotope ratios for their part suggest Sardinian and/or south Spanish copper ores as a

source for both the copper ingots and the copper of the bronzes. This would mean long-distance metal trade in the Later Bronze Age in both cases and would provide new insights into the interpretation of the prehistoric networks in Europe.

Keywords

Tin and copper ingots

Bronze

Bronze Age

Tin and copper isotopes

Metals trade

Provenance analysis

Recycling

1. Introduction

The Salcombe site is located in southwest Britain and comprises two underwater sites some 400 m apart within an open bay at the mouth of an estuary – Moor Sand and Salcombe B (Fig. 1). Archaeological work at Moor Sand was performed between 1977 and 1982 (Muckelroy, 1980; 1981), whilst work at Salcombe B started in 2004 and remains ongoing by the South West Maritime Archaeology Group (www.swmag.org). Since the beginning of these investigations some 400 bronze and other metal artefacts have been salvaged from the seabed. Extensive environmental, archaeometallurgical and archaeological analyses of the

earlier discoveries and surveys up until 2004 were published by Needham et al. (2013). Based on detailed typo-chronological analyses of diagnostic bronze and gold objects, which was supported by radiocarbon dates from terrestrial sites containing comparable metalwork, the Salcombe assemblage was dated to the Middle Bronze Age (MBA) Penard metalwork phase (ca. 1300–1150 BCE). Compositional analysis of the early finds revealed that the bronzes were consistent with this dating (Northover, 2013). The exception is one type Nantes bronze sword of the Late Bronze Age (LBA) Ewart Park metalwork phase (ca. 1000–800 BCE) (Needham and Giardino, 2008; Needham et al., 2013; Brandherm and Moskal-del Hoyo, 2014). Sea level history and coastal geomorphology, furthermore, demonstrated that coastal retreat cannot explain the distribution of the metalwork at the Moor Sand site, and it was therefore argued that the objects were transported to their location by a ship before having been dispersed on the seabed (Needham et al., 2013).

This assertion applies even more to the finds from between 2005 and 2013 from Salcombe B as it lies further outwards to the sea. They include 280 copper or copper alloy ingots and 40 bun-shaped tin ingots, as well as some bronze objects and gold ornaments. All finds were acquired by the British Museum, are registered and catalogued at Collections Online (https://www.britishmuseum.org/collection/term/x37148). Due to their extreme rarity and morphological simplicity, neither the tin nor the copper ingots are typologically diagnostic (Bachmann et al., 2004). However, following research on Late Bronze Age copper ingots in northwest France (Le Carlier et al., 2014), consistent differences in form can be identified according to whether they were cast in a shallow ceramic mould as with the copper ingots (Wang et al., 2018) or cast into the sand or earth (Wang et al., 2016). The Salcombe ingots are nonetheless dated by association with other artefacts either to ca. 1300–1150 BCE or 1000–800 BCE, as mentioned above, and have provided the most extensive, direct evidence

for Later Bronze Age tin and copper production and trade in northwestern Europe (Wang et al., 2016; 2018).

The ingots thus offer a very rare opportunity to analyse directly the Bronze Age (BA) 'metal trade'. Both the copper and tin ingots vary in size and weight as well as in shape although they are generally bun-shaped (plano-convex). The surface of the tin ingots is bumpy and covered with corrosion products, while the copper ingots appear smooth with a thin layer of surface corrosion (Fig. 2). Compositional analysis using ICP-AES and ICP-MS was carried out in two recent studies: The first included all the 40 Salcombe tin ingots and two morphologically similar tin ingots for comparison from the Erme Estuary site (also known as Bigbury Bay) that are thought to be Bronze or Iron Age (Fox, 1995; 1996; Wang et al., 2016). The second focussed on 25 of the Salcombe copper ingots, and also included two bronze artefacts from the site (Wang et al., 2018). Microstructural studies were performed on selected samples from both the ingots and artefacts following the compositional analysis to cover those ingots with different sizes, shapes and variable impurity levels.

In this paper we present isotopic data (tin, lead, copper) and trace element compositions of the Salcombe tin and copper ingots as well as a selection of bronze artefacts that were also found at the site. It was hoped that this multi-proxy approach would help determine the origin of the tin and the copper. The results will be discussed together with the data of the tin ingots from the Erme Estuary site and those found off the coast of Israel. The latter were recently published by Berger and co-workers (2019) and revealed a potential southwest British origin of the tin. Furthermore, the analyses should provide insights into the question of whether the bronze objects were directly produced from the ingots or derived from other metal sources.

This would help understand the bronze production practices and the raw material trade during the MBA and LBA in Europe.

2. Materials

2.1. Archaeological objects

The Salcombe assemblage to date encompasses nearly 400 artefacts. Beyond the 40 tin ingots and a small tin lump and the 280 copper ingots highlighted above (Fig. 2), there are 41 bronze weapons, tools and weights and 12 gold ornaments and fragments. The gold ornaments comprise two finely worked twisted wire bracelets dating to the MBA Penard metalwork phase (ca. 1300–1150 BCE) and are paralleled only by bracelets from hoards at Burton, north Wales and Saint-Marc-le-Blanc, northwest France. In contrast to these delicately crafted objects, the other gold ornaments include four plain penannular bar bracelets and three twisted gold torc fragments with the latter also typologically dating to the MBA Penard metalwork phase. They are paralleled throughout northwest Europe (Eogan 1967; Northover 1989; Eogan 1994), and were recently identified as being weight regulated (Rahmsdorf et al., 2019). The identification of a rare rectangular bronze block weight with a wavy moulding in the Salcombe assemblage and a another one without a groove (Fig. 3c) lends further support to the proposal of standardised weights being involved in the Salcombe cargo(es). The Salcombe piece with the wavy moulding is paralleled in southern Britain, France and Germany where the type dates to the late 14th–13th centuries BCE. This makes it contemporary to the gold twisted torc fragments (Needham 2017; Ialongo 2018; Rahmsdorf 2019).

The bronze tools comprise mainly palstave axes which also date to the Penard metalwork phase in types that are found in southern Britain and northern France (Fig. 3b). The weapons comprise swords and rapiers, with the fragmentary and worn condition of many of the blades making it impossible to determine the original form, let alone the type (Fig. 3a). Some swords were, however, identified earlier as possibly belonging to the Rosnoën type, so we will subsequently use this term to address the objects (Table 1). Together with two swords of the rod-tanged type (Fig. 3a, 1981,1103.1) and the Ballintober type (Fig. 3a, 2013,8032.34) they date to the Penard metalwork phase. In contrast, one sword of the Carp's Tongue type (Fig. 3a, 1983,1004.1) and another one of the Nantes or Meldreth type (Fig. 3a, 2010,8032.10) belong to the LBA Ewart Park metalwork phase (ca. 1000–800 BCE). The sword chronologies thus highlight that two distinct depositional events occurred during the MBA and the LBA, probably suggesting two wrecking events of ships. The sword type distributions in both periods span southern Britain, northwest France and south down the Atlantic coast and illustrate the long-distance connections of the assemblage. In addition, the presence of a bronze object identified as a *strumento con immanicatura a cannone* (not sampled) that had previously only ever been found in Sicily and dating to the 13th century BCE provides the strongest evidence for these long-distance connections (Needham and Giardino 2008).

2.2. Sampling

In this study a total of 34 samples from the Salcombe finds were analysed. This set comprises ten tin ingots, 19 bronze weapons – including ten complete and fragmentary swords (two LBA and eight MBA), eight palstaves and one rapier, two rectangular bronze blocks or

weights as well as three copper ingots (Figs. 2–3). The finds originate from both Moor Sand and Salcombe B (Table 1). It was attempted to examine any metallurgical association between the tin ingots, copper ingots and the bronze artefacts, and to explore differences or similarities between different types of objects, e.g. swords and palstaves as well as between the same type of objects (e.g. swords) of different periods, e.g. MBA and LBA. In addition to the listed objects, the irregular tin lump was also analysed (Table 1). It was found earlier at the Salcombe B site and is probably a remnant of an additional tin ingot (cf. Needham et al., 2013, Fig 3.21, S28). Two of the total 42 tin ingots from the Erme Estuary site were included for comparison (Fox, 1996), as both sites are less than 20 km apart (Fig. 1).

A sample of more than 20 mg from each ingot, and a smaller sample from each of the bronze artefacts was taken by drilling with a 1 mm high speed steel drill bit. To obtain uncorroded metal from the interior for a reliable analytical result, the corrosion from the surface was discarded and only the shiny metal drillings were used for the present study. Thicker areas on the tin ingots appeared to be corrosion ‘warts’; therefore, most drilling chips were extracted from the sides of the tin ingots. The corroded surface material was saved for X-ray diffraction analysis to identify the corrosion products, and will be used for evaluating whether tin corrosion products can provide reliable results for tin provenancing in a future study.

3. Analytical methods

3.1. Chemical analysis

All copper and most of the tin ingots from Salcombe and the Erme Estuary site that are considered in the present paper were chemically analysed in two previous studies with ICP-

AES and ICP-MS (Wang et al., 2016; 2018). The tin lump found earlier at Salcombe B was also analysed previously by Northover (2013) with electron probe micro analysis (EPMA). The EPMA data is not directly comparable with the ICP data of the ingots, especially regarding the trace elements that are often below 100 µg g^{-1} in unalloyed tin and thus below the detection limit of EPMA (Begemann et al., 1999; Northover and Gillis, 1999; Grant, 1999; Wang et al., 2016; Berger et al., 2019). We therefore re-analysed the lump with quadrupole mass spectrometry with inductively coupled plasma ionisation (ICP-Q-MS). The same was done with the bronze objects including those that have been examined by Northover (2013) with EPMA. Only those two bronzes that were analysed by Wang et al. (2018) previously (2010,8032.17 = MA-163268; 2010,8032.23 = MA-176569) were omitted from re-analysis. For better comparison, the data of these two as well as the data of the copper and tin ingots obtained earlier by Wang et al. (2016; 2018) were normalised to 100 % with sulphur content being omitted. The discrepancy with the original data is thus owed to re-calculation.

Samples of 5 to 33 mg of clean metal shavings (depending on the tin content) were dissolved overnight in a mixture of 6N HCl and H_2O_2. High purity water (18.2MΩ) and sub-boiled acids were used for the preparation of all solutions. An inductively coupled plasma ionisation quadrupole mass spectrometer with collision cell (ICP-Q-MS, XSeriesII, Thermo Scientific, Bremen, Germany) at the Curt-Engelhorn-Zentrum Archäometrie Mannheim, Germany (CEZA), was used for element analysis. ^{55}Mn, ^{57}Fe, ^{59}Co, ^{60}Ni, ^{63}Cu, ^{66}Zn, ^{75}As, ^{82}Se, ^{93}Nb, ^{107}Ag, ^{111}Cd, ^{113}In, ^{118}Sn, ^{121}Sb, ^{126}Te, ^{181}Ta, ^{182}W, ^{197}Au, ^{206}Pb and ^{209}Bi were determined. Calibration was performed with a set of selected MERCK and SPEX multi- and single standard solutions. ^{45}Sc, ^{169}Tm and ^{185}Re prepared from single stock solutions were added as internal standards. Spectral interferences on ^{113}In and ^{115}In were corrected using the

methodology of Xu et al. (2021). Three tin alloy reference materials (MBH 71X SR 2, 71 X SR3, 73X SC4) containing different amounts of In and Cd yielded correct In results within 9–20 %. For further quality control, a bronze reference material BAM 228 was treated the same way. Most results are in good agreement with the reported values of this reference material (<5 % Cu, Sn, Pb, 5–10 % Ni, Sb, Bi, <20 % for Fe and As).

3.2. Isotopic analysis

Tin, copper and lead isotope ratios of both the bronze artefacts and the ingots were determined using a Neptune Plus (Thermo Fisher Scientific, Bremen, Germany) HR-MC-ICP-MS at the CEZA. For this purpose, aliquots of the bronze solutions (see above) were diluted with deionised H_2O. Tin was digested the same way as bronze and an aliquot diluted with H_2O and HNO_3 and stabilised with concentrated HF. No chromatographic separation of the matrix element was necessary as the tin ingots consist of very pure tin (cf. Wang et al., 2016). The solutions were hence directly introduced into the mass spectrometer. In contrast, the tin of the bronze solutions had to be separated by column chemistry with TRU Resin (Eichrom Technologies, USA). After rinsing the resin with HCl, tin was eluted off the columns using HNO_3 and immediately stabilised with HF (details of the protocol can be found in Brügmann et al., 2017). An antimony reference solution (Specpure ICP–AES, Lot#. PSBH24/13, Fisher Chemical) was added to each aliquot of the bronze and tin solutions. The isotope ratios of tin were determined from the simultaneous measurement of seven stable tin isotopes (^{116}Sn, ^{117}Sn, ^{118}Sn, ^{119}Sn, ^{120}Sn, ^{122}Sn, ^{124}Sn). At the same time, the two stable antimony isotopes ^{121}Sb and ^{123}Sb were monitored for mass bias correction. The isotope ratios are expressed in the delta notation relative to an in-house standard, which was prepared

from an ultraclean tin metal (Puratronic, Batch W14222, Johnson Matthey, Royston, GB) by dissolving it in HCl. In order to make the isotopic data as comparable as possible to other research groups (there is still no internationally certified tin isotope reference material), all tin isotope values were re-calcualted to the NIST SRM 3161a tin standard solution using the specifications of Brügmann et al. (2017, Table 3). The resulting values were subjected to linear regression. The slope of the graph (theoretically all Sn isotope ratios align linearly) gives the tin isotopic composition δSn in permill per atomic mass unit (‰ u^{-1}) with the analytical uncertainty obtained from the regression procedure. The δSn will be used throughout the paper, but the original values referred to the Puratronic are given in the Supplementary Material (Supplementary Material S1).

Another two aliquots of each bronze solution served for copper and lead isotopic analysis, while aliquots of the tin solutions were analysed only for their lead isotope ratios. For this purpose, the solutions were evaporated to dryness and the residues picked up with 3N HNO_3. Columns filled with Sr Resin (Eichrom Technologies, USA) were used for the chromatographic separation of lead from the sample matrix. After multiple rinsing with 4N and 3N HNO_3, lead was eluted off the columns with 6N HCl and the solution evaporated to dryness again. After pick-up with 2 % HNO_3, doping with a thallium reference solution was performed in order to correct mass bias in the mass spectrometer. The same HR-MC-ICP-MS as for tin isotopic analysis was employed. Spectral interference on ^{204}Pb by ^{204}Hg was corrected by the measurement of ^{202}Hg assuming a $^{204}Hg/^{202}Hg$ ratio of 0.2293. The in-run precision amounts to 0.02 bis 0.05 % (2σ) depending on the isotope ratio.

No column chemistry was necessary for measuring the copper isotopic composition of the bronze solutions. Aliquots of the original bronze solutions were diluted with deionised H_2O

and 2 % HNO_3. A nickel reference solution (ROTI®Star, Nickel ICP Standard, Carl Roth GmbH + Co. KG, Karlsruhe, Germany) was added to each aliquot for mass bias correction. Besides ^{63}Cu and ^{65}Cu, the stable isotopes ^{60}Ni, ^{61}Ni, ^{62}Ni, ^{64}Ni and ^{66}Zn were measured with the Neptune Plus mass spectrometer. The $^{65}Cu/^{63}Cu$ isotope ratio is expressed as values of $\delta^{65}Cu/^{63}Cu$ in permill (‰) and given as $\delta^{65}Cu$ relative to the internationally used NIST SRM 976 copper isotope reference.

4. Results and discussion

4.1. Composition and origin of the tin in the ingots

Determining the sources of tin in metal artefacts is difficult. Almost every past analytical approach failed in finding suitable markers that can connect the metals with the ores. That is why the origin of the tin of the Bronze Age has been a 'mystery' for a long time (Muhly, 1973; Maddin, 1998; Giumlia-Mair and Lo Schiavo, 2003). A recent case study investigating LBA tin ingots from underwater sites in Israel (Hishuley Carmel, Kfar Samir, Haifa) (1300–1200 BCE), however, shed new light on this topic as it showed that a combination of geochemical parameters has great potential in tin sourcing (Berger et al., 2019). The most important proxy in this regard is the lead isotope ratios that allow discrimination between tin deposits formed at different times during Earth's history. For example, most European tin deposits including those in Cornwall/Devon, the Saxon-Bohemian Erzgebirge, on the Iberian peninsula or in Brittany and the French Massif Central formed 350 to 250 million years (Ma) ago during the Variscan orogeny, while Afghan and some European deposits or Egyptian sources are either much younger (Afghanistan: ~100–80 Ma) or older (Egypt: 650–530 Ma) (Del Moro et al., 1975; Willis-Richards and Jackson, 1989; Jackson et al, 1989; Babu, 1994;

Marignac and Cuney, 1999; Boni et al., 2003; Ludington and Peters, 2007; Neiva, 2008; Pavlova and Borisenko, 2009; Melcher et al., 2015; Chicharro et al., 2016; Romer et al., 2016; Lerouge et al., 2017; Rizvanova et al., 2017; Zhang et al. 2017; Moscati and Neymark, 2019; Lehmann et al., 2020; Powell et al. 2021). Using the $^{206}Pb/^{204}Pb$ and $^{207}Pb/^{204}Pb$ ratios instead of the conventional $^{207}Pb/^{206}Pb$ and $^{208}Pb/^{206}Pb$, all cassiterites that crystallised at the same time define a linear trend that is called an isochron (Nier et al., 1941; Molofsky et al., 2014). The underlying physical principle is the base for the U-Pb dating method (e.g. Zhang et al.; 2017; Neymark et al., 2018). The approach is, however, restricted to cassiterites that typically contain high concentrations of uranium and resulting high concentrations of uranogenic ^{206}Pb and ^{207}Pb. Furthermore, it is complicated by the possibility of contamination with foreign lead, e.g. during the pyrometallurgical processing of tin (smelting, refining, melting) or corrosion (Clayton, 2002), or when tin has been alloyed with lead metal. In all these cases, the lead isotopic signature of tin metal does not reflect that of the parental tin ore. Powell et al. (2021) most recently stressed the problem of contamination when discussing the available lead isotope data of the well-known tin ingots from the Uluburun wreck (from Oxalid database; with new isotope data from12 ingots). They emphasised that cassiterite is naturally lead-poor with lead concentrations normally below 4 µg g^{-1}. Lead concentrations in tin metal that exceed these values must therefore be due – at least in part – to impurities, e.g. from uranium- and lead-bearing minerals such as zircon or even from lead minerals (galena). The latter is not a problem if secondary cassiterite was mined from placer deposits. Lead minerals, which may introduce common lead into tin, are not resistant to weathering in fluvial environments compared with the highly resistant cassiterite. However, if more-resistant uranium-bearing minerals are mined alongside tin ores, radiogenic lead can be transferred into tin metal and dominate the lead signature (Powell et al., 2021). As long as these minerals are co-genetic with cassiterite, the slope of the isochron from the uranogenic lead isotopes

can be used to calculate a theoretical date (model age) which equals the formation age of the smelted cassiterite in tin deposits (Nier et al., 1941; Molofsky et al., 2014; Berger et al., 2019; Artioli et al., 2020; Powell et al., 2021).

Using the above approach, it was shown that the tin of the ingots from Israel must have been smelted from European sources (Berger et al., 2019). This result is in contrast to the previous view that suggested a central Asian origin (e.g. Afghanistan) for these tin ingots and bronze in the eastern Mediterranean and the Near East in general. This was concluded from both written sources and material evidence (e.g. lapis lazuli) (Muhly, 1985; Pigott, 1999; 2011; Galili et al., 2013). In the case of the Salcombe assemblage, lead isotope ratios are only available for six ingots, which is due to the very low lead concentrations in the tin (4.6–92 µg g^{-1}, cf. Wang et al., 2016). With sample sizes of 20 mg or less, there was often not enough lead in the digestion solutions to analyse them for their lead isotopic compositions. Thus, only those samples with more than 30 µg g^{-1} lead were analysed in this study, but they will consequentely contain foreign lead.

Nervertheless, five out of six tin ingots are characterised by highly radiogenic lead. They actually define an isochron in the $^{206}Pb/^{204}Pb$ vs. $^{207}Pb/^{204}Pb$ diagram (Fig. 4a; Table 2) whilst one specimen (MA-163251) falls significantly off the trend. The comparatively high concentration of lead and copper (87 µg g^{-1} and 2725 µg g^{-1}, see Supplementary Material S1) in MA-163251 compared to the other tin ingots could be due to contamination with common lead, e.g. from a furnace or a crucible. Hence its isotopic signature would not reflect that of the parental ore. That is the reason why the data of this sample was omitted from calculation of the model age. The remaining five items were used for calculation instead as it is likely

that contamination with radiogenic lead occurred during mining the cassiterite (e.g. from placer tin) or even originated from minerals intergrown with tin dioxide.

The slope of the isochron is 0.05422 ± 0.00310 (2SD) which relates to 380 ± 130 Ma. This is largely consistent with the European tin deposits and their formation during the Variscan orogeny. The high standard deviation is due to the small sample set and the lead isotopic compositions of the individual samples lying close together. When compared with the tin ingots found off the coast of Israel, however, it is obvious that they plot on the same trend line (Fig. 4a), not least because the slope of the isochron defined by the Israeli ingots (0.05213) is not changed significantly if the five ingots from Salcombe were included (0.05220). This suggests a common source area for the ingots from Salcombe and the different assemblages from Israel which must be on the European continent. Admittedly, the applied method cannot discriminate between sources with the same formation age, so Iberian, French, the Saxon-Bohemian and even Sardinian tin ores cannot be excluded by this approach as all formed in the same epoch. At this point, the tin isotope composition can be used to further narrow down the origin.

Although the various tin provinces as a whole cannot be differentiated by tin isotopes because of overlapping signatures, discrimination is principally possible when smaller regions (different granites) or units (mines) within the provinces are considered (Marahrens et al., 2016; Berger et al., 2019; Mason et al., 2020). If the isotopic composition of the ores is different from that in the artefacts, then the respective deposit can be excluded (exclusion principle). This approach is somewhat put into perspective by the potential mixing of tin ores or tin metal from various small (alluvial) workings in larger centres where ores and/or metal

were pyrometallurgically processed. So it could be more realistic to argue with averages of the potential tin suppliers rather than using isotopic values of individual cassiterite samples.

Figure 4b and Table 2 (see also Supplementary Material S1) summarise the tin isotopic composition of the Salcombe tin ingots and the lump. Overall, only positive values relative to NIST SRM 3161a are observed. The Salcombe tin exhibits a variation of 0.038 ‰ u^{-1} with values from 0.059 ± 0.001 to 0.097 ± 0.001 ‰ u^{-1} for the individual objects and an average isotopic composition of 0.073 ± 0.026 ‰ u^{-1} (2SD). The two bun ingots from the Erme Estuary site are very different from each other. While one of them has a δSn value of 0.058 ± 0.001 ‰ u^{-1} that is identical to some of the Salcombe ingots, the other has a tin isotopic composition of 0.111 ± 0.001 ‰ u^{-1} that is even heavier (i.e. more positive) than the heaviest one from the Salcombe site (Fig. 4b). Conversely, the tin lump from Salcombe B (MA-176602 = 2005,0503.19) is slightly lighter (i.e. more negative) (0.049 ± 0.001 ‰ u^{-1}) than the isotopically lightest ingot from the site, MA-163236 = 2010,8032.299 (0.059 ± 0.001 ‰ u^{-1}) (Table 2).

Figure 5 compares the δSn values of the Salcombe and Erme Estuary tin ingots with those of European tin deposits. Data of the latter have been acquired during our own research (Berger et al., 2019; Marahrens, forthcoming; Marahrens et al., forthcoming) and a parallel project of another group (Mason et al., 2020). The data is presented as box-whisker-plots including mean values to better illustrate the differences between the single tin ore regions and to account for possible tin (ore) mixing. The values of the artefacts have furthermore been corrected by –0.025 ‰ u^{-1} (coloured bars) to obtain δSn_{corr}. This was done for comparison with the ores, because mass dependent isotopic fractionation during the smelting process forces the isotopes toward heavier compositions (Berger et al., 2018; 2019). Without a

correction, direct comparison between ores and metals would lead to false interpretations. Referring to Figure 5, the following deposits can be excluded with great likelihood on a statistical base as sources for the Salcombe tin ingots since their isotopic signatures do not match those of the tin metal: the small occurrences on Sardinia, at Monte Valerio (Italy), the Mourne Mountains (North Ireland) and at Cerro de San Cristóbal near Logrosán (Spain). The larger ones like those of the Central part of the Erzgebirge, the German Fichtelgebirge and Vogtland, the Spanish deposits in the Salamanca, Ourense and A Coruña province, the ores from the St. Agnes Granite (Britain) and even the tin ores of Brittany and the French Massif Central are also less likely the sources due to partial overlap of their data with the artefacts and due to their deviating mean values.

The isotopic mismatch of the tin objects with the mean value and the median of the Breton tin ores is of particular interest. It strongly suggests that the nearby (alluvial) deposits in Brittany are not the source for the Salcombe tin. In contrast, the tin ingots show much better coincidence with the tin ores from the Carnmenellis and Land's End Granite areas in Britain. Finally, however, a lot of other deposits still remain as possible sources especially those of the Erzgebirge and Portugal, whose mean values show a good match with the respective objects (Fig. 5). Moreover, in a strict sense, also those areas with only partial overlap could still be a supplier for tin, at least for part of the ingots. On the one hand, tin ores could have been mixed across areas, smaller mines etc., thus homogenising the isotopic composition. On the other hand, the ingots must not necessarily originate from tin of the same deposit.

The latter conclusion could require further debate though. When the trace element pattern of the tin is evaluated (from the data reported in Wang et al., 2016 and Table 3), differences in the contents of indium (In), bismuth (Bi), lead (Pb) and antimony (Sb) can indicate different

origins. These elements turned out to be potentially diagnostic for tin deposits in previous studies (Rapp, 1978; Rapp et al., 1999; Berger et al., 2019). In the four-element diagram Pb/Bi vs. Sb/In covering all ingots analysed by Wang et al. (2016) at least two clusters can be distinguished, Group I and Group II (Fig. 6a). They follow distinct trends that are primarily due to the larger variation in the antimony and bismuth concentrations in the tin. Interestingly, five ingots within Group I (MA-163236, MA-163239, MA-163248, MA-163257, MA-163260) including those two with almost identical tin and lead isotope ratios as well as trace element signatures (MA-163239, MA-163260, cf. Table 2) show very good correlation in all four elements, strongly suggesting a common origin from the same tin deposit or mine (Fig. 6a). This is also reflected in their tin isotopic composition which correlates either negatively with bismuth or positively with iron, antimony, lead or Sb/In (Fig. 6b; Supplementary Material S2). According to Figure 6b, ingot MA-163251 falls in the same group whereas it does not in the four-element plot (Fig. 6a). This could in fact indicate contamination with lead as argued above.

Comparable relationships between tin isotopes and trace elements were recently recognised for the LBA tin ingots from Israel (Hishuley Carmel, Kfar Samir, Haifa), which, however, revealed negative correlations between tin isotopes and indium, lead and manganese (Berger et al., 2019). We interpreted this as indication of re-melting, probably due to refining. A relationship with the tin's pyrometallurgical *chaîne opératoire* (smelting, re-melting) cannot be ruled out for the Salcombe tin, but the correlation in the tin isotopes and trace element concentrations is more likely related with the mineralogical composition or paragenesis of the parental tin ores. Otherwise the increasing concentrations in antimony, arsenic and iron with increasing δSn values as observed (Supplementary Material S2) would be difficult to explain. Especially the concentrations of volatile antimony and arsenic would be expected to decrease

when the metal is re-melted manifold while the tin becomes isotopically heavier – at least in theory. Recent experiments by ourselves (Berger et al., forthcoming) actually show the tin isotopic composition of tin metal to remain unchanged, even when the metal is melted several times under extremely oxidising conditions. Moreover, the loss of antimony and arsenic from a tin melt could be small in the trace elemental range. So, finally, the observed correlations are most likely not related with the thermal processing of the tin, but a full assessment of the recognised elemental-isotopic dependencies requires further study.

The remaining five tin ingots from Salcombe as well as the tin lump roughly fall into Group II in the Pb/Bi vs. Sb/In diagram (MA-163233, MA-163242, MA-163245, MA-163251, MA-163254) and show a better match with the ingots from Israel (Fig. 6a). One ingot from the Erme Estuary site (MA-163263) with the lower δSn value falls into Group I while the other ingot from this site (MA-163266) with the higher ratio shows no coincidence with the two groups because of its unusually high bismuth content (1680 µg g^{-1}). Regarding the diagnostic trace elements, ingot no. MA-163263 corresponds well with the five Salcombe ingots from Group I as does also its tin isotopic composition (Fig. 4b and 6b). Hence, there is some probability that the respective ingots derive from tin ores of the same deposit or area, whereas it appears that the remaining ingots from Salcombe including the tin lump originate from other tin ores or from another area that could have also been the supplier for the tin ingots found off the coast of Israel. This latter statement is supported by the same variation in the tin isotope ratios of the Israeli tin (δSn = 0.05–0.10 ‰ u^{-1}) and its lead isotope signatures that indicate European tin sources in general (Fig. 4a; Berger et al., 2019).

Considering both trace elements and the smaller variation in the tin isotopic composition of Group I (δSn_{corr} = 0.034–0.060 ‰ u^{-1}), the provenance can be further confined for this group

of ingots. From the British sources for instance, only the tin ores from the Land's End and the St. Austell granites cover the whole range (Fig. 5). However, since the conclusions are similar for the other regions, a considerable number of other deposits remains possible. The chemical composition of the ores themselves with particular reference to the indium concentrations may help reduce the list of potential suppliers. Indium in tin indicates that the parental cassiterite ores were associated with indium-bearing sulphides (chalcopyrite, sphalerite, stannite) (Schwarz-Schampera and Herzig, 2002; Seifert and Sandmann, 2016; Goldmann, 2016; Werner et al., 2017; Andersen et al., 2018). The sulphides can be present as micro-inclusions or as associated minerals. The correlation of indium and bismuth in some of the Salcombe ingots (Group I) could further suggest a paragenesis with bismuth minerals such as bismuthinite and native bismuth or – more likely – their coexistence in the same sulphidic compounds such as sphalerite, chalcopyrite or stannite. Unfortunately, there is hardly any scientific study which provides enough analytical data allowing a complete assessment of diagnostic trace elements in cassiterite. Recent approaches at least demonstrate that indium rarely occurs at high concentrations (more than 100 µg g^{-1}) in European cassiterite mineralisation with the exception of the British ones and few locations in Brittany and Galicia (Abbaretz, Montbelleux, Macrofán) (Raimbault et al., 1999; Seifert and Sandmann, 2016; Werner et al., 2017; Lerouge et al., 2017; Andersen et al., 2018). If only the indium concentrations were considered one might thus conclude that British tin deposits rather than the other tin mineralisation throughout Europe are more likely the sources for the tin ingots. This conclusion, however, does not account for other trace elements such as antimony, bismuth and lead, mainly because a chemical reference database of tin ore deposits does not currently exist. Moreover, it disregards the behaviour of the chemical constituents during the pyrometallurgical processing steps. There is thus an urgent need for a comprehensive analytical study of tin ores (isotopic and chemical) from all over Europe and

beyond as well as systematic experiments regarding the behaviour of trace elements (and tin isotopes) during smelting and melting operations. At least, an analytical and experimental study of Cornish and Devonian ores is underway ('Project Ancient Tin' https://projectancienttin.wordpress.com/).

Unfortunately, the analytical limitations can hardly be compensated by archaeological considerations. The archaeological evidence for tin exploitation and extraction in the Bronze Age is not abundant despite the fundamental research of Penhallurick (1986) and more recent work by Timberlake (2017; Timberlake and Hartgroves, 2018) on the Cornwall and Devon evidence. This comprises several small assemblages of cassiterite grains from Bronze Age settlements of Trevisker (near St. Eval, Cornwall), Tremough (near Penryn, Cornwall) and Dean Moor on Dartmoor (Devon), which were quite recently complemented by an exceptional find of more than 10 kg of tin ore from two pits in EBA roundhouses at Tregurra Farm (near Truro, Cornwall) (Fox, 1957; ApSimon and Greenfield, 1972; Penhallurick, 1997; Jones et al., 2016; Carey et al., 2019). Aside from cassiterite, slag containing tin prills was unearthed from Dean Moor, as also was from a barrow at Caerloggas Downs, Treverbyn, Cornwall (Miles, 1975; Tylecote et al., 1989; Malham, 2010). These slags are the most convincing finds to date as they show that tin was actually extracted from tin ores quite early in southwest Britain. Even earlier evidence for tin exploitation from ca. 2300–2100 BCE (Bell Beaker phase) are likely provided by stone tools with small residues of tin recovered at Sennen Cove, Cornwall, which are thought to be related with the benefication of cassiterite (Carey et al., 2019). Timberlake (2017) furthermore mentions a couple of picks coming from alleged Bronze Age (open-cast) minings. One of these picks found in the Lower Carnon Valley, Cornwall, has been recently radiocarbon-dated to ca. 1600 BCE providing the first direct record for Bronze Age tin mining in Britain (Timberlake and Hartgroves, 2018).

Comparable vestiges are not available for the French Massif Central or the Saxon-Bohemian tin province, albeit excavations in the Aveyron department (Massif Central) and near Altenberg, Germany (Erzgebirge) revealed the first tentative evidence for the exploitation of alluvial tin during the EBA or the LBA (Cauuet, 2013; Tolksdorf et al., 2019). More significant records with direct relevance to Bronze Age tin extraction seems to exist from Brittany all of which are stanniferrous slags from different sites in the Délé valley near Saint Renan (Mahé-Le Carlier et al., 2001; Le-Carlier de Veslud et al., 2017). The disagreement in the tin isotopes, however, reduces the significance of this evidence with respect to our ingots as the Breton ores can most likely be excluded as their sources. Iberian tin ores are potential candidates regarding the tin isotopes (see Fig. 5). But apart from an Iron Age hillfort settlement at Carvalhelhos, Boticas, Portugal (Tylecote et al., 1989; Figueiredo et al., 2018), and the settlement near the Bronze Age tin mine of Cerro de San Cristóbal, Logrosán, Spain (Rodríguez Díaz et al., 2001; 2019), there is no other evidence for prehistoric tin production on the Iberian peninsula (note that the Salcombe ingots show a mismatch in the tin isotopes with the Logrosán cassiterites; Fig. 5). Given the fact that the tin ingots from Salcombe were found near one of the largest and most important European tin deposits with easily exploitable alluvial tin sources, it is not at all surprising that the Salcombe tin should originate, not from distant tin sources such as those on the Iberian peninsula, but from the geographical doorstep of southwest Britain.

4.2. Composition and origin of the copper in the ingots

The three copper ingots analysed in this study represent a small quantity (1 %) of the assemblage which comprises 280 ingots overall (Wang et al., 2018). Thus, the actual results only highlight a tiny fraction of the isotopic nature of the entire metal set, and the interpretations can therefore only be fragmentary. Nonetheless, the highly scattered data of both the lead and copper isotopes suggests apparent different origins for the copper of these three objects. While two ingots exhibit identical δ^{65}Cu values of –0.13 ± 0.01 ‰ and –0.16 ± 0.02 ‰ respectively, the isotopic composition of the third turned out to be isotopically extremely light with a δ^{65}Cu value of –1.56 ± 0.02 ‰ (Fig. 7a; Table 4). The picture is emphasised by the lead isotope ratios that cover a wide range from 0.84774 to 0.86070 in the ^{207}Pb/^{206}Pb and from 2.0912 to 2.1060 in the ^{208}Pb/^{206}Pb ratio (Fig. 7b; Table 4). Provided large-scale fractionation during pyrometallurgy can be excluded (Woodhead et al., 1999; Klein and Rose, 2020), from the copper isotopic composition just below 0 ‰ (relative to NIST SRM 976) it could be inferred that the copper of two ingots (MA-176597 and MA-176599) was smelted from primary sulphidic (hypogene) ores, such chalcopyrite. These ores mostly possess δ^{65}Cu values around 0 ‰ (Fig. 8). However, (supergene) oxide ores like malachite can also have negative δ^{65}Cu, although positive values are more typical (Fig. 8). Negative δ^{65}Cu values down to –2 ‰ apply even more to admixtures of secondary oxide minerals with relics of (secondary) sulphide ores that often occur at the interface between oxidation and cementation zone of ore bodies. That could be a likely explanation for the strongly negative δ^{65}Cu value of the third ingot (MA-176598). However, the use of purely oxidised copper ores such as malachite or azurite, that was speculated as a possibility by Wang et al. (2018), cannot be excluded from the δ^{65}Cu value alone since their isotopic variation is extremely broad (see Fig. 8) (Durali-Müller, 2005; Markl et al., 2006; Klein et al., 2009; 2010; Jansen et al., 2018; Mathur et al., 2018; Powell et al., 2018).

The above conclusions seem to agree with the elemental compositions of the copper. Although all three objects are rather pure copper (impurities <1.0 and <0.3 % ignoring sulphur) with similar sulphur contents of ca. 0.5 %, the two ingots with similar δ^{65}Cu values are richer in arsenic and tin, while the third one has considerably higher contents of zinc, silver, gold and lead than the others (Table 5). Sulphur could emphasise a sulphidic copper base for each of them, which was probably associated with some sphalerite (ZnS) and galena (PbS) in case of ingot MA-176598 indicated by its high zinc, silver, cadmium and lead concentrations. The low contents of iron in the three ingots (<200 µg g^{-1}) are striking and – as stated previously by Wang et al. (2018) – argue against chalcopyrite ore. Otherwise higher iron contents would be expected even if the copper had been refined (Craddock, 2000; Craddock and Meeks, 1987). The more likely metal base would thus be copper-rich secondary sulphides like chalcocite (Cu_2S), diginite (Cu_9S_5), djurleite ($Cu_{31}S_{16}$) or covelline (CuS). However, Tylecote (1976) and Craddock (1988) pointed out that copper smelted from oxide ores can contain about 0.5 to 0.7 % sulphur. So the presence of sulphur in the ingots alone can neither prove the use of copper-rich primary/secondary sulphides nor the use of oxide ores like malachite can be excluded. Considering the chemical and copper isotopic compositions and given the general rarity of pure secondary copper sulphides we thus assume that weathered copper ores containing both oxide and sulphide minerals were more likely the source for the copper ingots.

The copper isotopic composition is in the present case difficult to interpret and furthermore does not directly allow conclusions on the origin of the copper. This can be achieved by looking at the lead isotope ratios. Several ancient copper mines have been identified from Ireland and Britain, concentrating on the southwest of Ireland, northern to central Wales, the Isle of Man and central England that supplied oxide ores in the Bronze Age (Fig. 1; Ixer and

Budd, 1998; Timberlake, 2003; 2014; 2017; Timberlake and Marshall, 2014; 2018; O'Brien, 2015; Williams and Le Carlier de Veslud, 2019). The most important one was the Great Orme whose copper was used throughout Britain and beyond mainly between 1700 and 1300 BCE (Ixer and Budd, 1998; Williams and Le Carlier de Veslud, 2019). No Bronze Age copper mines have been identified so far in southwest Britain (Cornwall, Devon) apart from a potential but not confirmed candidate at Exmoor, Devon (Juleff and Bray, 2007). Copper isotopic composition is currently lacking for all of these copper mines and sources. Therefore, only lead isotopic data from the mines or deposits are compared with the ingots in Figure 9 along with isotopic data of galena, malachite and chalcopyrite ores from different mineralisation in Britain.

In general, there are matches either with the isotopic data of English ores (MA-176597; Fig. 9a–b) or ores from Wales (MA-176598 and MA-176599; Fig. 9c–d). On closer inspection, however, only ingot MA-176599 would be positively allocated to the Copa Hill mine (Cwmystwyth mine), Wales (see Fig. 1), because of its isotope ratios (Fig. 9c–d). Nonetheless, the use of the primary or secondary ores (chalcopyrite, secondary sulphides, malachite) of this deposit for the ingot is unlikely given the time of its main exploitation. Radiocarbon dates fixed the operating period to the EBA between 2100–1600 BCE (Timberlake and Marshall, 2014; 2018; O'Brien, 2015), although few later dates exist (Ixer and Budd, 1998). Comparable exploitation periods apply to several other British mines (Parys Mountain, Ecton, Alderley Edge, Nantyeira) with the exception of the Great Orme. From all known mines the Great Orme actually would be the most likely supplier because it operated until ca. 900 BCE with a peak between 1700 and 1300 BCE (Williams and Le Carlier de Veslud, 2019). Since the ingots show no convincing match in all lead isotope ratios the use of these ores can be excluded. Hence, sources on the continent or beyond must additionally be

considered not least because they became fundamentally important for the metal industry in Britain in the later 2nd millennium BCE (Northover, 1982; Williams and Le Carlier de Veslud, 2019; Ling et al., 2014; 2019). In this respect, the copper ores from Sardinia and southern Spain show the best match with two ingots (MA-176598 and MA-176599), while the third one (MA-176597) broadly falls into the isotopic field of the ores from Sardinia and the Slovakian Ore Mountains (Fig. 10). Overall, definite conclusions on the origin of the copper remain difficult because of extensive data overlap and the limited amount of analysed ingots.

The chemical characteristics of all 25 Salcombe ingots analysed previously (Wang et al., 2018), suggest that the above conclusions might be transferable to the entire assemblage. The chemical data is highly heterogeneous scattering over several orders of magnitude for some trace elements (e.g. As, Ag, Sb, Pb; Fig. 11). In addition, no trends, correlations or clusters are discernible, unlike most of the Bronze Age copper ingots from Sardinia and the Uluburun wreck. Both assemblages exhibit clusters in their chemistry (Wang et al., 2018). The Uluburun ingots also stand out by a narrow range in the lead isotopic compositions (Stos-Gale et al., 1998). Bearing in mind the large variations in the isotopic compositions of the (three) Salcombe ingots, one actually has to draw the conclusion that the assemblage comprises objects of different origins. It is also possible that they derive from a copper source with a large variation in both the chemical composition and the isotope abundance ratios. Whether further isotopic analyses of more copper ingots from the site can shed additional light on that issue remains to be investigated. This would probably also help to find evidence for or against mixing of copper ores or sources.

4.3. Relationship between ingots and bronze artefacts

4.3.1. Chemical and isotopic composition of the bronzes

Most bronze objects analysed chemically in this study by ICP-Q-MS were previously analysed by Rohl and Needham (1998) and Northover (2013) using EPMA. The results of both methods are not directly comparable due to various reasons (bulk analysis vs. micro-level analysis, detection limits, sensitivity), nevertheless the data of the sample sets shows good agreement (Fig. 11, grey symbols). Yet, from the present results, the interpretations are more far-reaching especially in combination with the isotopic compositions. Good agreement is also observed with the lead isotopic compositions of four artefacts (MA-176570; MA-176575, MA-176584, MA-176585) determined by Rohl and Needham (1998). There is just a slight systematic offset in the $^{206}Pb/^{204}Pb$ ratio (Supplementary Material S3), probably due to differences in precision between the employed analytical techniques (MC-ICP-MS used in this study; thermal ionisation mass spectrometry used by Rohl and Needham 1998).

The sword fragments of the Rosnoën type consist of bronze with tin contents between 7.2 and 10.6 % and an average of 9.2 ± 2.8 % (Table 6). The bronzes are characterised by medium levels of impurities that add up to 0.31–1.27 %. Strikingly, all trace elements (excluding Te) appear to be positively correlated among each other ($R > 0.6$) except for manganese and gold (Fig. 11–12; Supplementary Material S4). Also, the tin content shows no relationship with the trace elements. The other bronze swords studied here (Sn contents from 5.9 to 16.1 %), including the two LBA pieces, appeared similar in impurity pattern to the Rosnoën swords (Table 6) with significantly lower levels of cobalt, nickel, indium and bismuth. The contents of gold tend to be low as well apart from MA-176572 which has a very high gold content (Table 6). Moreover, unlike the Rosnoën group, lead contents are much more variable

between those swords. The LBA sword resembling the Carp's Tongue type (MA-176570) has an extremely high lead content of 29 %, followed by the MBA Ballintober type sword (MA-176574) with 5.1 %. The impurity pattern of the well-preserved MBA rod-tanged sword (MA-176575) shows the highest values of all the samples for cobalt, zinc, silver, indium, antimony and bismuth (Table 6). It was found to be closer to the Rosnoën fragments rather than the other swords.

The eight bronze palstaves from the site exhibit a variation in the tin contents comparable to the swords between 8.5 and 12.9 % (mean 10.6 ± 2.6 %; Table 6). The impurity pattern is very similar to the swords of the Rosnoën type, though the overall level of the trace elements tends to be slightly higher and more uniform (0.56–1.10 %). The largest differences are observed for cobalt, nickel, arsenic, silver and antimony whose mean values are 23 to 38 % higher compared with the Rosnoën swords (Table 6). Zinc, indium, lead and bismuth also exhibit higher averages than that in the swords with relative differences ranging 11 to 18 %. Concentrations of gold and tellurium are almost the same as that of the swords, whereas manganese and iron are relatively lower by 72 and 18 %, respectively. Figure 12 reveals again positive correlations for some elements such as cobalt, arsenic, silver, indium, antimony and bismuth. In the respective diagrams the absolute elemental concentrations are in the same order of magnitude as in the Rosnoën swords and so are the trends (Fig. 11). In contrast, there are considerable discrepancies to the other swords with the exception of the rod-tanged sword that is in line for most elements (Fig. 11).

The two rectanguloid blocks – called weights here – have very different tin contents (Table 6; Fig. 11). The smaller one (MA-176594) contains 10.0 % tin, while the second one with the wavy grooves (MA-176596) contains 19.7 %. Moreover, the latter artefact has higher

concentrations of iron, cobalt, zinc, antimony and lead, but lower concentrations of nickel, gold and bismuth. The concentrations of arsenic, silver and indium are similar, so is the manganese. Compared with the Rosnoën swords fragments and the palstave axes there are lot of similarities in the impurity pattern of the metal (Fig. 11).

The tin isotopic composition of the bronzes is displayed in Figure 4b and Table 7. A majority of eight swords, four palstaves and one weight have δSn values in a narrow range from 0.068 ± 0.001 ‰ u^{-1} to 0.089 ± 0.002 ‰ u^{-1}. The remaining objects are shifted to heavier (more positive) or lighter (more negative) tin isotopic compositions. The LBA Carp's Tongue sword (MA-176570) has a distinctly heavy composition of δSn = 0.104 ± 0.001 ‰ u^{-1}, whereas one palstave axe (MA-176584) is isotopically very light (0.055 ± 0.001 ‰ u^{-1}). The variation is also small for the copper isotopes. δ^{65}Cu values spread from –0.04 ± 0.02 ‰ to 0.14 ± 0.02 ‰ for the swords and from 0.07 ± 0.01 ‰ to 0.18 ± 0.01 ‰ for the palstaves and the weights (Table 7; Fig. 7a). Only one MBA sword (MA-163268) has a very positive copper isotopic composition of 0.73 ± 0.01 ‰. In terms of the lead isotope ratios, the Rosnoën sword fragments are less radiogenic than three of the other swords and scatter between 0.85768 and 0.86163 (^{207}Pb/^{206}Pb) and 2.1040 and 2.1115 (^{208}Pb/^{206}Pb) (Figs. 7b–d and 9–10). Almost the same range is observed for the palstaves (except for MA-163269) and one weight (MA-176594). The weight with the wavy grooves and one of the other swords (MA-176575) clearly fall off this range.

4.3.2. Recycling or not?

It is worth mentioning that there are striking correlations among trace elements and even between trace elements and isotopes (Fig. 12–13; Supplementary Material S4–6). This becomes particularly clear with the swords of the Rosnoën type exhibiting correlations between almost all elements except for tin, manganese and gold. Most accompanying elements are additionally correlated positively with the δ^{65}Cu values (Supplementary Material S6). Such correlations are not expected for independent artefacts. Rather, the chemical and the isotopic data would basically scatter if the artefacts are not directly linked. Thus, there is strong indication that the Rosnoën sword fragments are related with each other in that at least two copper batches have been mixed. Since the tin isotopic composition and the tin concentration are also correlated with the copper isotopes (Fig. 13a; Supplementary Material S6), there is further evidence that we are dealing with the mixing or recycling of bronzes because the parameters are independent isotopic features of the parental ores.

On the other hand, we can exclude fractionation during the pyrometallurgical processing of the bronzes as the reason for the negative correlation between δ^{65}Cu and δSn. The isotopic compositions of the elements would have been either constant under highly reducing or forced toward heavier compositions under oxidising conditions (Supplementary Material S7). Fractionation of the isotope systems into different directions (i.e. toward heavier for Sn and lighter for Cu, or reverse) is very unlikely, so that the present relationship in fact points to a mixture of bronzes.

This conclusion is additionally emphasised by the lead isotopic composition and the corresponding inverse lead content 1/Pb. Pollard and Bray (2015) used this data presentation to reveal mixing of metal batches in Sardinian copper artefacts, in which all objects deriving from mixing events define linear mixing lines. The same method was recently successfully

applied to EBA/MBA bronzes from Central Europe by Berger et al. (2021). Concerning the Rosnoën swords from Salcombe, linear trends can be observed for most of the objects (Fig. 7e–f). This result actually supports the theory of metal mixing or recycling following the argumentation of Pollard and Bray (2015). However, one sword (MA-176577) does not align with the other bronzes, and the object also clearly falls off trend in the diagram of the copper and tin isotope ratios (Fig. 13a). The same can be observed for another sword (MA-176578), though the shift is smaller than that for MA-176577. Instead, MA-176578 shows a striking mismatch with the trend line (= mixing line) established by the copper isotopic signatures and the tin contents because it is too low in tin (Supplementary Material S6; Fig. 13). If we postulate that the mixture or alloying with a third component does neither affect the tin isotopic nor the chemical signature but has slight effect on the copper isotopes towards higher compositions, these observations would be consistent. One possibility to achieve this is for instance alloying with another, chemically pure and isotopically heavier (i.e. more positive) copper source as this would have had lowered the tin concentration at the same time. So, in this case, there could be an indication of multiple or sequential alloying/mixing (Faure and Mensing, 2005, 348–329). The same practice could also explain why the isotopic values of the sword MA-176577 are inconsistent with the other items (Fig. 13). In this case, however, the copper must have been isotopically very light (i.e. more negative δ^{65}Cu) to yield the current isotopic composition.

The situation is comparable for the palstave axes. Their chemical and isotopic compositions match those of the Rosnoën swords in all points, especially in their absolute concentrations/values and the observed elemental correlations (Fig. 11–13). Part of the objects also show a mixing line between the lead isotope ratios and the inverse lead concentration (Fig. 7e–f). Thus, it is very likely that the axes and the Rosnoën swords

analysed here were made with the same metal sources. However, it is impossible that the bronze of one group served as base for the other, e.g. palstaves were remelted for producing swords. The $\delta^{65}Cu$ of the palstaves tend to be positively correlated with $^{207}Pb/^{206}Pb$ (and the other lead isotope ratios), while there is a negative relationship for the swords of the Rosnoën type (Figure 13b). The same picture is observed with the $\delta^{65}Cu$ values and tin contents (Supplementary Material S4). Although the sample set in this study is limited, mixtures of bronzes are very likely in both cases due to the linear dependency between copper and tin isotopes, hence the parental bronze batches must have been different. The poorer correlations between the copper isotopes and the trace elements could further suggest a stronger mixing with a third component, probably rather pure copper. This would have affected the copper isotopes more than the trace elements. Neglecting one outlier (MA-176584), the tin isotopic composition and its variation are similar to that of the Rosnoën swords, so the use of the same tin sources for the palstaves is possible (Fig. 4b).

4.3.3. Tin from the ingots?

Provided we are actually dealing with bronze mixing or recycling, the significance of the individual isotopic values of the objects is limited. When components are mixed, the isotopic compositions of the products should in theory equilibrate and lie between the isotopic composition of the end members (i.e. the starting bronzes or tin). This, however, would make the tin isotopic composition of the bronzes obsolete as a tool for provenance determination, because the isotopic signatures of the end members are often unknown. The situation is hence similar to the Salcombe tin ingots in certain points, for which we also had to consider mixing of tin or cassiterite charges (see 4.1.). Given the larger isotopic variation in the tin ingots

overtopping the entire range of isotopic compositions in the bronze artefacts (Fig. 4b) and accounting for the almost identical average values (Tables 2 and 7), it is yet possible that the Salcombe tin ingots or their source areas in general played a role in the manufacturing of the Rosnoën swords and the axes. This conclusion may be supported by the highly significant correlation in the indium and bismuth contents in the bronzes (Fig. 11f). This correlation seems to be mirrored in the respective concentration in the tin ingots (Fig. 12), which could be an additional indication for the same source area of the tin. A clear statement on that finally is not possible, not least there are too many unknowns. Nevertheless, the conclusions can be applied to the rectanguloid weights because they are similar to the other bronze artefacts in many ways (Fig. 11; 13). Following the above consideration, one would deduce tin sources other than the Breton ones for the bronzes, as their (corrected) isotopic compositions clearly differ from the ores in their average composition and median (Fig. 14). This would be particularly significant, as it suggests that the Rosnoën swords as a typical northern French artefact type were not made with local tin.

4.3.4. Copper from the ingots?

In contrast to tin, the copper ingots alone can hardly be the raw material of the bronze artefacts, especially the Rosnoën swords, palstave axes and weights. The diagrams in Figure 11 demonstrate that the ingots have much lower levels of impurities (especially Co, Ni, In, Pb, Bi), often by a factor of 10 or 100, than the bronzes. This observation cannot be compensated by the tin impurities either. Firstly, prehistoric tin has usually very low concentrations of (chalcophile) trace elements and secondly, the elemental concentrations are diluted by a factor of about 10 if tin is alloyed with copper. Thus, either an unusually impure

tin or copper (in the form of bronze) other than that of the Salcombe copper assemblage was used in the production of the bronze objects. The former is very unlikely as tin from placer cassiterite (most probably the main source in prehistory) is usually quite pure. The latter theory is on the one hand reinforced by the above observation that bronze batches were mixed. On the other, the sulphur concentration of one palstave and one Rosnoën sword are low (330 and 650 µg g^{-1}, analysed by Wang et al., 2018, Table 2, 2010,8032.23 = MA-163269, 2010,8032.17 = MA-163268) and their iron content (470 and 1470 µg g^{-1}) is similar or even higher than in the other bronze items analysed in this study (Table 4). This provides further evidence for a copper source other than the Salcombe ingots as the situation there is reversed. Their iron concentrations are very low throughout (<219 µg g^{-1}), while sulphur contents are distinctly higher (0.3–0.8 mass%) (Table 5; cf. Wang et al., 2018). If this copper would have been used exclusively to make the bronze, the iron contents in the bronze must be much lower, and those of sulphur higher. Thus, the ingot copper could not have been the sole base for the bronzes, which is also suggested by a mismatch in the copper isotope ratios (Fig. 7a). It is, however, not excluded by the above considerations that copper was alloyed with bronze as a third component during recycling. If this was the case, the copper isotopic composition could have been more affected than the trace elements, all the more so if the δ^{65}Cu value of the copper was strongly negative. Ingot no. MA-176598 is such a candidate with δ^{65}Cu = –1.56 ± 0.02 ‰. Assuming that e.g. the bronze of sword MA-176577 had an original δ^{65}Cu of 0.15 ‰ (to match the trend in Fig. 13a), only 10 % unalloyed copper similar to that of ingot no. MA-176598 was needed to change the copper isotopic composition of the bronze to the current value of –0.02 ‰.

The lead isotope ratios would not have been influenced significantly by this due to the comparable isotopic signature of the respective ingot with the swords. Nevertheless, when a

third component is alloyed with two other components, the lead isotope ratios generally form a mixing triangle between the three end members (Faure and Mensing, 2005, 350–355), which should include the bronze object in question (MA-176577) (Fig. 7b–d). Taking the analytical precision into consideration, this requirement is fulfilled for the sword. Even if the respective objects (bronzes and copper ingot MA-176598) are not directly related to each other (end members of mixing are not known), the mixing triangle can be interpreted as an additional reference to the alloying of some of the bronzes with fresh copper similar to ingot no. MA-176598. It should be noted that the sword MA-176577 has been identified as not following the mixing line of the lead isotopes and the inverse lead concentrations (Fig. 7e–f). This adds further evidence to the above considerations of more-component mixing. The combination of copper isotopes with other parameters therefore helps to reconstruct the potential use of Salcombe copper in recycling to produce the bronzes from the site.

The swords other than the Rosnoën type are certainly not related to the copper ingots from the site. Although most impurities of the swords are in the same magnitude of order as the ingots, their copper and lead isotopic compositions are different (Figs. 7 und 11).

4.3.5. Provenance of the bronze's copper

The above conclusions on recycling and alloying have implications for tracking the copper sources of the bronzes. If copper-tin alloys were mixed and alloying with fresh copper took place this would have had an effect on the lead isotope ratios. A proper provenancing of the copper with lead isotope abundance ratios is thus not feasible, nor is it possible with the copper isotopes and trace elements. Since the lead isotope signatures of most of the Rosnoën

swords exhibit straight lines that can be interpreted as mixing lines between two components (Figs. 7, 9–10), the original sources can at least be estimated. However, it is not a straightforward task to interpret the diagrams containing the data of various European copper deposits. A lot of sources show comparable ranges of isotopic compositions or data overlap. Especially the copper deposits of Sardinia, the southern and western Alpine region as well as southern Spain show similar ratios, which also applies to several British sources. Considering all isotope ratios, the archaeological objects (Rosnoën swords and axes) show best match with the ores from Sardinia (Iglesiente and Barbagia/Barbona region) and southern Spain (provinces of Huelva, Cadiz, Sevilla), though some locations of Wales (Copa Hill mine) and the Harz Mountains cannot be ruled out. In contrast to that, the ores of the Slovakian Ore Mountains are shifted to slightly more radiogenic ratios, whereas the lead isotopes signatures of the Mitterberg region in the eastern Alps (not shown in the diagrams) are significantly more radiogenic (Figs. 9–10). These ores can thus be excluded. Many other ore deposits such as those in Cyprus, the Erzgebirge, the western and southeastern Alps and even most of the ores in the British Mainland and Ireland can also be ruled out as the source of the these archaeological bronze artefacts, because their isotope ratios are either completely different or only partially match with those of the artefacts. Moreover, most deposits do not form mixing lines with the artefacts in all diagrams, and/or an exploitation for the respective time period is not assured. In contrast, there could have been mixing of different Sardinian copper sources and probabaly of Sardinian with Spanish ores when the mixture with three components is used as a basis (Fig. 10c–d). The conclusions raised here for the Rosnoën swords and palstaves are in line with the interpretations made earlier for other Penard phase metalwork by Rohl and Needham (1998, 179–180). They also concluded on material mixing, interestingly outside the British territory – i.e. somewhere on the continent. However, Rohl

and Needham (1998) were ultimately as unable to pinpoint the origin of the copper as ourselves.

The copper isotopic composition of the Rosnoën swords and palstave axes (δ^{65}Cu values between 0 and 0.2 ‰) strongly resemble that of sulphidic ores such as chalcopyrite or bornite. This impression is based on a vast data set of analyses on chalcopyrites and bornites from various locations, even though rarely from those minerals from which the presented lead isotope ratios originate. The mean δ^{65}Cu value of 0.22 ± 0.67 ‰ (2SD, n = 583) for chalcopyrite and 0.23 ± 0.88 ‰ (2SD, n = 77) for bornite are nevertheless in the same range as the artefacts (Fig. 8), so that sulphidic copper ores are most likely their sources. The conclusion is further suggested by the impurity pattern of the bronzes in general (low levels of impurities) and their elevated iron contents (0.05–0.40 %), whereas the low sulphur concentrations of two objects (0.03 and 0.06 %) seem to contradict the observation. However, the copper for the bronzes was certainly refined before it was used for alloying, which would have lowered the sulphur concentrations (and also those of Fe) considerably. On the other hand, we have to bear in mind the mixing or recycling that may have occurred. This could have had impact on the copper isotopes, especially when the values of the parental copper/bronze was very different. In such cases, the conclusions for the source of the bronzes are limited to what was seen in sword MA-176577, which might have experienced multiple or sequential alloying/recycling with quite different coppers. Nevertheless, for most of the Rosnoën swords and palstaves the copper isotopic compositions and impurity patterns are consistent with primary sulphidic ores, and thus expand the conclusions drawn from the lead isotope ratios.

Despite the likely prevalence of Iberian and/or Sardinian copper sources in the MBA artefacts of our sample set, ores from Britain were probably used to produce the LBA objects. This is demonstrated by the LBA Carp's Tongue sword (MA-176570) and the type Nantes sword (MA-176572). These two objects and the MBA sword of the Ballintober type (MA-176574) share lead isotope signatures with galena and malachite from the Alderley Edge mine (Fig. 9a–b). Two of the swords have very high lead levels of 5 and 29 % (Table 6). In those objects lead is an intentional alloying element, which source is thus tracked by the lead isotopic composition. Lead minerals, especially galena are abundantly present in some parts of the Alderley Edge deposit (Ixer and Vaughan, 1982), but whether lead could have been really obtained from the mine is debatable. Galena is often intergrown with chalcopyrite, but there is no evidence for ancient exploitation (Timberlake and Prag, 2005), and the mine obviously operated only earlier in the 2nd millennium BCE (O'Brien 2015, 151). Rohl and Needham (1998, 180) also proposed the potential use of the ores from Alderley Edge for a number of objects from Ewart Part metalwork. Additionally, they were unsure as to whether lead ores from the Mendip Hills, Somerset, played a role in the production of LBA metalwork. However, from the artefacts studied here, the lead from the Mendips could have been an alternative source for the MBA Ballintober type sword with 5 % lead (Fig. 9a–b). In contrast to that, the remaining two MBA swords (MA-163268 and MA-176575) and the two rectangular weights (MA-176594, -96) are different from the former three swords and share again isotopic characteristics with Sardinian or south Spanish copper (Fig. 10c–d). The strongly positive δ^{65}Cu value of sword MA-163268 (0.73 ± 0.01 ‰) could indicate a supergene nature of the parental copper ores (e.g. malachite), whereas the values of the other four swords and the weights (Fig. 7a) point to primary sulphidic sources like for the Rosnoën swords and palstaves. In this context, it would be worthwhile to investigate a continental counterpiece to the weight with the wavy moulding found in Wallerstädten, Germany, as to

its isotopic characteristics. The object shares a similar chemical signature and a high tin content (Berger 2012, Table A.8, 17), so that – besides typological coincidences – there is some likelihood for the use of the same metal bases.

Overall, our results on the bronze objects from the Penard and Ewart Park metalwork phases mirror to some extent the findings for comtemporary bronzes from Scandinavia. Ling et al. (2013; 2014; 2018, 2019) and Melheim et al. (2018) have recently presented a large corpus of isotopic and chemical data from Nordic Bronze Age bronzes and identified a diversity of possible copper suppliers. Among these, the Italian Alpine region along Sardinia and southern Spain seems to have dominated the Nordic metal industry from the 15th century BCE (periods II to V) onwards, while earlier metalwork (periods LN I and I) was mainly produced with copper from deposits in the eastern Alps (Mitterberg, Tyrol), Slovakia and the British Isles (Ling et al., 2013; 2014; 2018, 2019; Vandkilde et al., 2017; Melheim et al., 2018; Radivojević et al., 2019; Nörgaard et al., 2019; 2021). It is evident that our findings fit into the picture of long-distance metal trade established by large-scale analytical programs in recent years. In the case of Scandinavia, the metal input was dependant on extensive networks and likely two different trade routes, one of which was termed the Atlantic 'maritime route' (Ling et al., 2014). In this scenario, the British Isles – and in particular the ore-rich regions of Cornwall and Devon – played a central role, acting as some kind of stopping point or entrepôt in the metals trade between southern and northern Europe. The British tin sources may have been a crucial factor for this route, and the hypothesis of Ling et al. (2014) relies heavily on the analysis of an annular tin ingot from Vårdinge, Sweden, which was thought to come from Cornish tin deposits. The lead isotopic composition of this ring of Period V of the Nordic Bronze Age (900–700 BCE) actually matches perfectly the isochron defined by the tin ingots from Salcombe and Israel. Moreover, it fits exactly with two Late

Bronze Age tin finds from Flag Fen, Britain (Fig. 4a; Rohl and Northover, 1994). It is of course not known how precisely the artefacts from Salcombe relate to Scandinavian metalwork and whether the alleged ships could have been part of the 'maritime route'. There is even uncertainty about the exact relationship between the raw products (ingots) and the bronzes studied. However, if the MBA bronzes and the ingots from Salcombe date from the same period and were part of the same cargo, it is not unreasonable to assume that the metal artefacts were destined for northern Europe. To transport tin ingots for the local demand across the sea by ship is unlikely, so a supraregional destination is more plausible, be it in northern Europe or somewhere else.

5. Synthesis and conclusions

The analytical work carried out in this study improves our knowledge of the MBA/LBA Salcombe metal assemblage and the relationship between the specific artefact types considerably. The tin ingots from the site were most likely produced from ores of two different tin deposits in southwest Britain. Despite an extensive data set for tin objects comprising tin and lead isotopes as well as trace elements, however, incontrovertible evidence is still missing. This is mainly due to the lack of ore data, with further isotopic and chemical analyses from British and other European tin sources needed to overcome this limitation. Producing these ore data is at the core of a new research project involving several of the authors (*Project Ancient Tin* https://projectancienttin.wordpress.com/).

The striking isotopic and chemical coincidence of the tin ingots found off the coasts of Salcombe, southwest Britain, and Israel, nevertheless, suggests an origin from the same

sources (primarily from the source of chemical Group II; cf. Fig. 6), thus corroborating the theory of long-distance trade networks voiced by Berger et al. (2019). Although concerns have recently been raised over the idea of a northwestern European-Mediterranean tin trade route (Powell et al., 2021), the data presented here provides new evidence for the interpretations of Berger et al. (2019). This is further underlined by the slightly later Early Iron Age (7th–6th century BCE) tin ingots from the shipwreck off Rochelongue, Cap d'Agde, France (Hugues, 1965; Bouscaras and Hugues, 1972; Aragón et al., 2022), which are very much on the riverine and maritime route from Cornwall to the Levant. Two tin objects from the site share the same geochemical characteristics (data to be published in a future paper) with the ingots from Salcombe and Israel.

The geographical distance and socio-cultural contrasts between the small farming communities in southwest Britain and the palaces, cities and states of the Levant in the mid-late 2nd millennium BCE have potentially dissuaded many scholars from exploring potential trade dynamics. Whilst there is no evidence to suggest that any direct connections between southwest Britain and the Levant, there is an emerging connectivity spanning these disparate regions. Recent research on the weight systems across sites and networks spanning Mesopotamia, Aegean-Anatolia and Europe sees the origins of a pan-western Eurasian regulated weight system at ca. 1300 BCE with distribution of balance weights in central and western Europe, including those found at Salcombe (Ialongo, 2019), and a common use of weighing technology by ca. 1000 BCE (Ialongo et al., 2021). It is thought that metals were widely used in weight-based transactions, though such activities may have been initially restricted in western Europe to elite groups (Poigt et al., 2021). Whilst silver is widely attested as weighed currency in the Levant, weight regulation in gold has been demonstrated as occurring with Penard (1300–1150 BCE) gold torcs and fragments, including those found

at Salcombe (Rahmstorf, 2019). Beyond gold, the potential use of bronze objects and fragments as pan-European currency during the 2nd millennium BCE has been highlighted in several extensive and persuasive studies (Kuijpers et al., 2021; Ialongo and Lago, 2021). This connectivity during the 2nd millennium BCE is reflected in the widespread distribution of distinctive bronze artefact types, not only across the Mediterranean, but also in north and northwest Europe. Earlier examples include the Cypriot hook tang weapons, with finds including a hoard at Sidmouth, just along the coast from Salcombe, now sadly lost (Brandherm, 2017; Harding, 2021). By the 13th century BCE, there is not only the *strumento* found at Salcombe but also razors, fleshhooks and shaft-hole axes across southern England which are paralleled across France, Iberia and the Netherlands but have their core distributions in the central Mediterranean (Needham and Giardino, 2008). It is also during the 13th century BCE that oxhide copper ingots, previously an ingot form associated with the east Mediterranean, are found in high numbers in the central Mediterranean and, in particular, in Sardinia (Sabatini, 2016a; 2016b). This distribution not only reflects the changing dynamics in the Mediterranean metals trade but also the close connections between Cyprus and Sardinia at this time (Lo Schiavo and Sabatini, 2020). Finally, the 13th century BCE also sees the widespread adoption across Europe of one of the most distinctive bronze technology, complex sheet-metalworking as demonstrated in cauldrons (Gerloff, 2010) and shields (Uckelmann, 2012), as well as one of the most important and transformative bronze objects, the sword (Colquhoun and Burgess, 1988; Hermann et al., 2020). These are both represented in the Salcombe assemblage with a cauldron handle and the two earliest main sword types in the Channel region, Rosnoën and rod-tanged (Needham et al., 2013). Within the context of this increasingly inter-connected world, the possibility of a network of traders responsible for tin ingots from Cornwall being discovered at shipwreck sites off the coasts of southwest

Britain and Israel no longer seems implausible. Nevertheless, there might have been more than one such trade route, especially in other periods of the Bronze Age.

The situation appears to be the inverse of the tin for the Salcombe copper ingots. The lead isotopes suggest Sardinian and/or Spanish rather than British or Irish sources. Based on the copper isotopes and the chemical composition, these ores could have been of mixed oxidic/sulphidic character, but more than three objects have to be analysed in order to make a statistically significant statement. This is all the more important when the heterogeneous nature of the Salcombe copper assemblage is considered (Wang et al., 2018), which is not least reflected in the isotopic characteristics of the copper. The recent trace element and lead isotope analysis of several plano-convex copper ingots found at the Rochlongue shipwreck indicated a similar diversity in distant provenances ranging from Iberia to the Eastern Alps and potentially additional Mediterranean sources (Aragón et al., 2022).

With the available findings, the Salcombe copper ingots could only have been an additional component rather than the sole base for the bronze objects found in association with them on the same site. The elevated levels of impurities as well as the differing copper and lead isotope ratios of the Rosnoën swords and palstave axes indicate other ore sources, such as chalcopyrite from Sardinia and/or southern Spain. Mixing lines/triangles in the lead isotopes, however, could point to the alloying of bronze with Salcombe copper as a third component.

The tin of the bronzes exhibit the same isotopic range as the tin ingots, so the production of the bronzes with Salcombe tin would principally have been possible. Given the correlations between copper and tin isotopes and between copper isotopes and trace elements observed in the Rosnoën swords and the palstaves, however, this conclusion is put into perspective. The

bronzes were verifiably made by mixing either bronze ingots or scrap bronze as indicated by the highly significant correlations between copper and tin isotopes and between copper isotopes and trace elements. This result is the most tangible evidence to date for the mixing/recycling of bronze in the Middle Bronze Age and thus supports the assessment of many previous studies on the subject. However, if the tin ingots were actually used to make the bronze artefacts from the site, then one must assume that first discrete bronze batches were produced, which were then mixed several times with the use of scrap metal. Because it seems unlikely that this was done in the same workshop we thus argue the history of the tin ingots and the history of the bronzes are different. This conclusion does not rule out British tin for the bronzes, since the tin isotopic composition of the bronzes match that of British and hardly that of the nearby Breton tin ores. The question of where the bronze objects were produced remains nevertheless elusive without a closer archaeological examination. However, given the identical chemical and isotopic features, it is almost certain that the palstave axes and the Rosnoën swords were made from the same metal bases and even were part of the same cargo. The other bronzes from the site (except the LBA objects) could have been related closer to these objects, but how exactly is difficult to decide due to the deviating scientific data.

When the analysed metals are considered in the context of Bronze Age maritime activity off the coast of Salcombe, any interpretation is complicated by the typo-chronological evidence for two potential shipwreck events. Whilst the majority of the typologically diagnostic bronze and gold objects date to the Penard metalwork phase (ca. 1300–1150 BCE) rather than the Ewart Park metalwork phase (ca. 1000–800 BCE), this does not mean that the 40 tin ingots and 280 copper ingots can be dated to the earlier period. The spatial distribution of the Bronze Age finds in the Salcombe assemblage does not provide evidence for two distinct

groupings with a secure location and context of deposition for the objects being compromised by the highly dynamic nature of the seabed in this coastal area. There is no clear compositional or isotopic evidence for dividing the analysed copper or bronze objects into two groups and, whilst the tin ingots can be divided into two groups by means of the archaeometric data, a chronological attribution for either group would be difficult to demonstrate. That the tin ingots were most likely produced locally from tin deposits in southwest Britain whereas the copper ingots seem to have been produced from European rather than British ore sources (e.g. Spain or Sardinia) is supported by related archaeological and archaeometallurgical scholarship for each metal. It is also entirely feasible that both the copper and tin ingots were part of the same cargo despite their very different origins. The association of objects of completely different origins is well-known from other Bronze Age shipwrecks (Uluburun, Gelidonya, Early Iron Age Rochelongue) and could be a characteristic feature of long-distance trade networks (Hauptmann et al. 2002; Stos, 2009; Aragón et al., 2022). Thus, it is readily conceivable that both ingot types and the Salcombe assemblage as a whole (except for the LBA bronzes) were integrated into a supra-regional network concerning the metals trade. If this could have been related to northern Europe must remain speculative at present as it requires further research. Also, there is an urgent need for a comprehensive analytical study of tin ores (isotopic and chemical) from all over Europe and beyond with systematic smelting experiments as well as further work on more of the Salcombe copper ingots to provide clearer evidence regarding the European tin and copper trade and sources. Overall, the Salcombe ingots and metalwork provide further evidence of long-distance European metal trade networks in the Later Bronze Age and that the British tin sources are likely to have played a prominent part, with tentative indications that the tin reached as far as the eastern Mediterranean.

Acknowledgements

The authors would like to thank Neil Wilkin, the current Bronze Age curator of the Department of Britain, Europe and Prehistory of the British Musuem for his support in the project. We further acknowledge the assistance of Janeta Marahrens, Bernd Höppner and Sigrid Klaus, CEZA Mannheim, in the preparation and analysis of the metal samples. Most of the analyses and the work on the topic were funded by the European Research Council (ERC Advanced Grant Project G.A. no. 323861 to EP) within the project 'BRONZEAGETIN – Tin isotopes and the sources of Bronze Age tin in the Old World'. The lead isotopic analyses of the tin ingots were funded by the British Museum Research Fund.

References

Andersen, J.C.Ø., Stickland, R.J., Rollinson, G.K., Shail, R.K., 2016. Indium mineralisation in SW England: Host parageneses and mineralogical relations, Ore Geology Reviews 78, 213–238.

ApSimon, A., Greenfield, E., 1972. The excavation of Bronze Age and Iron Age settlements at Trevisker, St. Eval, Cornwall. Proceedings of the Prehistoric Society 38, 302–381.

Aragón, E., Montero-Ruiz, I., Polzer, M.E., van Duivenvoorde, W., 2022. Shipping metal: Characterisation and provenance study of the copper ingots from the Rochelongue underwater site (Seventh–Sixth century BCE), West Languedoc, France. Journal of Archaeological Science: Reports, 41, 103286, DOI:10.1016/j.jasrep.2021.103286.

Arribas, A., Tosdal, R.M., 1994. Isotopic composition of Pb in ore deposits in the Beltic Cordillera, Spain: Origin and relationship to other European deposit. Economic Geology 89(5), 1074–1093.

Artioli, G., Angelini, I., Nimis, P., Villa, I.M., 2016. A lead-isotope database of copper ores from the Southeastern Alps: A tool for the investigation of prehistoric copper metallurgy. J. Archaeol. Sci. 75, 27–39.

Artioli, G., Canovaro, C., Nimis, P., Angelini, I., 2020. LIA of prehistoric metals in the Central Mediterranean area: A Review. Archaeometry 62, 53–85. https://doi.org/10.1111/arcm.12542

Asael, D., Matthews, A., Bar-Matthews, M., Halicz, L., 2007. Copper isotope fractionation in sedimentary copper mineralization (Timna Valley, Israel). Chemical Geology, 243(3–4),

Asael, D., Matthews, A., Oszczepalski, S., Bar-Matthews, M., Halicz, L., 2009. Fluid speciation controls of low temperature copper isotope fractionation applied to the Kupferschiefer and Timna ore deposits. Chemical Geology 262(3–4), 147–158.

Babu, T.M., 1994. Tin in India. Geological Society of India, Bangalore.

Bachmann, H.-G., Jockenhövel, A., Spichal, U., Wolf, G., 2004. Zur bronzezeitlichen Metallversorgung im mittleren Westdeutschland: Von der Lagerstätte zum Endprodukt. Berichte der Kommission für Archäologische Landesforschung in Hessen 7 (2002/2003), 67–120.

Begemann, F., Schmitt-Strecker, S., Pernicka, E., Lo Schiavo, F., 2001. Chemical composition and lead isotopy of copper and bronze from Nuragic Sardinia. European Jorunal of Archaeology 4(1), 43–85.

Begemann, F., Kallas, K., Schmitt-Strecker, S., Pernicka, E., 1999. Tracing ancient tin via isotope analyses, in: Hauptmann, A., Pernicka, E., Rehren, T., Yalcin, Ü. (Eds.), The beginnings of metallurgy: Proceedings of the International Conference 'The Beginnings of Metallurgy', Bochum 1995, Der Anschnitt, Beiheft 9. Deutsches Bergbau-Museum, Bochum, pp. 277–284.

Berger, D., 2012. Bronzezeitliche Färbetechniken an Metallobjekten nördlich der Alpen: Eine archäometallurgische Studie zur prähistorischen Anwendung von Tauschierung und Patinierung anhand von Artefakten und Experimenten. Forschungsberichte des Landesmuseums für Vorgeschichte Halle 2. Landesmuseums für Vorgeschichte, Halle (Saale).

Berger, D., Figueiredo, E., Brügmann, G., Pernicka, E., 2018. Tin isotope fractionation during experimental cassiterite smelting and its implication for tracing the tin sources of prehistoric metal artefacts, Journal of Archaeological Science 92, 73–86.

Berger, D., Brügmann, G., Bunnefeld, J.-H., Pernicka, E., 2021. Identifying mixtures of metals by multi-isotope analysis: Disentangling the relationships of the Early Bronze Age swords of the Apa-Hajdúsámson type and associated objects. Archaeometry. https://doi.org/10.1111/arcm.12714

Berger, D., Brügmann, G., Pernicka, E., 2019. On smelting cassiterite in geological and archaeological samples: Preparation and implications for provenance studies on metal artefacts with tin isotopes, Archaeological and Anthropological Science 11(1), 293–319.

Berger, D., Soles, J.S., Giumlia-Mair, A.R., Brügmann, G., Lockhoff, N., Galili, E., Pernicka, E., 2019. Isotope systematics and chemical composition of tin ingots from Mochlos (Crete) and other Late Bronze Age sites in the eastern Mediterranean Sea: An ultimate key to tin provenance?, PLoS ONE 14(6), e0218326. https://doi.org/10.1371/journal.pone.0218326

Berger, D., Brügmann, G., Pernicka, A., forthcoming. Pyrometallurgy, corrosion and tin isotopes: Constraints for provenance research from experimental archaeology and isotopic analyses, in: Pernicka, E., Berger, D., Brügmann, G., Frank, C., Marahrens, J., Nessel, B. (Eds.), BRONZE AGE TIN: Geological sources, production, and distribution of tin in Bronze Age Eurasia. Proceedings of the international workshop held at the Reiss-Engelhorn-Museen in Mannheim, Germany, 14–16 March 2018. Forschungen zur Archäometrie und Altertumswissenschaft 7. Marie Leidorf GmbH, Rahden/Westf.

Boni, M., Köppel, V., 1985. Ore-lead isotope pattern from the Iglesiente-Sulcis Area (SW Sardinia) and the problem of remobilization of metals. Mineralium Deposita 20(3), 185–193.

Boni, M., Stein, H.J., Zimmermann, A., Villa, I.M., 2003. Re-Os age for molybdenite from SW Sardinia (Italy): A comparison with $^{40}Ar/^{39}Ar$ dating of Variscan granitoids, in: Eliopoulos, D. (Ed.), Mineral exploration and sustainable development: Proceedings of the seventh biennial SGA meeting on mineral exploration and sustainable development, Athens, Greece, August 24–28, 2003. Millpress, Rotterdam, pp. 247–250.

Bouscaras, A., Hugues, C., 1972. La cargaison des bronzes de Rochelongues (Agde, Hérault). Revue d'Études Ligures 33, 173–184.

Brandherm, D., Moskal-del Hoyo, M., 2014. Both sides now: The Carp's Tongue complex revisited. Antiquaries J. 94, 1–47.

Brandherm, D., 2017. Zyprische Griffangelklingen & Co. aus West- und Mitteleuropa? Noch einmal zur Problematik einer Quellengruppe der frühen und mittleren Bronzezeit, in:

Brandherm, D. (Ed.), Memento dierum antiquorum: Festschrift für Majolie Lenerz-de Wilde zum 70. Geburtstag. Curach Bhan, Hagen, pp. 45–70.

Carey, C., Jones, A.M., Allen, M.J., Juleff, G., 2019. The social organisation of metalworking in southern England during the Beaker period and Bronze Age: absence of evidence or evidence of absence? Internet Archaeology 52. https://doi.org/10.11141/ia.52.4

Cattin, F., Guénette-Beck, B., Curdy, P., Meisser, N., Ansermet, S., Hofmann, B., Kündig, R., Hubert, V., Wörle, M., Hametner, K., Günther, D., Wichser, A., Ulrich, A., Villa, I.M., Besse, M., 2011. Provenance of Early Bronze Age metal artefacts in western Switzerland using elemental and lead isotopic compositions and their possible relation with copper minerals of the nearby Valais. Journal of Archaeological Science 38, 1221–1233.

Cauuet, B., 2013. Les ressources métallifères du Massif Central et ses marges, in: Verger, S., Pernet, L. (Dir.), Une Odyssée gauloises: Parures de femmes à l'origine des premiers échanges entre la Grèce et la Gaule. Collection archéologie de Montpellier Agglomération 4. Editions Errance, Arles, pp.74–83.

Chicharro, E., Boiron, M.-C., López-García J.Á., Barfod, D.N., Villaseca, C., 2016. Origin, ore forming fluid evolution and timing of the Logrosán Sn–(W) ore deposits (Central Iberian Zone, Spain), Ore Geology Reviews 72(1), 896–913.

Clayton, R.E., 2001. Lead isotopes in cassiterite and tin metal: Further data and experimental results applied to the provenance of tin in antiquity, Revue d'Archéométrie 25, 79–86.

Colquhoun, I., Burgess, C., 1988. The swords of Britain. Prähistorische Bronzefunde IX, 5. Beck, Munich.

Craddock, P.T., 1988. The composition of the metal finds, in: Rothenberg, B. (Ed.), The Egyptian mining temple at Timna. Institute for Archaeo-Metallurgical Studies, London, pp. 169–181.

Craddock, P.T., 2000, From hearth to furnace: Evidences for the earliest metal smelting technologies in the Eastern Mediterranean, Paléorient, 26(2), 151–165.

Craddock, P.T., Meeks, N.D., 1987. Iron in ancient copper. Archaeometry 29(2), 187–204.

Del Moro, A., Di Simplicio, P., Ghezzo, C., Guasparri, G., Rita, F., Sabatini, G., 1975. Radiometric data and intrusive sequence in the Sardinian Batholith, Neues Jahrbuch für Mineralogie, Abhandlungen 126, 28–44.

Durali-Müller, S., 2005. Roman lead and copper mining in Germany: Their origin and development through time deduced from lead and copper isotopes provenance studies. PhD thesis University Frankfurt, Frankfurt. available from http://publikationen.ub.uni-frankfurt.de/frontdoor/index/index/docId/2824

Eogan, G. 1967. The associated finds of gold bar torcs. The Journal of the Royal Society of Antiquaries of Ireland 97, 129–175.

Eogan, G. 1994. The accomplished art: Gold and gold-working in Britain and Ireland during the Bronze Age (c. 2300–650 BCE), Oxford.

Faure, G., Mensing, T. M., 2005. Isotopes: Principles and applications. Wiley and Sons, Hoboken.

Figueiredo, E., Fonte, J., Lima, A., Veiga, J.P., Silva, R.J.C., Mirão, J., 2018. Ancient tin production: Slags from the Iron Age Carvalhelhos hillfort (NW Iberian Peninsula). Journal of Archaeological Science 93, 1–16.

Fox, A., 1957. Excavations on Dean Moor in the Avon valley 1954–1956: The late Bronze Age settlement. Transactions of the Devon Association 89, 18–77.

Fox, A., 1995. Tin ingots from Bigbury Bay, South Devon. Devon Archaeology Society Proceedings 53, 11–23.

Fox, A., 1996. Tin ingots from Bigbury Bay, South Devon. Mining History: Bull. Peak Dist. Mines Hist. Soc. 13 (2), 150–151.

Frotzscher, M., 2012. Geochemische Charakterisierung von mitteleuropäischen Kupfervorkommen zur Herkunftsbestimmung des Kupfers der Himmelsscheibe von Nebra. Forschungsberichte des Landesmuseums für Vorgeschichte Halle 1. Landesmuseum für Vorgeschichte, Halle (Saale).

Gale, N.H., 2005. Die Kupferbarren von Uluburun, T.2: Bleiisotopenanalysen von Bohrkernen aus den Barren, in: Yalçin, Ü., Pulak, C., Slotta, R. (Eds.), Das Schiff von Uluburun: Welthandel vor 3000 Jahren. Katalog der Ausstellung des Deutschen Bergbau-Museums Bochum vom 15. Juli 2005 – 16. Juli 2006, Veröffentlichungen aus dem Deutschen Bergbau-Museum 138. Deutsches Bergbau-Museum, Bochum, pp. 141–148.

Gale, N.H., Stos-Gale, Z.A., 2005. Zur Herkunft der Kupferbarren aus dem Schiffswrack von Uluburun und der spätbronzezeitliche Metallhandel im Mittelmeerraum, in: Yalçin, Ü., Pulak, C., Slotta, R. (Eds.), Das Schiff von Uluburun: Welthandel vor 3000 Jahren. Katalog der Ausstellung des Deutschen Bergbau-Museums Bochum vom 15. Juli 2005 - 16. Juli 2006, Veröffentlichungen aus dem Deutschen Bergbau-Museum 138. Deutsches Bergbau-Museum, Bochum, pp. 117–132.

Gale, N.H., Stos-Gale, Z.A., Maliotis, G., Annetts, N., 1997. Lead isotope data from the Isotrace Laboratory, Oxford: Archaeometry data base 4. Ores from Cyprus. Archaeometry 39(1), 237–246.

Gauß, R., 2015. Zambujal und die Anfänge der Metallurgie in der Estremadura (Portugal): Technologie der Kupfergewinnung, Herkunft des Metalls und soziokulturelle Bedeutung der Innovation. Früher Bergbau und Metallurgie auf der Iberischen Halbinsel, Faszikel 1. Iberia archaeologica 15, Tübingen.

Gerloff, S., 2010. Atlantic cauldrons and buckets of the Late Bronze Age and Early Iron Ages in Western Europe. Prähistorische Bronzefunde II, 18. Franz Steiner, Stuttgart.

Giumlia-Mair, A.R., Lo Schiavo, F., 2003. The problem of early tin: Acts of the XIVth UISPP Congress, University of Liège, Belgium, 2–8 September 2001. BAR International Series 1199, Oxford.

Goldmann, S., 2016. Mineralogical-geochemical characterisation of cassiterite and wolframite ores for an analytical fingerprint: Focus on trace element analysis by LA-ICP-MS, PhD thesis, Hannover.

Grant, M.R., 1999. The sourcing of southern African tin artefacts. Journal of Archaeological Science 26(8), 1111–1117.

Hamelin, B., Dupré, B., Brévart, O., Allègre, C.J., 1988. Metallogenesis at Paleo-spreading centers: Lead isotopes in sulfides, rocks and sediments from the Troodos Ophiolite (Cyprus). Chemical Geology 68(3–4), 229–238.

Harding, A., 2021. The movement of commodities in Europe, in: Rahmstorf, L., Barjamovic, G., Ialongo, N. (Eds.), Merchants, measures and money: Understanding technologies of early trade in a comparative perspective. Weight & value, Volume 2. Wachholtz Verlag, Kiel/Hamburg, pp. 127–140.

Hauptmann, A., Maddin, R., Prange, M., 2002. On the structure and composition of copper and tin ingots excavated from the shipwreck of Uluburun. Bulletin of the American Schools of Oriental Research 328, 1–30.

Hermann, R., Dolfini, A., Crellin, R.J., Wang, Q, Uckelmann, M., 2020. Bronze Age swordsmanship: New insights from experiments and wear analysis. Journal of Archaeological Method and Theory 27, 1040–1083.

Huelga-Suarez, G., Moldovan, M., Suárez Fernández, M., De Blas Cortina, M.A., Vanhaecke, F., García Alonso, J.I., 2012. Lead isotopic analysis of copper ores from the Sierra El Aramo (Asturias, Spain). Archaeometry 54(4), 685–697.

Huelga-Suarez, G., Moldovan, M., Suárez Fernández, M., De Blas Cortina, M.A., García Alonso, J.I., 2014. Isotopic composition of lead in copper ores and copper artefacts from the La Profunda mine (León, Spain). Archaeometry 56(4), 651–664.

Hugues, C., 1965. La découverte sous-marine de Rochelongue, Agde (Hérault). Comptes rendus des séances de l'Académie des Inscriptions et Belles-Lettres 109, 176–178.

Ialongo, N., 2018. The earliest balance weights in the west: Towards an independent metrology for Bronze Age Europe. Cambridge Archaeological Journal 29, 103–124.

Ialongo, N., 2019. The earliest balance weights in the West: Towards an independent metrology for bronze Age Europe. Cambridge Archaeological Journal 29, 103–124.

Ialongo, N., Hermann, R., Rahmstorf, L., 2021. Bronze Age weight systems as a measure of market integration in Western Eurasia. Proceedings of the National Academy of Sciences, 118(27), e2105873118. DOI: 10.1073/pnas.2105873118.

Ialongo, N., Lago, G., 2021. A small change revolution: Weight systems and the emergence of the first Pan-European money. Journal of Archaeological Science 129, 105379. DOI:10.1016/j.jas.2021.105379

Ixer, R.A., Budd, P., 1998. The mineralogy of Bronze Age copper ores from the British Isles: Implications for the composition of early metalwork. Oxford Journal of Archaeology 17(1), 15–41.

Ixer, R.A., Vaughan, D.J., 1982. The primary ore mineralogy of the Alderley Edge deposit, Cheshire. Mineralogical Magazine 46, 485–492.

Jackson, N.J., Willis-Richards, J., Manning, D.A.C., Sams, M.S., 1989. Evolution of the Cornubian Ore Field, Southwest England: Part II, Mineral deposits and ore-forming processes, Economic Geology 84(5), 1101–1133.

Jansen, M., Hauptmann, A., Klein, S., Seitz, H.-M., 2018. The potential of stable Cu isotopes for the identification of Bronze Age ore mineral sources from Cyprus and Faynan: Results from Uluburun and Khirbat Hamra Ifdan. Archaeological and Anthropological Sciences 10, 1485–1502.

Joel, E.C., Taylor, T., Ixer, R.A., Goodway, M., 1997. Lead isotope analysis and the Great Orme mine, in: Sinclair, A., Slater, E., Gowlett, J. (Eds.), Archaeological sciences 1995, Oxford: Proceedings of a conference on the application of scientific techniques to the study of archaeology, Liverpool, July 1995. Oxbow monograph 64. Oxbow, Oxford. pp. 129–137.

Jones, A.M., Gossip, J., Quinnell, H., 2016. Meet the smiths: Bronze Age settlement in Tremough, Cornwall. British Archaeology 146, 24–29.

Juleff, G., Bray, L., 2007. Minerals, metal, colours and landscape: Exmoor's Roman Lode in the Early Bronze Age. Camb. Archaeol. J. 17(3), 285–296.

Kinnaird, J.A., Ixer, R.A., Barreiro, B., Nex, P.A.M., 2002. Contrasting sources for lead in Cu-polymetallic and Zn-Pb mineralisation in Ireland: Constraints from lead isotopes. Mineralium Deposita 37(5), 495–511.

Klein, S., Domergue, C., Lahaye, Y., Brey, G.P., von Kaenel, H.-M., 2009. The lead and copper isotopic composition of copper ores from the Sierra Morena (Spain). Journal of Iberian Geology 35(1), 59–68.

Klein, S., Brey, G.P., Durali-Müller, S., Lahaye, Y., 2010. Characterisation of the raw metal sources used used for the production of copper and copper-based objects with copper isotopes. Archaeological and Anthropological Journal 2(1),45–56.

Klein, S., Rose, T., 2020. Evaluating copper isotope fractionation in the metallurgical operational chain: An experimental approach. Archaeometry 62(S1), 134–155.

Kuijpers, M.H.G., Popa, C.N., Biehl, P.F., 2021. The origins of money: Calculation of similarity indexes demonstrates the earliest development of commodity money in prehistoric Central Europe. PLoS ONE, 16(1), e0240462. DOI:10.1371/journal.pone.0240462

Larson, P.B., Maher, K., Ramos, F.C., Chang, Z., Gaspar, M., Meinert, L.D., 2003. Copper isotope ratios in magmatic and hydrothermal ore-forming environments. Chemical Geology 201(3–4), 337–350.

Le Carlier de Veslud, C., Edme, M., Fily, M., 2014. Lingots et déchets de fonderie dans les dépôts de l'horizon de l'épée à pointe en langue de carpe (Bronze final IIIb): Proposition de typologie. Bulletin de la Societé Préhistorique Française 111(3), 509–522.

Le-Carlier de Veslud, C., Siepi, C., Le-Carlier de Veslud, C., 2017. Tin production in Brittany (France): A rich area exploited since Bronze Age, in: Montero-Ruiz, I., Perea, A. (Eds.), Archaeometallurgy in Europe IV. Consejo Superior de Investigaciones Científicas, Madrid, pp. 91–103.

Lehmann, B, Zoheir, B., Neymark, L., Zeh, A., Emam, A., Radwan, A., Zhang, R., Moscati, R., 2020, Monazite and cassiterite UPb dating of the Abu Dabbab rare-metal granite, Egypt: Late Cryogenian metalliferous granite magmatism in the Arabian-Nubian Shield. Gondwana Research 84, 71–80.

Lerouge, C., Gloaguen, E., Wille, G., Bailly, L., 2017. Distribution of In and other rare metals in cassiterite and associated minerals in Sn ± W ore deposits of the western Variscan Belt. European Journal of Mineralogy 29(4), 739–753.

Lévêque, J., Haack, U., 1993. Lead isotopes of hydrothermal ores in the Harz. Monograph Series on Mineral Deposits 30, 197–210.

Ling, Johan; Hjärthner-Holdar, Eva; Grandin, Lena; Stos-Gale, Zofia; Kristiansen, Kristian; Melheim, Anne Lene; Artioli, Gilberto; Angelini, Ivana; Krause, Rüdiger; Canovaro, Caterina

Ling, J., Hjärthner-Holdar, E., Grandin, L., Billström, L., Persson, P-O., 2013. Moving metals or indigenous mining? Provenancing Scandinavian Bronze Age artefacts by lead isotopes and trace elements. Journal of Archaeological Science 40(1), 291–304.

Ling, J., Stos-Gale, Z., Grandin, L., Billström, L., Hjärthner-Holdar, E., Persson, P-O., 2014. Moving metals II: Provenancing Scandinavian Bronze Age artefacts by lead isotope and elemental analyses. Journal of Archaeological Science 41(1), 126–132.

Ling, J., Hjärthner-Holdar, E., Grandin, L., Stos-Gale, Z., Kristiansen, K., Melheim, A.L., Artioli, G., Angelini, I., Krause, R., Canovaro, C., 2019. Moving metals IV: Swords, metal sources and trade networks in Bronze Age Europe. Journal of Archaeological Science: Reports 26, 101837.

Lo Schiavo, F., Sabatini, S., 2020. Late Bronze Age metal exploitation and trade: Sardinia and Cyprus. Material and Manufacturing Processes 35(13), 1501–1518. DOI:10.1080/10426914.2020.1758329

Ludington, S.D., Peters, S.G., 2007. Tin and tungsten deposits, in: Peters, S.G., Ludington, S.D., Orris, G.J., Sutphin, D.M., Bliss, J.D., Rytuba, J.J. (Eds.), Preliminary non-fuel mineral resource assessment of Afghanistan 2007, USGS Open-File Report, vol. 2007–1214. U.S.

Geological Survey, Reston, pp. 106–117. Available from: https://pubs.usgs.gov/of/2007/1214/

Maddin, R., 1998. Early metallurgy: The tin mystery, in: Proceedings of the fourth international conference on the beginning of the use on metals and alloys (BUMA-IV): May 25–27, 1998, Kunibiki Messe, Matsue, Shimane, Japan, Matsue. pp. 1–4.

Malham, A., 2010. The classification and interpretation of tin smelting remains from South West England: A study of the microstructure and chemical composition of tin smelting slags from Devon and Cornwall, and the effect of technological developments upon the character of slags. Unpublished PhD thesis, University of Bradford.

Mahé-Le Carlier, C., Lulzac, Y., Giot, P.R., 2001. Etude des déchets de réduction provenant de deux sites d'exploitation d'étain armoricain de l'âge du Bronze et du Moyen Age, Revue Archéologique de l'Ouest 18, 45–56.

Maher, K.C., 2005, Analysis of copper isotope ratios by multi-collector inductively coupled plasma mass spectrometry and interpretation of copper isotope ratios from copper mineralization. Phd thesis. Washington State University.

Marahrens, J., forthcoming. Tin isotope analysis of tin ore deposits in Europe and Central Asia in view of the tin provenance in archaeological metal objects. PhD thesis University Heidelberg.

Marahrens, J., Berger, D., Brügmann, G., Pernicka, E., 2016. Vergleich der stabilen Zinn-Isotopenzusammensetzung von Kassiteriten aus europäischen Zinn-Lagerstätten, in: Greiff, S., Kronz, A., Schlütter, F., Prange, M. (Eds.), Archäometrie und Denkmalpflege 2016: Jahrestagung an der Georg-August-Universität Göttingen, 28. September bis 1. Oktober 2016. Metalla, Sonderheft 8. Deutsches Bergbau-Museum, Bochum. pp. 190–193.

Marahrens, J. Brügmann, G., Berger, D., forthcoming. Tin isotopic composition of tin ore deposits in Europe, in: Pernicka, E., Berger, D., Brügmann, G., Frank, C., Marahrens, J., Nessel, B. (eds.), BRONZE AGE TIN: Geological sources, production, and distribution of tin in Bronze Age Eurasia. Proceedings of the international workshop held at the Reiss-Engelhorn-Museen in Mannheim, Germany, 14–16 March 2018. Forschungen zur Archäometrie und Altertumswissenschaft 7. Marie Leidorf GmbH, Rahden/Westf.

Marcoux, E., 1998. Lead isotope systematics of the giant massive sulphide deposits in the Iberian Pyrite Belt. Mineralium Deposita 33(1–2), 45–58.

Maréchal, C.N., Télouk, P., Albarède, F., 1999. Precise analysis of copper and zinc isotopic compositions by plasma-source mass spectrometry. Chemical Geology 156(1-4), 251–273.

Marignac, C., Cuney, M., 1999. Ore deposits of the French Massif Central: Insight into the metallogenesis of the Variscan collision belt, Mineralium Deposita 34(5–6), 472–504.

Markl, G., Lahaye, Y., Schwinn, G., 2006. Copper isotopes as monitors of redox processes in hydrothermal mineralization. Geochimica et Cosmochimica Acta 70(16), 4215–4228.

Mason, A.H., Powell, W.G., Bankoff, H.A., Mathur, R., Price, M., Bulatovic, A., Filipovic, V. 2020. Provenance of tin in the Late Bronze Age balkans based on probabilistic and spatial analysis of Sn isotopes. Journal of Archaeological Science 122, 105181.

Mathur, R., Ruiz, J., Titley, S., Liermann, L., Buss, H., Brantley, S., 2005. Cu isotopic fractionation in the supergene environment with and without bacteria. Geochimica et Cosmochimica Acta 69(22), 5233–5246.

Mathur, R., Titley, S., Barra, F., Brantley, S., Wilson, M., Phillips, A., Munizaga, F., Maksaev, V., Vervoort, J., Hart, G., 2009. Exploration potential of Cu isotope fractionation in porphyry copper deposits. Journal of Geochemical Exploration 102(1), 1–6.

Mathur, R., Falck, H., Belogub, E., Milton, J., Wilson, M., Rose, A., Powell, W., 2018. Origins of chalcocite defined by copper isotope values. Geofluids 2018, 1–9.

Melcher, F., Graupner, T., Gäbler, H.-E., Sitnikova, M., Henjes-Kunst, F., Oberthür, T., Gerdes, A., Dewaele, S., 2015. Tantalum-(niobium-tin) mineralisation in African pegmatites and rare metal granites: Constraints from Ta-Nb oxide mineralogy, geochemistry and U-Pb geochronology, Ore Geology Reviews 64, 667–719.

Melheim, A.L., Grandin, L., Persson, P.-O., Billström, K., Stos-Gale, Z., Ling, J., Williams, A., Angelini, I., Canovaro, C., Hjärthner-Holdar, E., Kristiansen, K., 2018. Moving metals III: Possible origins for copper in Bronze Age Denmark basedon lead isotopes and geochemistry. Journal of Archaeological Science 96, 85–105.

Merideth, C., 1998. La Mina El Cerro de San Cristobal. Papers from the Institute of Archaeology 9, 57–69.

Miles, H., 1975, Barrows on the St Austell Granite, Cornwall, Cornish Archaeology 14, 5–81.

Molofsky, L.J., Killick, D., Ducea, M.N., Macovei, M., Chesley, J.T., Ruiz J., Thibodeau A., Popescu, G.C., 2014. A novel approach to lead isotope provenance studies of tin and bronze: Applications to South African, Botswanan and Romanian artifacts. J. Archaeol. Sci. 50, 440–450.

Montero Ruiz, I., Murillo-Barroso, M., 2010. La producción metalúrgica en las sociedades argáricas y sus implicaciones sociales: Una propuesta de investigación. Menga, Revista de Prehistoria de Andalucía 1, 37–52.

Moscati, R.J., Neymark, L.A, 2019. U–Pb geochronology of tin deposits associated with the Cornubian Batholith of southwest England: Direct dating of cassiterite by in situ LA-ICPMS, Mineralium Deposita. Available from: https://doi.org/10.1007/s00126-019-00870-y.

Muckelroy, K., 1980. Two Bronze Age cargoes in British waters. Antiquity 54, 100–109.

Muckelroy, K., 1981. Middle Bronze Age trade between Britain and Europe: A maritime perspective. Proc. Prehist. Soc. 47, 275–298.

Muhly, J.D., 1973. Copper and tin: The distribution of mineral resources and the nature of the metals trade in the Bronze Age. Transactions of the Connecticut Academy of Arts and Sciences 43. Academy of Arts and Sciences, Hamden.

Muhly, J.D., 1985. Sources of tin and the beginnings of bronze metallurgy. American Journal of Archaeology 89(2), 275–291.

Murillo-Barroso, M., Montero-Ruiz, I., Nieto, J.M., Camalich Massieu, M.D., Martín Socas, D., Martinón-Torres, M., 2019. Trace elements and lead isotopic composition of copper deposits from the eastern part of the Internal Zone of the Betic Cordillera (SE Iberia): Application to provenance of archaeological materials. Journal of Iberian Geology 45, 585–608.

Needham, S. 2017. Transmanche in the Penard/Rosnoën stage. Wearing the same sleeve or keeping at arm's length?, in Lehoërff, A., Talon, M. (Eds.), Movement, exchange and identity in Europe in the 2nd and 1st millennia BCE: Beyond frontiers. Oxbow, Oxford, pp. 31–48.

Needham, S., Giardino, C., 2008. From Sicily to Salcombe: A Mediterranean Bronze Age object from British coastal waters. Antiquity 82, 60–72.

Needham, S., Parham, D., Frieman, C.J., 2013. Claimed by the Sea: Salcombe, Langdon Bay, and other marine finds of the Bronze Age, CBA Research Report 173. Council for British Archaeology, York.

Neiva, A.M.R., 2008. Geochemistry of cassiterite and wolframite from tin and tungsten quartz veins in Portugal, Ore Geology Reviews 33(3–4), 221–238.

Niederschlag, E., Pernicka, E., Seifert, T., Bartelheim, M., 2003. The determination of lead isotope ratios by multiple ICP-MS: A case study of Early Bronze Age artefacts and their possible relation with ore deposits of the Erzgebirge. Archaeometry 45(1), 61–100.

Nier, A.O., Thompson, R.W., Murphy, B.F., 1941. The isotopic constitution of lead and the measurement of geological time III, Physical Review 60(2), 112–116.

Neymark, L.A., Holm-Denoma, C.S., Moscati, R.J., 2018. In situ LA-ICPMS U-Pb dating of cassiterite without a known-age matrix-matched reference material: Examples from worldwide tin deposits spanning the Proterozoic to the Tertiary. Chemical Geology 483, 410–425.

Nørgaard, H.W., Pernicka, E., Vandkilde, H., 2019. On the trail of Scandinavia's early metallurgy: Provenance, transfer and mixing. PLoS ONE 14(7), e0219574.

Nørgaard, H.W., Pernicka, E., Vandkilde, H., 2021. Shifting networks and mixing metals: Changing metal trade routes to Scandinavia correlate with Neolithic and Bronze Age transformations. PLoS ONE 16, 1–42. https://doi.org/10.1371/journal.pone.0252376

Northover, J.P., 1982. The exploration of the long distance movement of bronze in Bronze and Early Iron Age Europe. Bulletin of the Institute of Archaeology 19, 45–72.

Northover, J.P., 1989. The gold torc from Saint Helier, Jersey. Annual Bulletin of the Société Jersiaise 25, 112–137.

Northover, J.P., 2013. Metal analyses, in: Needham, S., Parham, D., Frieman, C.J., Claimed by the Sea: Salcombe, Langdon Bay, and other marine finds of the Bronze Age, CBA Research Report 173. Council for British Archaeology, York, pp. 101–112.

Northover, J.P., Gillis, C., 1999. Questions in the analysis of ancient tin, in: Young, S.M., Pollard, A.M., Budd, P., Ixer, R.A. (Eds.), Metals in antiquity, BAR International Series 792. BAR Publishing, Oxford, pp. 78–85.

O'Brien, W., 2015. Prehistoric copper mining in Europe: 5500–500 BCE. Oxford University Press, Oxford.

Pavlova, G.G., Borisenko, A.S., 2009. The age of Ag-Sb deposits of central Asia and their correlation with other types of ore systems and magmatism, Ore Geology Reviews 35(2), 164–185.

Penhallurick R.D. 1986. Tin in antiquity, its mining and trade throughout the ancient world with particular reference to Cornwall. Institute of Metals, London.

Penhallurick, R.D., 1997. The evidence for prehistoric mining in Cornwall, in: P. Budd, D. Gale (Eds.), Prehistoric extractive metallurgy in Cornwall. Cornwall County Council, Truro, 1997, pp. 23–34.

Pernicka, E., Lutz, J., Stöllner, T., 2016. Bronze Age copper produced at Mitterberg, Austria, and its distribution. Archaeologia Austriaca 100, 19–55.

Pigott, V.C., 1999, The archaeometallurgy of the Asian old world. MASCA research papers in science and archaeology 16. University Museum, University of Pennsylvania, Philadelphia.

Pigott, V.C., 2011. Sources of tin and the tin trade in southwest Asia: Recent research and its relevance to current understanding, in Betancourt, P.P., Ferrence, S.C. (Eds.) Metallurgy: Understanding how, learning why. Studies in honor of James D. Muhly, INSTAP Academic Press, Philadelphia, pp. 273–291.

Poigt, T., Comte, F., Adam, A., 2021. How accurate was Bronze Age weighing in Western Europe?. Journal of Archaeological Science: Reports 40, 103221. DOI:10.1016/j.jasrep.2021.103221

Pollard, A.M., Bray, P.J., 2015. A new method for combining lead isotope and lead abundance data to characterize archaeological copper alloys. Archaeometry 57(6), 996–1008.

Powell, W., Mathur, R., Bankoff, H.A, Mason, A., Bulatovi, A., Filipovi, V., Godfrey, L., 2018. Digging deeper: Insights into metallurgical transitions in European prehistory through copper isotopes. Journal of Archaeological Science 88, 37–46.

Powell, W., Johnson, M., Pulak, C., Yener, K.A., Mathur, R., Bankoff, H.A., Godfrey, L., Price, M., Galili, E., 2021. From peaks to ports: Insights into tin provenance, production, and

distribution from adapted applications of lead isotopic analysis of the Uluburun tin ingots. Journal of Archaeological Science 134, 105455. https://doi.org/10.1016/j.jas.2021.105455

Radivojević, M., Roberts, B.W., Pernicka, E., Stos-Gale, Z., Martinón-Torres, M., Rehren, T., Bray, P., Brandherm, D., Ling, J., Mei, J., Vandkilde, H., Kristiansen, K., Shennan, S.J., Broodbank, C., 2019. The provenance, use, and circulation of metals in the European Bronze Age: The state of debate. Journal of Archaeological Research 27, 131–185.

Rahmstorf, L., 2019. Scales, weights and weight-regulated artefacts in Middle and Late Bronze Age Britain. Antiquity 93, 1197–1210.

Raimbault, L., Alexandrov, P., Nong, L.X., 1999. Behaviour of indium and gallium in hydrothermal cassiterites, in: Stanley, C.J. et al. (Eds.), Mineral Deposits: Processes to Processing. A.A. Balkema, Rotterdam, pp. 421–424.

Rapp, G., 1978. Trace element as a guide to the geographical source of tin ore: Smelting experiments, in: A.D. Franklin, J.S. Olin, T.A. Wertime (Eds.), The search for ancient tin. U. S. Government Printing Office, Washington D.C., pp. 59–63.

Rapp, G., Rothe, R., Jing, Z., 1999. Using neutron activation analysis to source ancient tin (cassiterite), in: Young, S.M., Pollard, A.M., Budd, P., Ixer, R.A. (Eds.), Metals in antiquity, BAR International Series 792. BAR Publishing, Oxford, pp. 153–162.

Rizvanova, N.G., Skublov, S.G., Cheremazova, E.V., 2017. Age of hydrothermal processes in the central Iberian Zone according to U-Pb dating of cassiterite and apatite, Journal of Mining Institute 225, 275–283.

Rodríguez Díaz, A., Pavon Soldevilla, I., Merideth, C., Tresserras, J.J.I., 2001. El Cerro de San Cristóbal, Logrosán, Extremedura, Spain: The archaeometallurgical excavation of a Late Bronze Age tin-mining and metalworking site. First excavation season 1998. BAR International Series 922. BAR Publishing, Oxford.

Rodríguez Díaz, A., Pavón, I., Duque Espino, D.M., 2019. La explotación tartésica del estaño en San Cristóbal de Logrosán (Cáceres, España): Arqueología y recuperación de un paisaje minero. BAR International Series 2944. BAR Publishing, Oxford.

Rohl, B.M., 1995. Application of lead isotope analysis to Bronze Age metalwork from England and Wales. PhD Thesis, Oxford University, Oxford.

Rohl, B.M., 1996. Lead isotope data from the Isotrace Laboratory, Oxford: Archaeometry data base 2. Galena from Britain and Ireland. Archaeometry 38(1), 165–180.

Rohl, B.M., Needham, S., 1998. The circulation of metal in the British Bronze Age: The application of lead Isotope analysis. Occasional Paper 102. British Museum, London.

Romer, R.L., Thomas, R., Stein, H.J., Rhede, D., 2007. Dating multiply overprinted Sn-mineralized granites: Examples from the Erzgebirge, Germany, Mineralium Deposita 42(4), 337–359.

Rohl, B.M., Northover, P., 1994. The metalwork from Flag Fen. Historical Metallurgy 18(2), 103–111.

Rouxel, O., Fouquet, Y., Ludden, J., 2004. Copper isotope systematics of the Lucky Strike, Rainbow, and Logatchev sea-floor hydrothermal fields on the mid-atlantic ridge. Economic Geology 99(3), 585–600.

Sabatini, S., 2016. Late Bronze Age oxhide and oxhide-like ingots from areas other than the Mediterranean: Problems and challenges. Oxford Journal of Archaeology 35, 29–45.

Sabatini, S., 2016. Revisiting Late Bronze Age copper oxhide ingots: Meanings, questions and perspectives, in: Aslaksen, O.C. (Ed.), Local and global perspectives on mobility in the Eastern Mediterranean. Norwegian Institute in Athens, Athens, pp. 15–62.

Santos Zalduegui, J.F., García de Madinabeitia, S., Gil Ibarguchi, J.I., and Palero, F., 2004. A lead isotope database: The Los Pedroches–Alcudia area (Spain). Implications for archaeometallurgical connections across southwestern and southeastern Iberia. Archaeometry 46(4), 625–634.

Schreiner, M., 2007. Erzlagerstätten im Hrontal, Slowakei: Genese und prähistorische Nutzung. Forschungen zur Archäometrie und Altertumswissenschaft 3. Marie Leidorf, Rahden/Westfalen.

Schwarz-Schampera, U., Herzig, P.M., 2002. Indium: Geology, Mineralogy, and Economics. Springer Verlag, Berlin.

Seifert, T., Sandmann, D., 2006. Mineralogy and geochemistry of indium-bearing polymetallic vein-type deposits: Implications for host minerals from the Freiberg district, Eastern Erzgebirge, Germany, Ore Geology Reviews 28(1), 1–31.

Stos, Z.A., 2009. Across the wine dark seas... Sailor tinkers and royal cargoes in the Late Bronze Age eastern Mediterranean, in: Shortland, A.J., Freestone, I.C., Rehren, T. (Eds.), From mine to microscope: Advances in the study of ancient technology. Oxbow Books, Oxford, pp. 163–180.

Stos-Gale, Z.A., Gale, N.H., Houghton, J., Speakman, R., 1995. Lead isotope data from the Isotrace Laboratory, Oxford: Archaeometry data base 1. Ores from the Western Mediterranean. Archaeometry 37(2), 407–415.

Stos-Gale, Z.A., Gale, N.H., Bass, G., Pulak, C., Galili, E., Sharvit, J., 1998, The copper and tin ingots of the Late Bronze Age Mediterranean: New scientific evidence, in: The fourth international conference on the beginning of the use on metals and alloys (BUMA-IV), May 25–27, 1998 Kunibiki Messe, Matsue, Shimane, Japan. pp. 115–126.

Timberlake, S., 2003. Excavations on Copa Hill, Cwmystwyth (1986–1999): An Early Bronze Age copper mine within the Uplands of Central Wales. BAR British Series 348, Archaeopress, Oxford.

Timberlake, S., 2009. Copper mining and metal production at the beginning of the British Bronze Age, in P. Clark (Ed.), Bronze Age Connections. Oxbow, Oxford. pp. 95–122.

Timberlake, S., 2014. Prehistoric copper extraction in Britain: Ecton Hill, Staffordshire. Proceedings of the Prehistoric Society 80, 159–206.

Timberlake, S., 2017. New ideas on the exploitation of copper, tin, gold, and lead ores in Bronze Age Britain: The mining, smelting, and movement of metal. Materials and Manufacturing Processes 32(7–8), 709–727.

Timberlake, S., Hartgroves, S., 2018. New evidence for Bronze Age tin and gold mining in Cornwall: the date of the antler pick from the Carnon valley streamworks, Devoran, near Truro. Cornish Archaeology 57, 107–122.

Timberlake, S., King, C., 2005. Archaeological excavations at Engine Vein, Alderley Edge, 1997, in: Timberlake, S., Prag, A. (Eds.), The archaeology of Alderley Edge: Survey, excavation, and experiment in an Ancient Mining Landscape. BAR British Series 396, John Hedges, Oxford. pp. 33–57.

Timberlake, S., Marshall, P., 2014. The beginnings of metal production in Britain: A new light on the exploitation of ores and the dates of Bronze Age mines. Historical Metallurgy 47(1), 75–92.

Timberlake, S., Marshall, P., 2018. Copper mining and smelting in the British Bronze Age: New evidence of mine sites including some re-analysis of dates and ore sources, in: Ben-Yosef, E. (Ed.), Mining for ancient copper: Essays in memory of Beno Rothenberg, Monograph Series 37. Eisenbrauns, Winona Lake. pp. 418–431.

Timberlake, S., Prag, A., 2005. The archaeology of Alderley Edge: Survey, excavation, and experiment in an Ancient Mining Landscape. BAR British Series 396, John Hedges, Oxford.

Tolksdorf, J.F., Schröder, F., Petr, L., Herbig, C., Kaiser, K., Kočár, P., Fülling, A., Heinrich, S., Hönig, H., Hemker, C., 2019. Evidence for Bronze Age and Medieval tin placer mining in the Erzgebirge mountains, Saxony (Germany), Geoarchaeology. DOI: 10.1002/gea.21763

Tylecote, R.F., 1976. Properties of copper ingots of Late Bronze Age type. In: Mitscha-Märheim, H., Friesinger, H., Kerchler, H. (Eds.), Festschrift für Richard Pittioni zum siebzigsten Geburtstag, Volume 2. Archaeologia Austriaca, Beiheft 14. Deuticke, Vienna. pp. 157–172.

Tylecote, R.F., Photos, E., Earl, B., 1989. The composition of tin slags from the Southwest of England. World Archaeology 20(3), 434–445.

Uckelmann, M., 2012. Die Schilde der Bronzezeit in Nord-, West- und Zentraleuropa. Prähistorische Bronzefunde III, 4. Steiner, Stuttgart.

Vandkilde, H., Northover, P., Becker, K., Stos-Gale, Z., 2017. The Metal Hoard from Pile in Scania, Sweden: Place, things, time, metals, and worlds around 2000 BCEE. The Swedish History Museum Studies and Aarhus University Press, Aarhus.

Valera, R.G., Valera, P.G., 2003. Tin in the Mediterranean area: History and geology, in: Giumlia-Mair, A., Lo Schiavo, F. (Eds.), The problem of early tin: Acts of the XIVth UISPP

Congress, University of Liège, Belgium, 2–8 September 2001, BAR International Series 1199. BAR Publishing, Oxford. pp. 3–14.

Velasco, F., Pesquera, A., Herrero, J.M., 1996. Lead isotope study of Zn-Pb ore deposits associated with the Basque-Cantabrian basin and Paleozoic basement, Northern Spain. Mineralium Deposita 31(1–2), 84–92.

Wang, Q., Strekopytov, S., Roberts, B.W., Wilkin, N., 2016. Tin ingots from a probable Bronze Age shipwreck off the coast of Salcombe, Devon: Composition and microstructure. J. Archaeol. Sci. 67, 80–92.

Wang, Q., Strekopytov, S., Roberts, B.W., 2018. Copper ingots from a probable Bronze Age shipwreck off the coast of Salcombe, Devon: Composition and microstructure. J. Archaeol. Sci. 97, 102–117.

Warner, R.B., Moles, N.R., 2015. Radiocarbon-dated charcoal from fluvial sediments in the Mourne Mountains, Northern Ireland: Neolithic forest clearance and tin and gold recovery in the Early Bronze Age? The Journal of Irish Archaeology Volume 24, 97–114.

Warner, R.B., Moles, N.R., Chapman, R., 2015. Evidence for Early Bronze Age tin and gold extraction in the Mourne Mountains, County Down. Journal of the Mining Heritage Trust of Ireland 10, 20–36.

Wedepohl, K.H., Delevaux, M.H., Doe, B.R., 1978. The potential source of lead in the Permian Kupferschiefer bed of Europe and some selected Paleozoic mineral deposits in the Federal Republic of Germany. Contributions to Mineralogy and Petrology 65(3), 273–281.

Werner, T.T., Mudda, G.M., Jowitt, S.M., 2017. The world's by-product and critical metal resources part III: A global assessment of indium, Ore Geology Reviews 86, 939–956.

Williams, R.A., 2013. Linking Bronze Age copper smelting slags from Pentrwyn on the Great Orme to ore and metal. Historical Metallurgy 47(1), 93–110.

Williams, R.A., 2017. The Great Orme Bronze Age copper mine: Linking ores to metals by developing a geochemically and isotopically defined mined-based metal group metallurgy, in: Montero-Ruiz, I., Perea, A. (Eds.), Archaeometallurgy in Europe IV. Consejo Superior de Investigaciones Científicas, Madrid. pp. 29–47.

Williams, R.A., Le Carlier de Veslud, C., 2019. Boom and bust: Major copper production in Bronze Age Britain from the Great Orme mine and European trade c.1600–1400 BCE. Antiquity 93, 1178–1196.

Willis-Richards, J., Jackson, N.J., 1989. Evolution of the Cornubian Ore Field, Southwest England: Part I, Mineral deposits and ore-forming processes, Economic Geology 84(5), 1078–1100.

Woodhead, A.P., Gale, N.H., Stos-Gale, Z.A., 1999. An investigation into the fractionation of copper isotopes and its possible application to archaeometallurgy, in: Young, S.M.M.,

Pollard, A.M., Budd, P., Ixer, R.A. (Eds.), Metals in antiquity, BAR International Series 792. BAR Publishing, Oxford. pp. 134–139.

Xu, J., Cook, N.J., Ciobanu, C.L., Kontonikas-Charos, A., Gilbert, S., Lv, Y., 2021, Indium distribution in sphalerite from sulfide-oxide-silicate skarn assemblages: A case study of the Dulong Zn-Sn-In deposit, Southwest China, Mineralium Deposita 56, 307–324.

Yalçın, Ü., Pulak, C., Slotta, R., 2005. Das Schiff von Uluburun: Welthandel vor 3000 Jahren. Katalog der Ausstellung des Deutschen Bergbau-Museums Bochum vom 15. Juli 2005 bis 16. Juli 2006, Deutsches Bergbau-Museum, Bochum.

Zhang, R., Lehmann, B., Seltmann, R., Sun, W., Li, C., 2017. Cassiterite U-Pb geochronology constrains magmatic-hydrothermal evolution in complex evolved granite systems: The classic Erzgebirge tin province (Saxony and Bohemia), Geology 45(12), 1095–1098.

Captions

Fig. 1

Map of Great Britain and Ireland with the locations and copper/lead mines mentioned in the text (green). Additional mines are the yellow dots; red shaded areas are tin mineralisation. 1 – Moor Sand and Salcombe B, 2 – Erme Estuary (Bigbury Bay), 3 – Dean Moor, 4 – Caerloggas Downs, 5 – Trevisker, 6 – Tremough, 7 – Carrigacat, 8 – Ross Island, 9 – Derrycarhoon, 10 – Mount Gabriel, 11 – Toormore, 12 – Ballyrisode Hill, 13 – Boulysallagh, 14 – Callaros Oughter, 15 – Tooreen, 16 – Canshanavoe, 17 – Crumpane, 18 – Reentrusk, 19 – Coad Mountain, 20 – Parys Mountain, 21 – Great Orme, 22 – Park Lodge (Ogof Wyddon), 23 – Nantyreira, 24 – Copa Hill (Cwmystwyth), 25 – Grogwynion, 26 – Tyn-y-fron, 27 – Twll-y-mwyn, 28 – Erglodd, 29 – Pwll Roman, 30 – Llangynfelyn, 31 – Balkan Hill, 32 – Panteidal, 33 – Alderley Edge, 34 – Ecton, 35 – Isle of Man, 36 – Exmoor, 37 – Mendip Hills, 38 – Tregurra Farm; C/D – large tin mineralisation in Cornwall and Devon, M – minor tin mineralisation in the Mourne Mountains, North Ireland (map: D. Berger, C. Frank after information in O'Brien, 2015; ApSimon and Greenfield, 1972; Carey et al., 2019; Fox, 1957; Jones et al., 2016; Miles, 1975; Penhallurick, 1997; Timberlake and Marshall, 2018; Warner et al., 2015; Warner and Moles, 2015).

Fig. 2

Selection of copper and tin ingots from the Salcombe B site (photo: © Southwest Maritime Archaeology Group).

Fig. 3

Middle Bronze Age swords/rapiers (a), palstave axes (b) and weights (c) found in the bay of Salcombe (Moor Sand and Salcombe B sites). Some of the objects examined in this study are labelled with their original and CEZA laboratory numbers, also tabulated in Table 1 (photo: after Wang et al., 2016, Fig. 2, © the British Museum Trustees).

Fig. 4

Lead isotopic composition ($^{206}Pb/^{204}Pb$ vs. $^{207}Pb/^{204}Pb$) of the Salcombe tin ingots and comparison with the tin ingots found off the coast of Israeli, at Vårdinge and Flag Fen (a). The black solid isochron (and the black formula) refers to the material from Salcombe, while the grey dotted line (and formula) derives from the Israeli ingots. The tin isotopic composition (δSn, 2SD) of the tin ingots and bronze artefacts from Salcombe and the Erme Estuary is shown in (b). Swords other than the Rosnoën type are subsumed as 'various swords' with the two LBA items with lighter orange symbols (diagrams: D. Berger; data: G. Brügmann, B. Höppner; data for the Israeli ingots from Berger et al., 2019; data Vårdinge from Ling et al., 2014, Table 3; data Flag Fen from Rohl and Northover, 1994, Table 4).

Fig. 5

Comparison of the tin isotopic composition of the tin objects examined in this study with European tin ores. The horizontal bars reflect the isotopic composition of the artefacts after subtracting 0.025 ‰ u^{-1} as the pyrometallurgical fractionation (cf. Berger et al., 2018) from the measured values ($=Sn_{corr}$) to yield the estimated original isotopic composition of the ores (diagram: D. Berger; data: G. Brügmann; Marahrens, forthcoming; Marahrens et al., forthcoming; Mason et al., 2020).

Fig. 6

Four-element diagram of ‘diagnostic elements’ (a) and tin isotopic composition vs. Sb/In (b) of the tin ingots from Salcombe and the Erme Estuary compared to the ingots from Israel. The dark grey circles refer to all tin ingots from Salcombe, while the green symbols represent those objects analysed in this study (diagram: D. Berger; data: G. Brügmann, N. Lockhoff; chemical data Salcombe: Wang et al., 2016; data Israel: Berger et al., 2019).

Fig. 7

Copper isotopic composition (δ^{65}Cu, 2SD) and lead isotope ratios of the copper ingots and bronze artefacts from Salcombe. Swords other than the Rosnoën type are subsumed under ‘various swords’ with the two LBA items with lighter orange symbols. In (a) the labels of the y-axis on the left hand side only apply to the copper ingots (grey shaded area), while the labels on the right only apply to the bronzes (white area). In (b) to (d) the relation between the Rosnoën swords are indicated by mixing lines (Rosnoën ML), while the alleged mixing of bronzes with copper (three components) is indicated by mixing triangles (MT). For the dark grey triangle the bronzes MA-176576 and MA-176580 as well as the copper ingot MA-176598 are assumed as end members. Since the end members are unknown the mixing triangle could be larger as indicated by the light grey area. In (e) and (f) the lead isotope ratios are plotted against 1/Pb. The numbers with two digits correspond to the Rosnoën swords with MA-1765xx. Legend in (a) is valid for all diagrams (diagrams: D. Berger; data: G. Brügmann, B. Höppner, N. Lockhoff).

Fig. 8

Histograms showing the copper isotopic composition in bornite, chalcopyrite, chalcocite and malachite ores of different locations all over Europe. The orange area symbolises the variation in the bronzes from Salcombe, the red bars signify the composition of the copper

ingots (diagrams: N. Lockhoff; data: compiled from Mar´echal et al., 1999; Larson et al., 2003; Rouxel et al., 2004; Durali Müller, 2005; Maher, 2005; Mathur et al., 2005, 2009, 2018; Markl et al., 2006, Asael et al., 2007, 2009).

Fig. 9

Lead isotopic composition of the copper ingots and bronze artefacts from Salcombe compared with ores from England and Ireland (a–b) and from Wales (c–d). Legends apply to all diagrams in the respective columns (diagrams: D. Berger; artefact data: B. Hoeppner; ore data: Rohl, 1995; 1996; Kinnaird et al., 2002; Rohl and Needham, 1998; Joel et al., 1997; Williams and Le Carlier de Veslud, 2019; Oxalid database).

Fig. 10

Lead isotopic composition of the copper ingots and bronze artefacts from Salcombe compared with ores from Continental Europe, Sardinia and Cyprus. Legends apply to all diagrams in the respective columns (diagrams: D. Berger, artefact data: B. Hoeppner; ore data: Pernicka et al., 2016; Schreiner, 2007; Niederschlag et al., 2003; Wedepohl et al., 1978; Lévêque and Haack, 1993; Niederschlag et al., 2003; Frotzscher, 2012; Artioli et al., 2016; Cattin et al., 2011; Boni and Köppel, 1985; Stos-Gale et al., 1995; Begemann et al., 2001; Hamelin et al., 1988; Gale et al., 1997; Arribas and Tosdal, 1994; Stos-Gale et al., 1995; Velasco et al., 1996; Marcoux, 1998; Santos Zalduegui et al., 2004; Montero-Ruiz and Murillo-Barroso, 2010; Huelga-Suarez et al., 2012; 2014; Gauss, 2015; Murillo-Barroso et al., 2019; Oxalid database).

Fig. 11

Bivariate plots of minor and trace elements in the copper ingots and bronze artefacts from

Salcombe. Legend in (e) applies to all diagrams. The dotted lines specify the detection limit of the ICP-MS of respective element (diagrams: D. Berger; data bronzes: N. Lockhoff; Wang et al., 2018; data copper ingots: Wang et al., 2018; data bronzes (literature): Rohl and Needham, 1998; Northover, 2013).

Fig. 12

A fragment of Pearson correlation matrix (determination factors R^2) and corresponding binary plots of trace element concetrations of the Rosnoën swords (squares), the palstaves (diamonds) and the the tin ingots (circles). The complete matrixes with correlation factors R including Mn, Fe, Co and Au are provided in Supplementary Material S4 and S5. Highly significant R^2 factors (> 0.7) are highlighted; concentrations given in µg g^{-1} (diagrams: D. Berger; data: N. Lockhoff; data tin ingots: Wang et al., 2016).

Fig. 13

Bivariate plots of the tin, copper and lead isotopic composition of the copper and bronze objects (a–c) and copper isotopes against Sn, Ni and As concentrations. Legend is valid for all diagram (diagrams: D. Berger; data: G. Brügmann, B. Höppner, N. Lockhoff).

Fig. 14

Comparison of the tin isotopic composition of the bronze objects examined in this study with European tin ores. The horizontal bars reflect the isotopic composition of the artefacts after subtracting 0.025 ‰ u^{-1} as the pyrometallurgical fractionation (cf. Berger et al., 2018) from the measured values (=Sn_{corr}) to yield the estimated original isotopic composition of the ores (diagram: D. Berger; data: G. Brügmann; Marahrens, forthcoming; Marahrens et al., forthcoming; Mason et al., 2020).

Table 1

Objects analysed in this study with the CEZA lab numbers of the samples and the corresponding British Museum (BM) accession numbers of the artefacts. The last column summarises the analytical methods applied to the samples: TIA – tin isotopic analysis, CIA – copper isotopic analysis, LIA – lead isotopic analysis, ICP-Q-MS – chemical analysis with quadrupole mass spectrometry.

Table 2

Tin and lead isotopic composition of the tin ingots and the lump from Salcombe and the Erme Estuary site. Tin isotope values specified as δSn in ‰ u^{-1} relative to NIST SRM 3161a; n. a. means no data is available (data: G. Brügmann, B. Höppner).

Table 3

Chemical composition of the tin lump with tin values given in mass% and all other elements in µg g^{-1} (data: N. Lockhoff).

Table 4

Copper and lead isotopic composition of the copper ingots from Salcombe analysed in this study. Copper isotope values specified as δ^{65}Cu in ‰ relative to NIST SRM 976 (data: G. Brügmann, B. Höppner).

Table 5

Chemical composition of the three copper ingots (in µg g^{-1}, except for Cu in mass%) investigated isotopically in this study. Data is reproduced from Wang et al. (2018, Table 2), but has been normalised to 100 % ignoring sulphur to be compared with the data of the bronze artefacts (cf. Table 6). The original sulphur contents from Wang et al. (2018) are given in italics for the sake of information (for original IDs of the objects see Table 1).

Table 6

Chemical composition of the bronze artefacts. Copper and tin values are given in mass%, all other elements are given in µg g^{-1} (data: N. Lockhoff, except for those tagged with $^{\#}$).

Table 7

Isotopic composition of the bronze artefacts with δSn in ‰ u^{-1} relative to NIST SRM 3161a and δCu in ‰; n. a. means no data is available (data: G. Brügmann, B. Höppner).

Supplementary Material S1

Complete isotopic and chemical data of the tin, copper and bronze objects investigated in this study. The original analysis of the tin isotope ratios was performed after a standard-sample-bracketing protocol and using the Puratronic in-house standard of CEZA. The data has been re-calculated relative to the NIST SRM3161a and subjected to linear regression to obtain δSn in ‰ u^{-1}. The individual tin isotope ratios are reported in ‰. Chemical data of the tin and copper ingots from Wang et al., 2016, 2018 after re-calculation; italic values reported in %, all other in µg g^{-1} (data: G. Brügmann, B. Höppner, N. Lockhoff).

Supplementary Material S2

Tin isotopic composition vs. trace elements of the tin ingots (Group I and II) and lump from Salcombe and the Erme Estuary site as well as tin ingots from Israel (diagrams: D. Berger; data: G. Brügmann, N. Lockhoff; chemical data Salcombe and Erme Estuary: Wang et al., 2016; data tin ingots Israel: Berger et al., 2019).

Supplementary Material S3

Comparison of $^{207}Pb/^{206}Pb$ and $^{206}Pb/^{204}Pb$ ratios of this study with TIMS data from Rohl and Needham (1998) for the same bronze objects from Moor Sand, even though not the same samples (diagram: D. Berger, data: B. Höppner and Rohl and Needham, 1998, Appendix 2; data reproduced in Needham et al., 2013 with British Museum accession numbers).

Supplementary Material S4

Pearson correlation matrix with correlation factors R of major, minor and the trace elements of the swords of the Rosnoën type.

Supplementary Material S5

Pearson correlation matrix with correlation factors R of major, minor and the trace elements of the palstave axes.

Supplementary Material S6

Isotopic composition vs. trace elements of the investigated bronzes from Salcombe (diagrams: D. Berger; data: G. Brügmann, B. Höppner, N. Lockhoff, Wang et al., 2018).

Supplementary Material S7

Fractionation of copper and tin isotopes during experimental melting of bronze in the laboratory under highly oxidising conditions. Both tin and copper isotopes in the melting products are shifted to heavier compositions relative to the starting material (diagram: D. Berger; data: G. Brügmann).

Tables

Table 1

Site	Lab. no. (CEZA)	Reg. no. (BM)	Period	Object	Metal type	Analysis (this study)
Salcombe B	MA-163233	2010,8032.295	BA	Bun ingot	Tin	TIA
Salcombe B	MA-163236	2010,8032.299	BA	Ingot fragment	Tin	TIA
Salcombe B	MA-163239	2010,8032.301	BA	Ingot fragment	Tin	TIA, LIA
Salcombe B	MA-163242	2010,8032.316	BA	Bun ingot	Tin	TIA
Salcombe B	MA-163245	2010,8032.318	BA	Bun ingot	Tin	TIA
Salcombe B	MA-163248	2010,8032.322	BA	Ingot fragment	Tin	TIA, LIA
Salcombe B	MA-163251	2010,8032.323	BA	Ingot fragment	Tin	TIA, LIA
Salcombe B	MA-163254	2013,8032.3	BA	Bun ingot	Tin	TIA, LIA
Salcombe B	MA-163257	2013,8032.8	BA	Bun ingot	Tin	TIA, LIA
Salcombe B	MA-163260	2013,8032.11	BA	Bun ingot	Tin	TIA, LIA
Salcombe B	MA-176602	2005,0503.19	BA	Lump/ingot	Tin	TIA, ICP-Q-MS
Salcombe B	MA-176597	2010,8032.254	BA	Bun ingot	Copper	CIA, LIA
Salcombe B	MA-176598	2010,8032.261	BA	Bun ingot	Copper	CIA, LIA
Salcombe B	MA-176599	2010,8032.267	BA	Bun ingot	Copper	CIA, LIA
Moor Sand	MA-176575	1981,1103.1	MBA	Sword, rod-tanged type	Bronze	TIA, CIA, LIA, ICP-Q-MS
Moor Sand	MA-176570	1983,1004.1	LBA	Sword, Carp’s Tongue type	Leaded bronze	TIA, CIA, LIA, ICP-Q-MS
Salcombe B	MA-163268	2010,8032.17	MBA	Rapier, unknown type	Bronze	TIA, CIA, LIA, ICP-Q-MS
Salcombe B	MA-176574	2013,8032.34	MBA	Sword, Ballintober type	Leaded bronze	TIA, CIA, LIA, ICP-Q-MS
Salcombe B	MA-176576	2005,0503.8	MBA	Sword, Rosnoën type	Bronze	TIA, CIA, LIA, ICP-Q-MS
Salcombe B	MA-176577	2005,0503.9	MBA	Sword, Rosnoën type	Bronze	TIA, CIA, LIA, ICP-Q-MS
Salcombe B	MA-176578	2005,0503.13	MBA	Sword, Rosnoën type	Bronze	TIA, CIA, LIA, ICP-Q-MS
Salcombe B	MA-176580	2005,0503.14	MBA	Sword, Rosnoën type	Bronze	TIA, CIA, LIA, ICP-Q-MS
Salcombe B	MA-176582	2005,0503.15	MBA	Sword, Rosnoën type	Bronze	TIA, CIA, LIA, ICP-Q-MS
Salcombe B	MA-176583	2005,0503.16	MBA	Sword, Rosnoën type	Bronze	TIA, CIA, LIA, ICP-Q-MS

Salcombe B	MA-176572	2010,8032.10	LBA	Sword, Nantes/Meldreth type	Bronze	TIA, CIA, LIA, ICP-Q-MS
Moor Sand	MA-176584	1981,0305.1	MBA	Palstave	Bronze	TIA, CIA, LIA, ICP-Q-MS
Moor Sand	MA-176585	1981,0305.2	MBA	Palstave	Bronze	TIA, CIA, LIA, ICP-Q-MS
Salcombe B	MA-176586	2005,0503.4	MBA	Palstave	Bronze	TIA, CIA, LIA, ICP-Q-MS
Salcombe B	MA-176587	2005,0503.5	MBA	Palstave	Bronze	TIA, CIA, LIA, ICP-Q-MS
Salcombe B	MA-176588	2005,0503.6	MBA	Palstave	Bronze	TIA, CIA, LIA, ICP-Q-MS
Salcombe B	MA-176589	2005,0503.7	MBA	Palstave	Bronze	TIA, CIA, LIA, ICP-Q-MS
Salcombe B	MA-176592	2010,8032.22	MBA	Palstave	Bronze	TIA, CIA, LIA, ICP-Q-MS
Salcombe B	MA-176569	2010,8032.23	MBA	Palstave	Bronze	TIA, CIA, LIA, ICP-Q-MS
Salcombe B	MA-176594	2005,0503.18	Possibly MBA	Rectanguloid block/weight	Bronze	TIA, CIA, LIA, ICP-Q-MS
Salcombe B	MA-176596	2010,8032.35	BA	Rectanguloid block/weight	Bronze	TIA, CIA, LIA, ICP-Q-MS
Erme Estuary	MA-163263	2013,8031.1	BA	Bun ingot	Tin	TIA
Erme Estuary	MA-163266	2013,8031.2	BA	Bun ingot	Tin	TIA

Table 2

Site	Lab. no. (CEZA)	$\delta Sn_{NIST\ SRM\ 3161a}$	2SD	$^{208}Pb/^{206}Pb$	2SD	$^{207}Pb/^{206}Pb$	2SD	$^{206}Pb/^{204}Pb$	2SD	$^{208}Pb/^{204}Pb$	2SD	$^{207}Pb/^{204}Pb$	2SD
Salcombe													
Tin ingot	MA-163233	0.070	0.001	n. a.	-	n. a.	-	n. a.	-	n. a.	-	n. a.	-
Tin ingot	MA-163236	0.061	0.001	n. a.	-	n. a.	-	n. a.	-	n. a.	-	n. a.	-
Tin ingot	MA-163239	0.059	0.001	1.8794	0.0001	0.76817	0.00002	20.478	0.001	38.487	0.003	15.731	0.001
Tin ingot	MA-163242	0.073	0.000	n. a.	-	n. a.	-	n. a.	-	n. a.	-	n. a.	-
Tin ingot	MA-163251	0.068	0.001	2.0830	0.0001	0.84493	0.00006	18.550	0.002	38.640	0.010	15.674	0.001
Tin ingot	MA-163254	0.097	0.000	1.8916	0.0001	0.76277	0.00001	20.640	0.001	39.043	0.001	15.744	0.001
Tin ingot	MA-163257	0.071	0.001	1.9556	0.0001	0.79854	0.00002	19.644	0.001	38.416	0.006	15.687	0.001
Tin ingot	MA-163260	0.061	0.001	1.8797	0.0003	0.76825	0.00006	20.475	0.002	38.487	0.024	15.730	0.003
Tin ingot	MA-163245	0.093	0.001	n. a.	-	n. a.	-	n. a.	-	n. a.	-	n. a.	-
Tin ingot	MA-163248	0.076	0.001	1.8697	0.0001	0.76569	0.00002	20.549	0.001	38.421	0.003	15.734	0.001
	average	**0.073**	**0.026**										
Salcombe, tin lump													
Tin lump	MA-176602	0.049	0.001	n. a.	-	n. a.	-	n. a.	-	n. a.	-	n. a.	-
Erme Estuary													
Tin ingot	MA-163263	0.058	0.000	n. a.	-	n. a.	-	n. a.	-	n. a.	-	n. a.	-
Tin ingot	MA-163266	0.111	0.001	n. a.	-	n. a.	-	n. a.	-	n. a.	-	n. a.	-
	average	**0.085**	**0.038**										

Table 3

Object	Lab. no.	Cu	Sn	Mn	Fe	Co	Ni	Zn	As	Ag	In	Sb	Te	Au	Pb	Bi
Tin lump	MA-176602	1350	100	20.6	390	<15	68	<4.7	<196	<1	29.0	18.4	<1.3	<0.32	30	6.4

Table 4

Object	**Lab. no. (CEZA)**	**δ^{65}Cu**	**2SD**	**^{208}Pb/^{206}Pb**	**2SD**	**^{207}Pb/^{206}Pb**	**2SD**	**^{206}Pb/^{204}Pb**	**2SD**	**^{208}Pb/^{204}Pb**	**2SD**	**^{207}Pb/^{204}Pb**	**2SD**
Copper ingot	MA-176597	–0.13	0.01	2.0912	0.0001	0.84774	0.00002	18.450	0.002	38.582	0.013	15.641	0.002
Copper ingot	MA-176598	–1.56	0.02	2.0966	0.0001	0.85791	0.00001	18.208	0.001	38.175	0.009	15.621	0.001
Copper ingot	MA-176599	–0.16	0.02	2.1060	0.0001	0.86070	0.00001	18.162	0.001	38.249	0.007	15.632	0.001

Table 5

Object	**Lab. no.**	**Cu**	**Sn**	**S**	**Mn**	**Fe**	**Co**	**Ni**	**Zn**	**As**	**Ag**	**In**	**Sb**	**Te**	**Au**	**Pb**	**Bi**
Copper ingot	MA-176597	99.8	170	*4800*	<15	<95	1.7	440	<7.0	650	86	<0.4	360	<0.2	<0.3	600	7.6
Copper ingot	MA-176598	98.9	<5	*5600*	<15	98	2.1	220	907	83	2900	3.2	470	<0.2	2.6	6200	5.9
Copper ingot	MA-176599	99.7	22.1	*4300*	<15	200	0.6	180	<7.0	1700	180	0.9	470	0.4	<0.3	660	18.7

Table 6

Object	**Lab. no.**	**Cu**	**Sn**	**Mn**	**Fe**	**Co**	**Ni**	**Zn**	**As**	**Ag**	**In**	**Sb**	**Te**	**Au**	**Pb**	**Bi**
Swords, various types																
Moor Sand	MA-176570	65	5.9	8.4	70.0	36	240	13.0	540	500	3.5	1220	2.3	1.1	289000	22.0
Moor Sand	MA-176575	89	9.8	2.0	2000	410	208	770	500	1010	126	1520	4.6	6.0	6200	290
Salcombe B[#]	MA-163268	86	11.6	47	1470	7.9	154	19.3	1140	600	<3	79	<6	<0.33	7300	29.3
Salcombe B	MA-176572	83	16.1	55	350	3.8	216	45	1000*	250	5.0	129	<12.7	3800	70	19.0
Salcombe B	MA-176574	86	8.6	14.6	880	10.2	470	11.0	340	480	3.2	950	2.7	4.2	51000	25.6
	average	**82**	**10.4**	**25.4**	**960**	**94**	**260**	**172**	**630**	**570**	**34**	**780**	**-**	**960**	**71000**	**77**
	2SD	*19*	*7.6*	*48*	*1600*	*360*	*250*	*670*	*700*	*560*	*122*	*1300*	-	*3800*	*250000*	*240*

Swords, Rosnoën type																
Salcombe B	MA-176576	88	9.9	128	860	193	1050	67	800	320	33	420	2.8	10.0	640	111
Salcombe B	MA-176577	92	7.9	219	1460	59	630	22.5	400*	111	9.6	146	<7.9	47	174	11.0
Salcombe B	MA-176578	92	7.2	5.8	1610	310	1780	67	990	560	43	470	2.7	13.8	1270	203
Salcombe B	MA-176580	88	10.6	36	3010	310	1870	196	1150	510	62	970	<3.8	14.6	4400	162
Salcombe B	MA-176582	89	10.5	43	2530	135	1440	32	800	219	20.4	420	<4	12.6	790	47
Salcombe B	MA-176583	90	9.4	27.5	1000	80	760	20.0	440	155	18.7	173	<4.2	5.7	420	42
	average	**90**	**9.2**	**77**	**1750**	**180**	**1250**	**67**	**770**	**310**	**31.1**	**430**	**-**	**17.3**	**1280**	**96**
	2SD	*3.8*	*2.8*	*163*	*1710*	*220*	*1050*	*133*	*590*	*370*	*38*	*590*	-	*30.0*	*3130*	*151*
Palstaves																
Moor Sand	MA-176584	89	10.8	27.2	390	250	2540	27.0	1000	240	21.8	440	2.4	14.8	1100	45
Moor Sand	MA-176585	91	8.5	74	171	193	1740	34	920	460	40	710	<4.7	25.5	1070	133
Salcombe B[#]	MA-163269	88	9.8	18.8	470	184	2310	23.0	1360	400	28.3	770	<6	11.1	3400	59
Salcombe B	MA-176586	86	12.9	77	2220	390	1390	260	1730	700	62	760	8.5	21.6	960	202
Salcombe B	MA-176587	89	10.1	6.5	710	290	1830	141	1230	500	52	710	<4.9	20.3	1890	159
Salcombe B	MA-176588	89	10.2	36	1520	190	2450	26.8	1350	310	27.2	770	4.2	15.0	830	69
Salcombe B	MA-176589	88	11.3	73	3010	120	1480	86	620	200	18.1	350	3.4	7.1	690	49
Salcombe B	MA-176591	88	11.1	43	3220	282	2190	46	1620	700	54	940	4.8	18.9	1670	169
	average	**88**	**10.6**	**45**	**1460**	**237**	**1980**	**80**	**1230**	**440**	**38**	**680**	**-**	**16.8**	**1430**	**111**
	2SD	*2.8*	*2.6*	*55*	*2440*	*170*	*880*	*166*	*740*	*380*	*33*	*380*	-	*11.9*	*1760*	*124*
Weights																
Salcombe B	MA-176594	89	10.0	54	2800	350	3400	27.9	1840	590	51	1120	6.3	38	900	149
Salcombe B	MA-176596	79	19.7	42	5000	810	1550	510	1500	450	58	1920	<11.5	8.5	6300	107
	average	**84**	**14.8**	**48.4**	**3900**	**580**	**2480**	**270**	**1670**	**510**	**54.8**	**1520**	**-**	**23.4**	**3600**	**128**
	2SD	*14.1*	*13.7*	*17.0*	*3100*	*650*	*2620*	*680*	*500*	*160*	*9.9*	*1130*	-	*42*	*7600*	*60*

Note: Values tagged with an asterisk (*) were determined with EDXRF due to isobaric interferences during measurements with ICP-Q-MS. Samples tagged with a hashtag ([#]) were already analysed in Wang et al. (2018) and are reproduced here after normalisation to 100 % for the sake of better comparison.

Table 7

Site	Lab. no.	$\delta Sn_{NIST\ SRM\ 3161a}$	2SD	$\delta^{65}Cu$	2SD	$^{208}Pb/^{206}Pb$	2SD	$^{207}Pb/^{206}Pb$	2SD	$^{206}Pb/^{204}Pb$	2SD	$^{208}Pb/^{204}Pb$	2SD	$^{207}Pb/^{204}Pb$	2SD
Swords, various types															
Moor Sand	MA-176570	0.104	0.001	0.09	0.03	2.0809	0.0001	0.84750	0.00001	18.422	0.001	38.335	0.003	15.613	0.001
Moor Sand	MA-176575	0.089	0.002	–0.04	0.02	2.1219	0.0001	0.86919	0.00002	17.981	0.001	38.153	0.001	15.629	0.001
Salcombe B	MA-163268	0.084	0.002	0.73	0.01	2.1052	0.0001	0.85614	0.00001	18.319	0.001	38.564	0.002	15.683	0.001
Salcombe B	MA-176572	0.080	0.001	0.11	0.004	2.0818	0.0001	0.84737	0.00001	18.418	0.001	38.343	0.008	15.607	0.001
Salcombe B	MA-176574	0.081	0.001	0.11	0.01	2.0822	0.0001	0.84640	0.00002	18.473	0.001	38.464	0.010	15.636	0.001
Swords, Rosnoën type															
Salcombe B	MA-176576	0.081	0.001	0.05	0.02	2.1115	0.0001	0.86163	0.00003	18.148	0.001	38.319	0.001	15.637	0.001
Salcombe B	MA-176577	0.068	0.001	–0.02	0.03	2.1040	0.0001	0.85871	0.00001	18.194	0.001	38.280	0.006	15.624	0.001
Salcombe B	MA-176578	0.081	0.002	0.11	0.01	2.1053	0.0001	0.85812	0.00001	18.229	0.001	38.377	0.002	15.643	0.001
Salcombe B	MA-176580	0.071	0.002	0.14	0.02	2.1040	0.0002	0.85768	0.00004	18.241	0.001	38.381	0.001	15.645	0.002
Salcombe B	MA-176582	0.079	0.001	0.09	0.04	2.1081	0.0001	0.85971	0.00002	18.194	0.001	38.355	0.007	15.642	0.001
Salcombe B	MA-176583	0.087	0.001	0.03	0.01	2.1093	0.0001	0.86001	0.00001	18.184	0.002	38.357	0.010	15.639	0.002
	average	**0.078**	**0.014**	**0.07**	**0.11**	**2.1070**	**0.0062**	**0.85931**	**0.00289**	**18.198**	**0.067**	**38.345**	**0.077**	**15.638**	**0.015**
Palstave axes															
Moor Sand	MA-176584	0.055	0.001	0.12	0.01	2.1059	0.0001	0.85967	0.00003	18.175	0.001	38.275	0.010	15.625	0.002
Moor Sand	MA-176585	0.071	0.002	0.18	0.005	2.1059	0.0002	0.85874	0.00005	18.213	0.001	38.356	0.001	15.641	0.001
Salcombe B	MA-163269	0.078	0.001	n.a.	n.a.	2.0865	0.0001	0.84852	0.00001	18.413	0.001	38.419	0.005	15.624	0.001
Salcombe B	MA-176586	0.077	0.002	0.08	0.01	2.1064	0.0001	0.85853	0.00002	18.216	0.001	38.371	0.002	15.639	0.001
Salcombe B	MA-176587	0.070	0.002	0.12	0.02	2.1061	0.0001	0.85869	0.00001	18.213	0.001	38.358	0.005	15.639	0.001
Salcombe B	MA-176588	0.073	0.001	0.14	0.01	2.1095	0.0001	0.86108	0.00002	18.153	0.002	38.292	0.010	15.631	0.001
Salcombe B	MA-176589	0.086	0.001	0.07	0.01	2.1019	0.0001	0.85670	0.00001	18.254	0.001	38.368	0.007	15.638	0.001
Salcombe B	MA-176591	0.078	0.001	0.10	0.01	2.1057	0.0001	0.85859	0.00003	18.216	0.002	38.358	0.020	15.640	0.002
	average	**0.076**	**0.011**	**0.12**	**0.07**	**2.1035**	**0.0143**	**0.85757**	**0.00771**	**18.232**	**0.159**	**38.350**	**0.092**	**15.635**	**0.014**

Weights															
Salcombe B	MA-176594	0.081	0.001	0.13	0.01	2.1121	0.0001	0.86163	0.00002	18.171	0.002	38.378	0.014	15.657	0.002
Salcombe B	MA-176596	0.073	0.001	0.16	0.02	2.0955	0.0001	0.85388	0.00002	18.289	0.002	38.325	0.012	15.617	0.002
	average	**0.077**	**0.011**	**0.14**	**0.03**	**2.1038**	**0.0001**	**0.85780**	**0.00002**	**18.230**	**0.002**	**38.352**	**0.013**	**15.637**	**0.002**

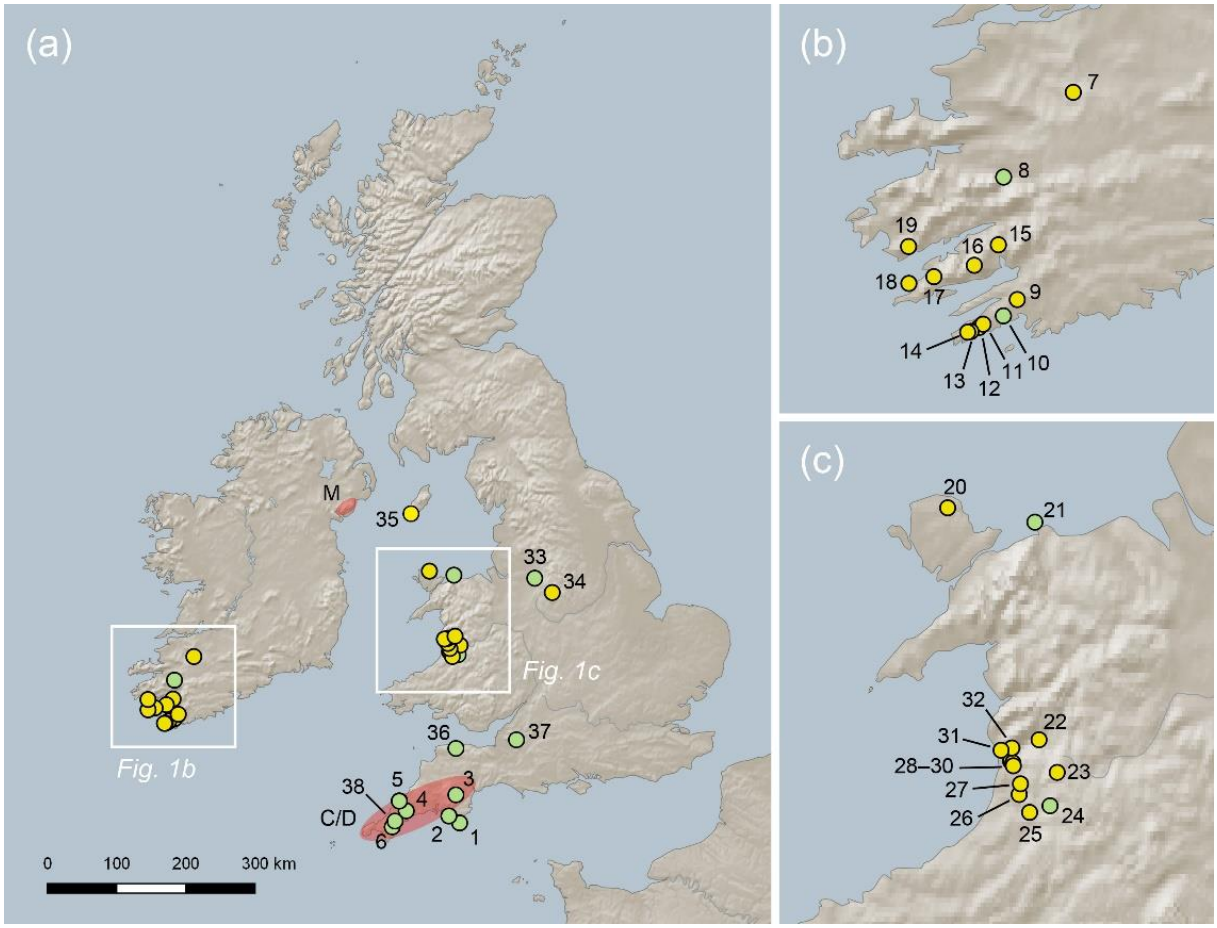
(a)
(b)
(c)
M
35
33
34
Fig. 1c
Fig. 1b
36
37
38
5
3
4
C/D
6
2
1
0
100
200
300 km
7
8
19
16
15
18
17
9
14
13
12
11
10
20
21
32
22
31
28–30
23
27
26
24
25

Fig. 1

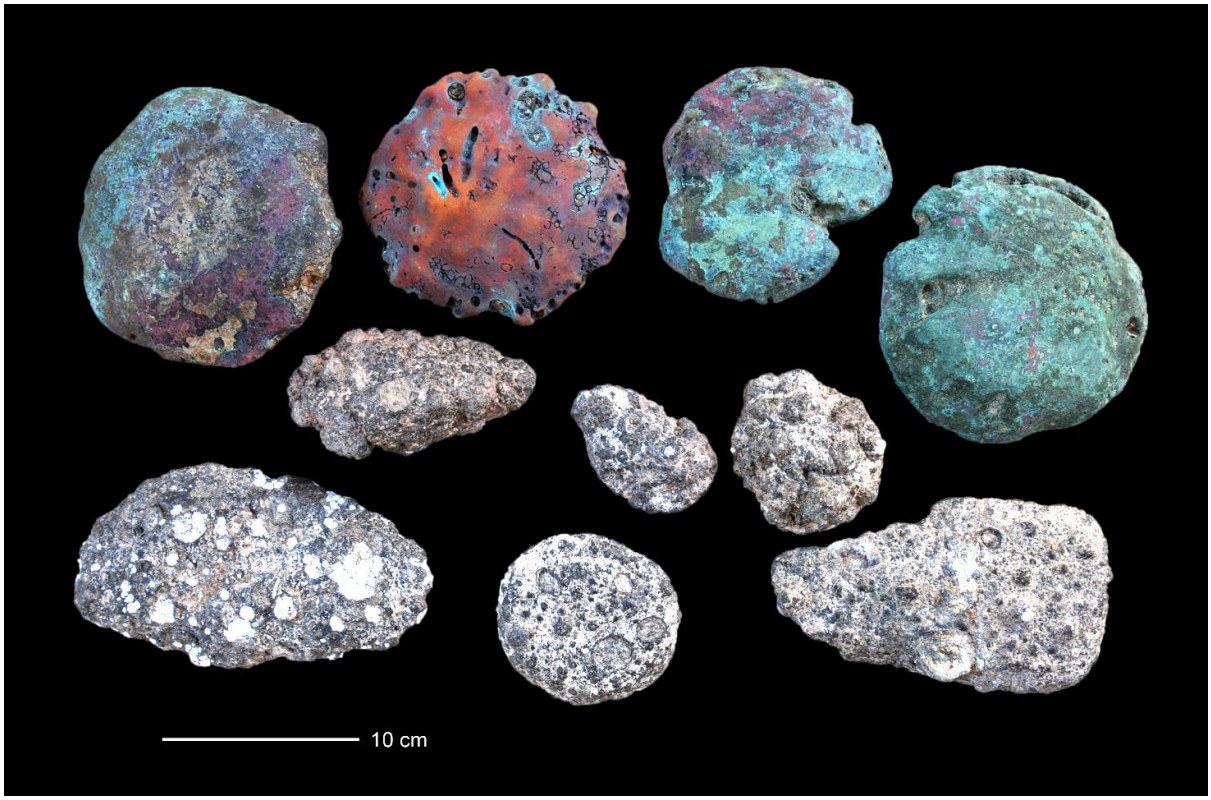

Fig. 2

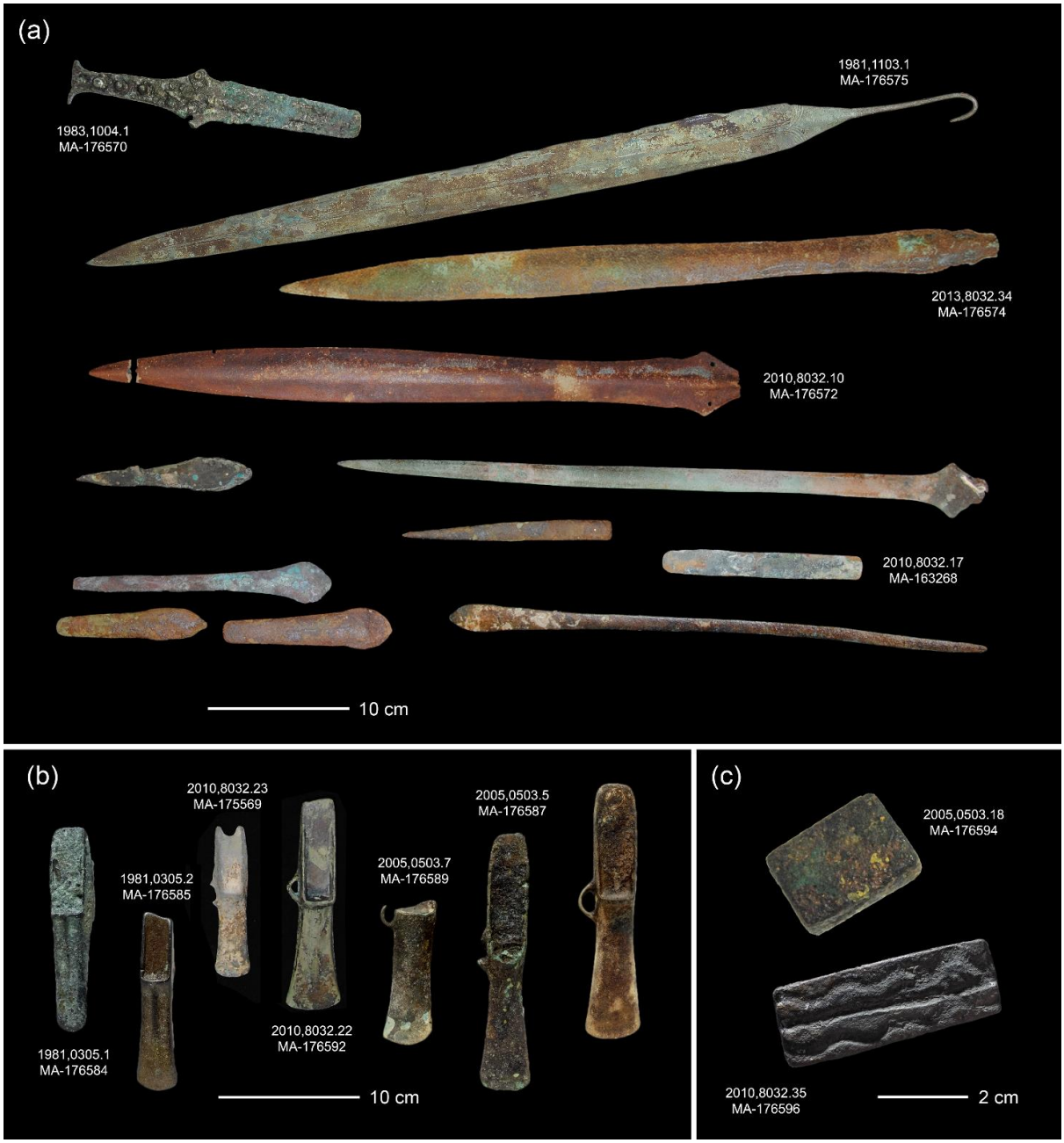
(a)
1983,1004.1
MA-176570
1981,1103.1
MA-176575
2013,8032.34
MA-176574
2010,8032.10
MA-176572
2010,8032.17
MA-163268
10 cm
(b)
2010,8032.23
MA-175569
1981,0305.2
MA-176585
2005,0503.5
MA-176587
2005,0503.7
MA-176589
1981,0305.1
MA-176584
2010,8032.22
MA-176592
10 cm
(c)
2005,0503.18
MA-176594
2010,8032.35
MA-176596
2 cm

Fig. 3

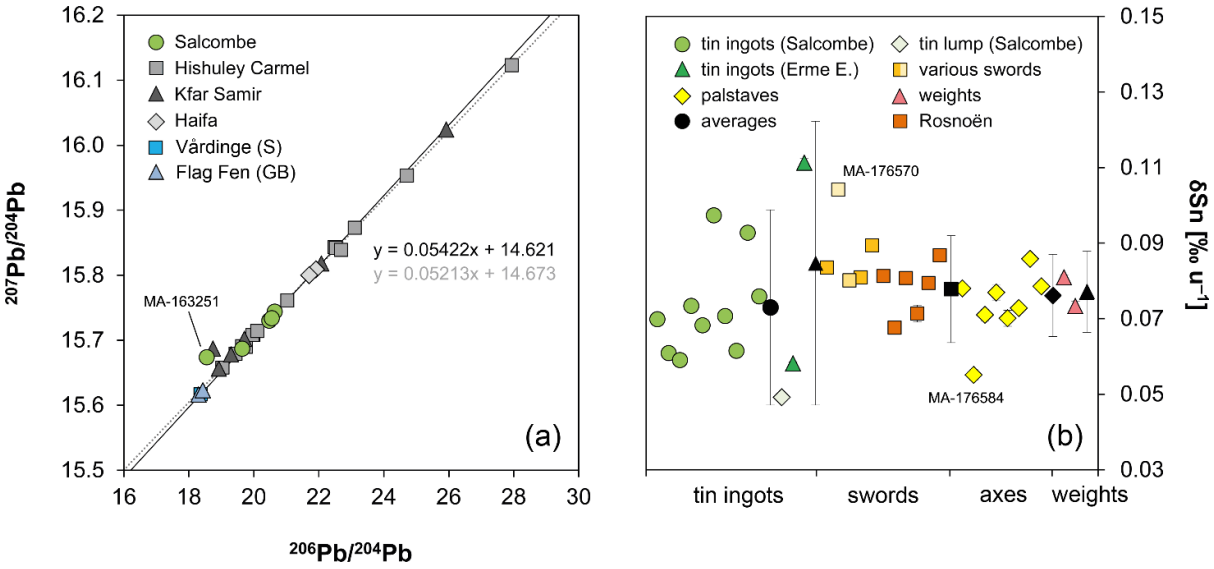
Salcombe
Hishuley Carmel
Kfar Samir
Haifa
Vårdinge (S)
Flag Fen (GB)
y = 0.05422x + 14.621
y = 0.05213x + 14.673
MA-163251
(a)
$^{207}Pb/^{204}Pb$
$^{206}Pb/^{204}Pb$
tin ingots (Salcombe)
tin ingots (Erme E.)
palstaves
averages
tin lump (Salcombe)
various swords
weights
Rosnoën
MA-176570
MA-176584
(b)
δSn [‰ u⁻¹]
tin ingots
swords
axes
weights

Fig. 4

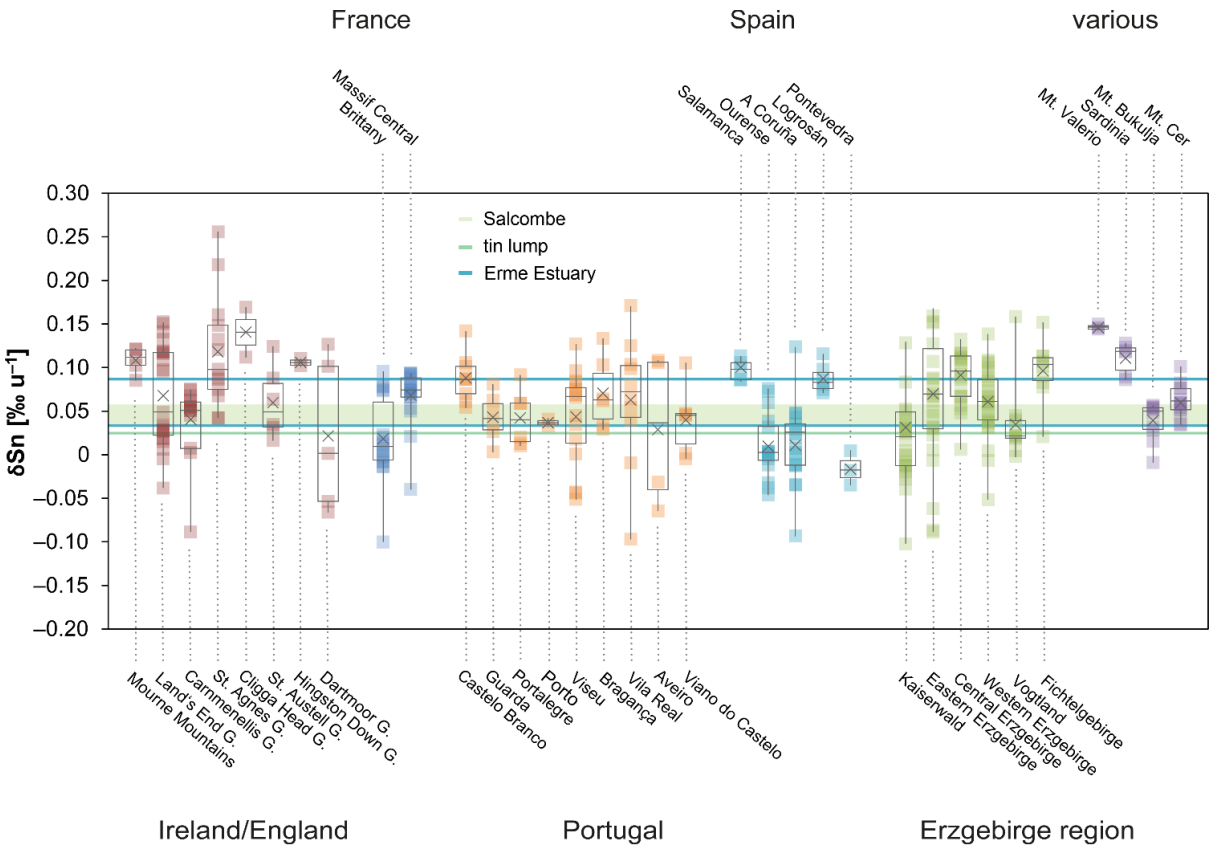
France
Spain
various
Massif Central
Brittany
Salamanca
Ourense
A Coruña
Pontevedra
Logrosán
Mt. Valerio
Sardinia
Mt. Bukulja
Mt. Cer
Salcombe
tin lump
Erme Estuary
δSn [‰ u⁻¹]
Mourne Mountains
Land's End G.
Carnmenellis G.
St. Agnes G.
Cligga Head G.
St. Austell G.
Hingston Down G.
Dartmoor G.
Castelo Branco
Guarda
Portalegre
Porto
Viseu
Bragança
Vila Real
Aveiro
Viano do Castelo
Kaiserwald
Eastern Erzgebirge
Central Erzgebirge
Western Erzgebirge
Vogtland
Fichtelgebirge
Ireland/England
Portugal
Erzgebirge region

Fig. 5

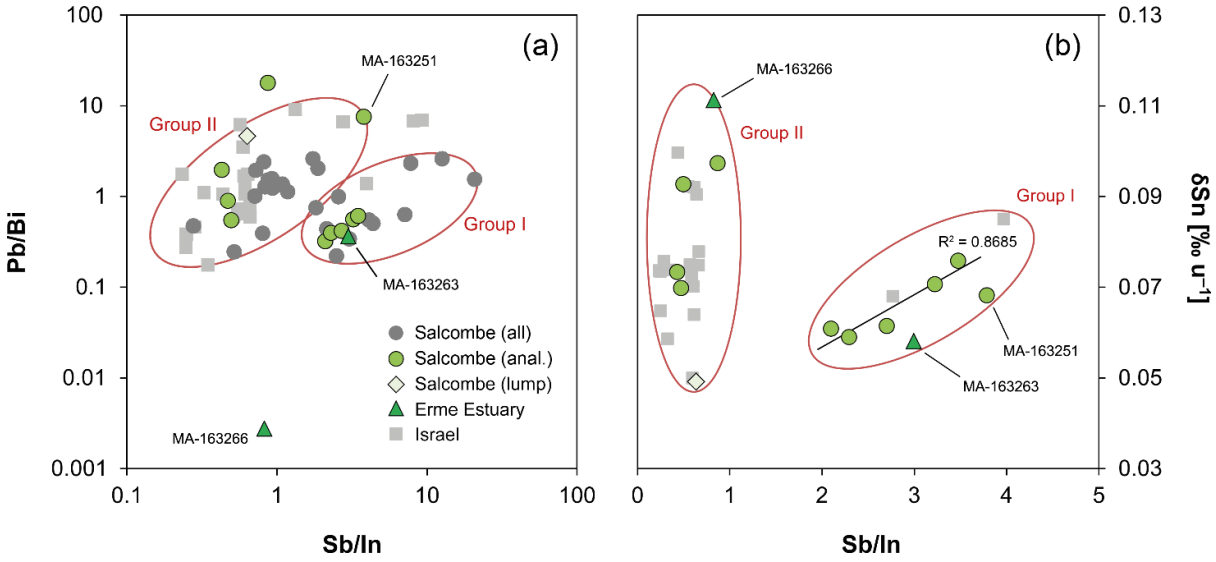
(a)
(b)
Pb/Bi
Sb/In
δSn [‰ u⁻¹]
Group I
Group II
MA-163251
MA-163263
MA-163266
Salcombe (all)
Salcombe (anal.)
Salcombe (lump)
Erme Estuary
Israel
R² = 0.8685
100
10
1
0.1
0.01
0.001
0.13
0.11
0.09
0.07
0.05
0.03
0
1
2
3
4
5

Fig. 6

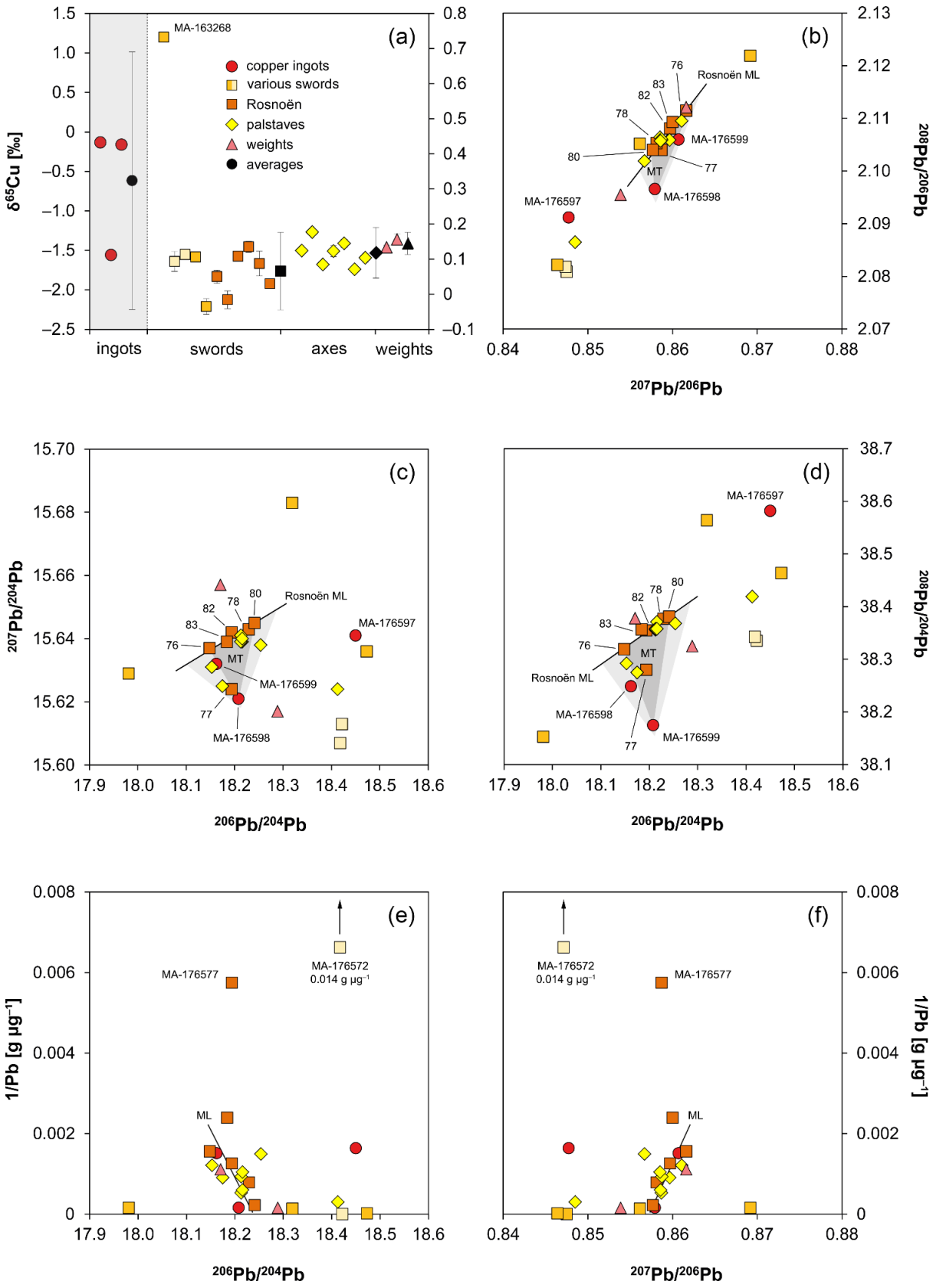
(a)
MA-163268
copper ingots
various swords
Rosnoën
palstaves
weights
averages
δ65Cu [‰]
ingots
swords
axes
weights
(b)
Rosnoën ML
MA-176599
MT
MA-176597
MA-176598
208Pb/206Pb
207Pb/206Pb
(c)
Rosnoën ML
MA-176597
MA-176599
MT
MA-176598
207Pb/204Pb
206Pb/204Pb
(d)
MA-176597
Rosnoën ML
MT
MA-176598
MA-176599
208Pb/204Pb
206Pb/204Pb
(e)
MA-176577
MA-176572
0.014 g µg−1
ML
1/Pb [g µg−1]
206Pb/204Pb
(f)
MA-176572
0.014 g µg−1
MA-176577
ML
1/Pb [g µg−1]
207Pb/206Pb

Fig. 7

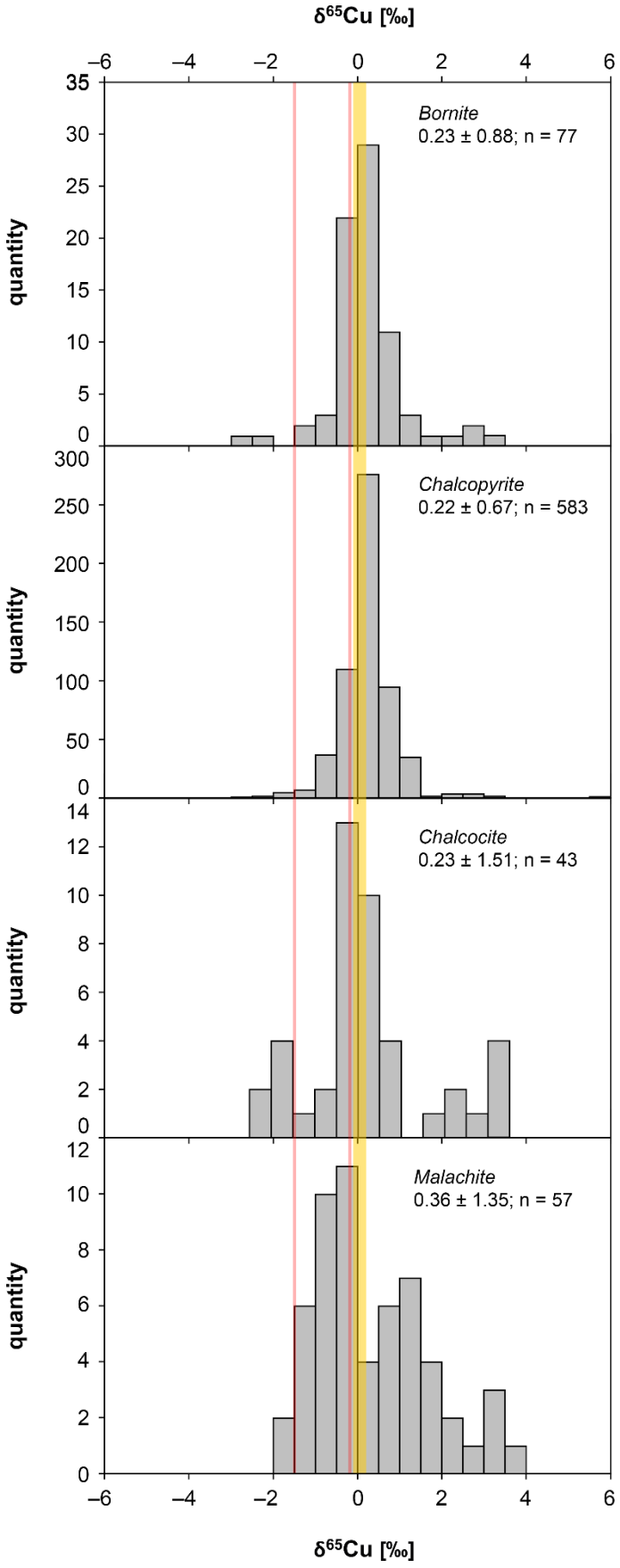
δ65Cu [‰]
Bornite
0.23 ± 0.88; n = 77
Chalcopyrite
0.22 ± 0.67; n = 583
Chalcocite
0.23 ± 1.51; n = 43
Malachite
0.36 ± 1.35; n = 57
quantity
δ65Cu [‰]

Fig. 8

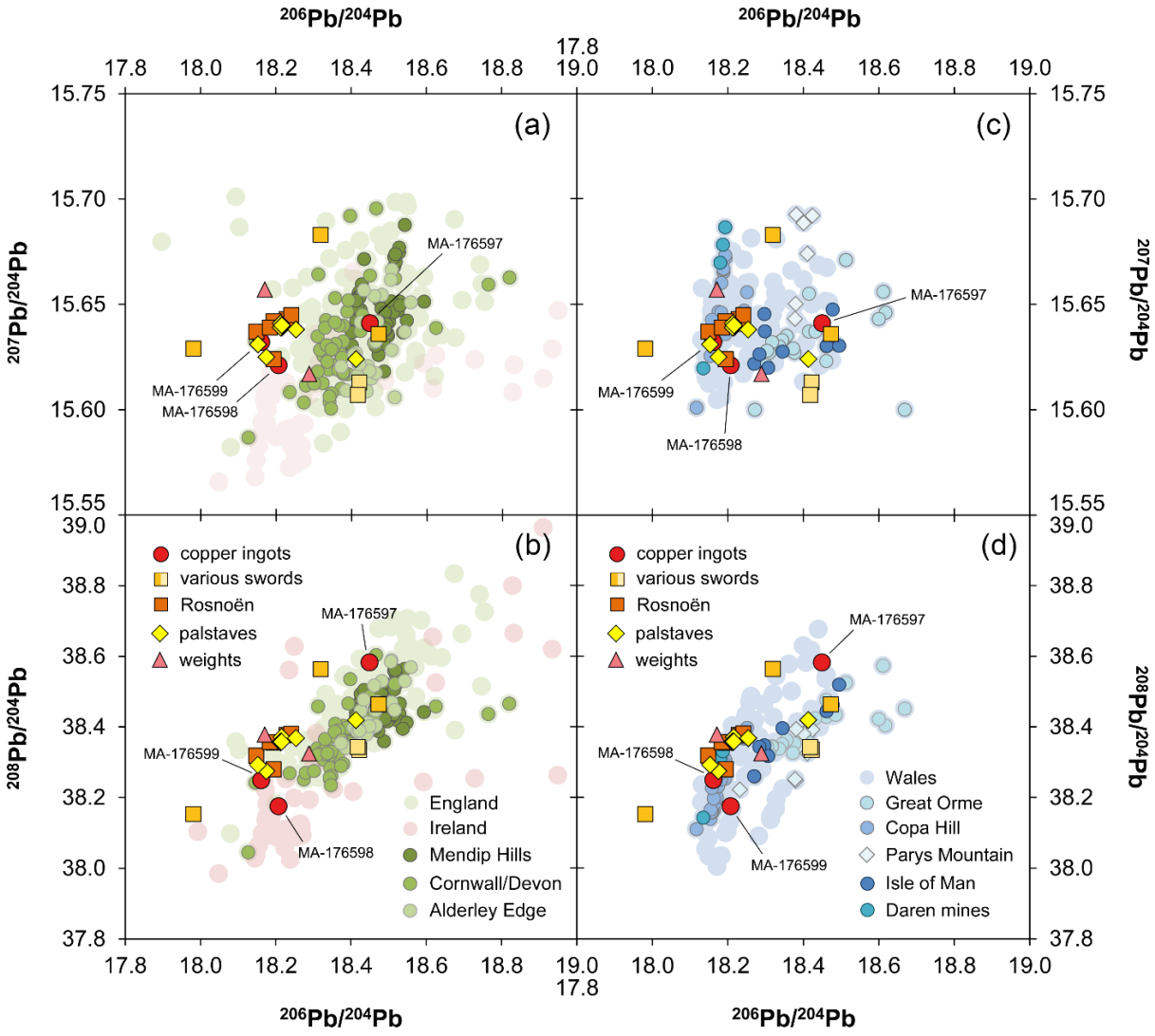
(a)
(b)
(c)
(d)
$^{206}Pb/^{204}Pb$
$^{207}Pb/^{204}Pb$
$^{208}Pb/^{204}Pb$
MA-176597
MA-176599
MA-176598
copper ingots
various swords
Rosnoën
palstaves
weights
England
Ireland
Mendip Hills
Cornwall/Devon
Alderley Edge
Wales
Great Orme
Copa Hill
Parys Mountain
Isle of Man
Daren mines

Fig. 9

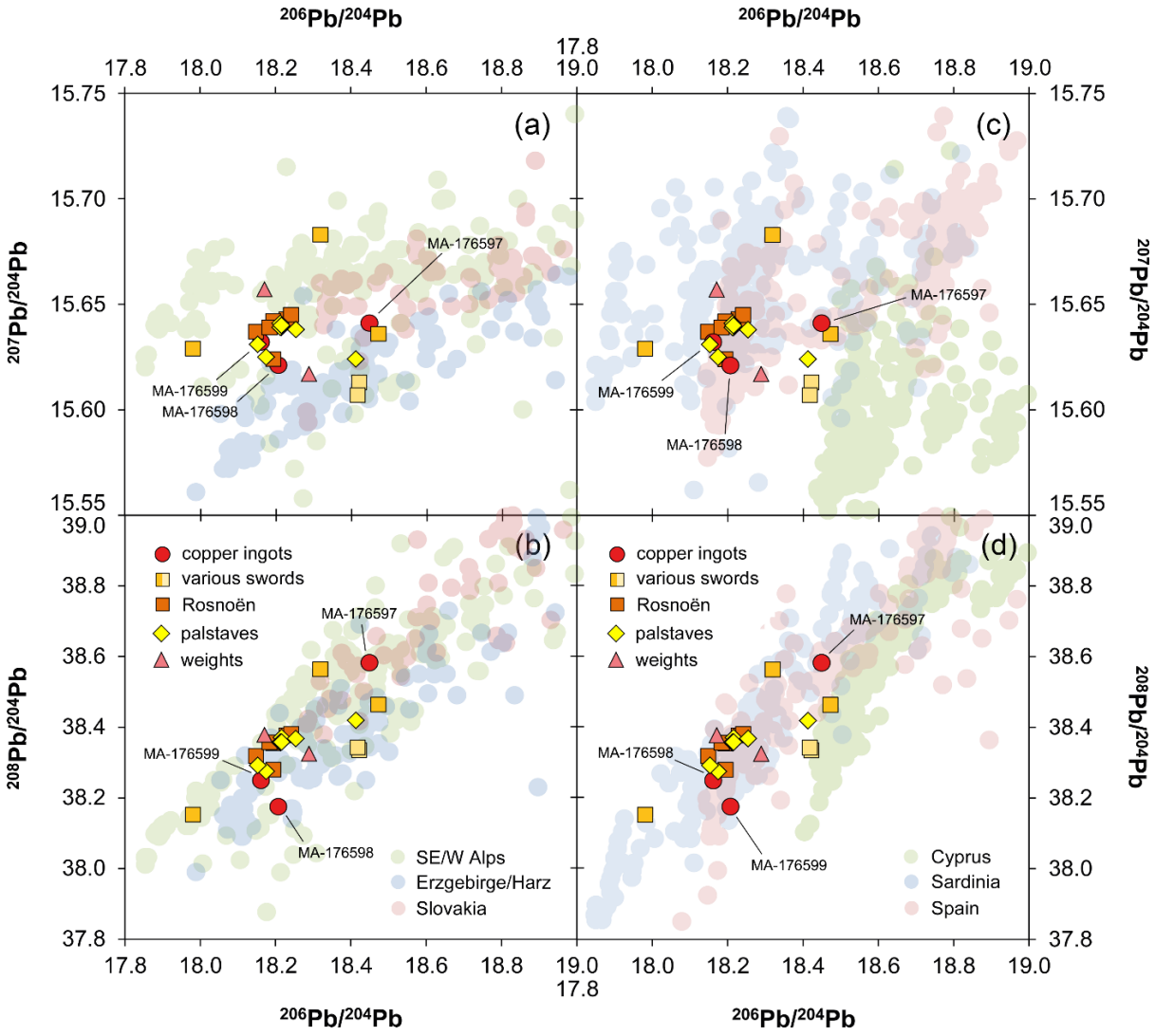
(a)
(b)
(c)
(d)
$^{206}Pb/^{204}Pb$
$^{207}Pb/^{204}Pb$
$^{208}Pb/^{204}Pb$
MA-176597
MA-176599
MA-176598
copper ingots
various swords
Rosnoën
palstaves
weights
SE/W Alps
Erzgebirge/Harz
Slovakia
Cyprus
Sardinia
Spain

Fig. 10

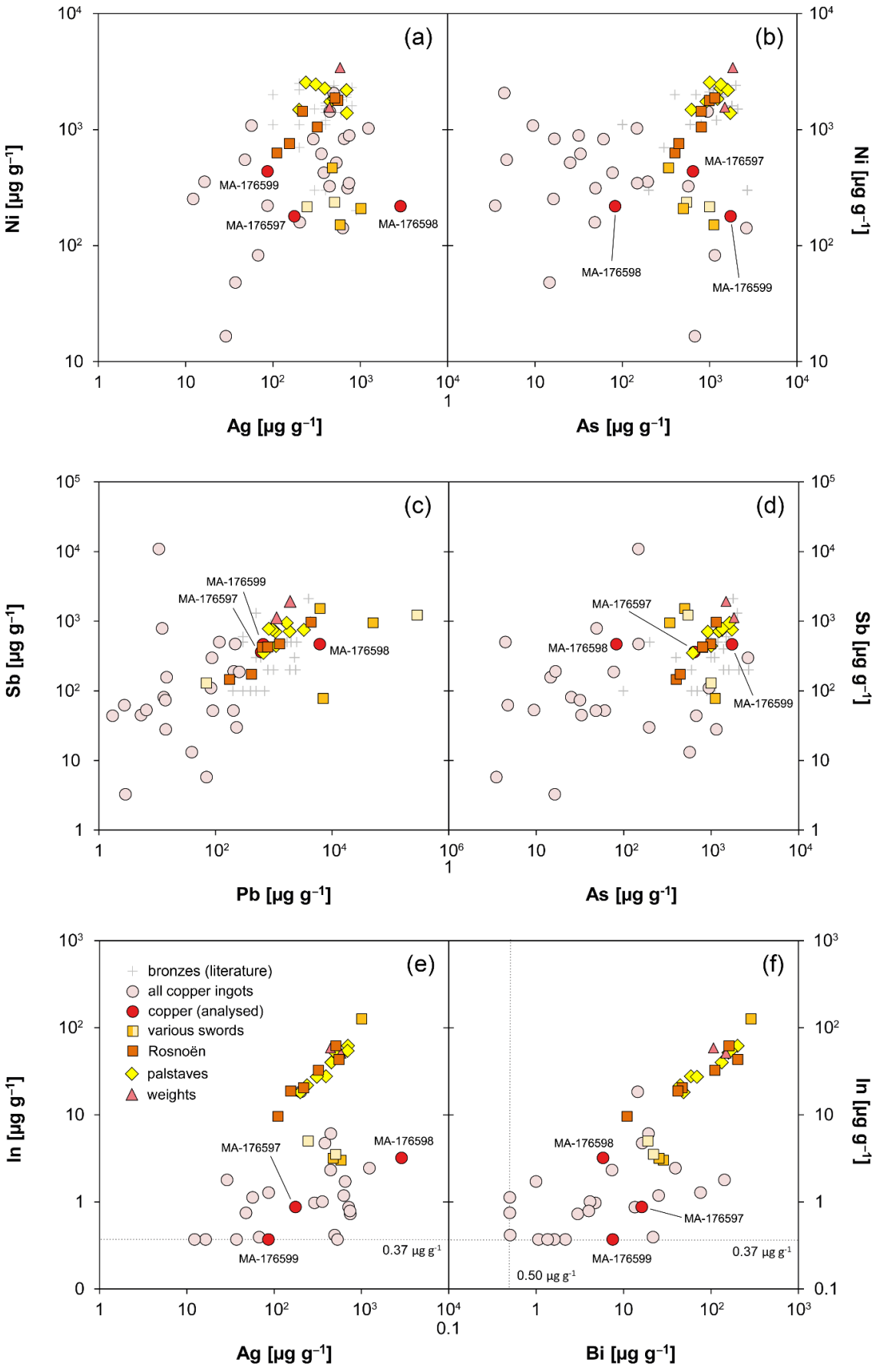
(a)
(b)
(c)
(d)
(e)
(f)
Ni [µg g⁻¹]
Ag [µg g⁻¹]
As [µg g⁻¹]
Sb [µg g⁻¹]
Pb [µg g⁻¹]
In [µg g⁻¹]
Bi [µg g⁻¹]
MA-176599
MA-176597
MA-176598
bronzes (literature)
all copper ingots
copper (analysed)
various swords
Rosnoën
palstaves
weights
0.37 µg g⁻¹
0.50 µg g⁻¹

Fig. 11

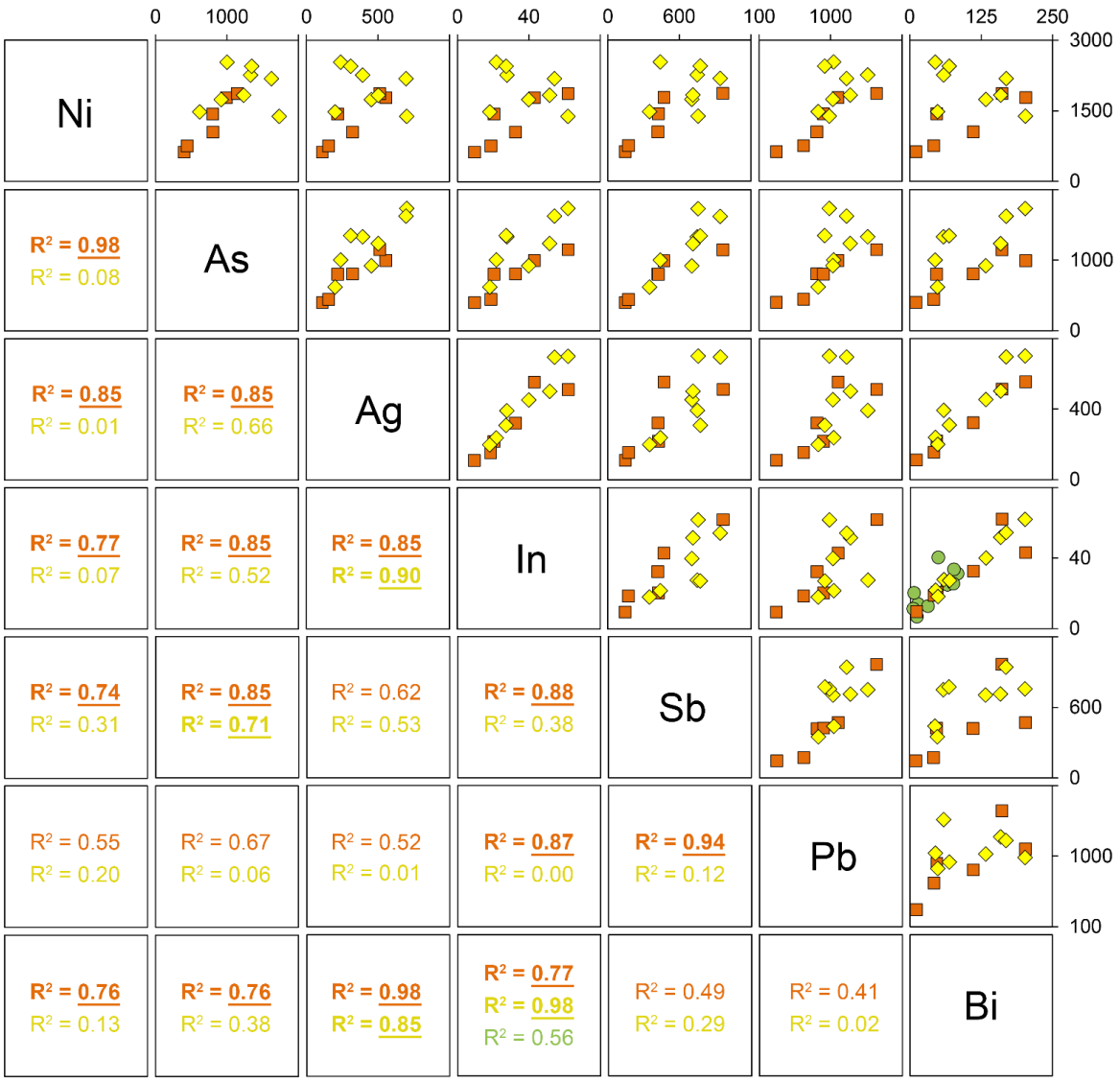
0 1000
0 500
0 40
0 600
100 1000
0 125 250
3000
1500
0
1000
0
400
0
40
0
600
0
1000
100
Ni
As
Ag
In
Sb
Pb
Bi
R² = 0.98
R² = 0.08
R² = 0.85
R² = 0.01
R² = 0.85
R² = 0.66
R² = 0.77
R² = 0.07
R² = 0.85
R² = 0.52
R² = 0.85
R² = 0.90
R² = 0.74
R² = 0.31
R² = 0.85
R² = 0.71
R² = 0.62
R² = 0.53
R² = 0.88
R² = 0.38
R² = 0.55
R² = 0.20
R² = 0.67
R² = 0.06
R² = 0.52
R² = 0.01
R² = 0.87
R² = 0.00
R² = 0.94
R² = 0.12
R² = 0.76
R² = 0.13
R² = 0.76
R² = 0.38
R² = 0.98
R² = 0.85
R² = 0.77
R² = 0.98
R² = 0.56
R² = 0.49
R² = 0.29
R² = 0.41
R² = 0.02

Fig. 12

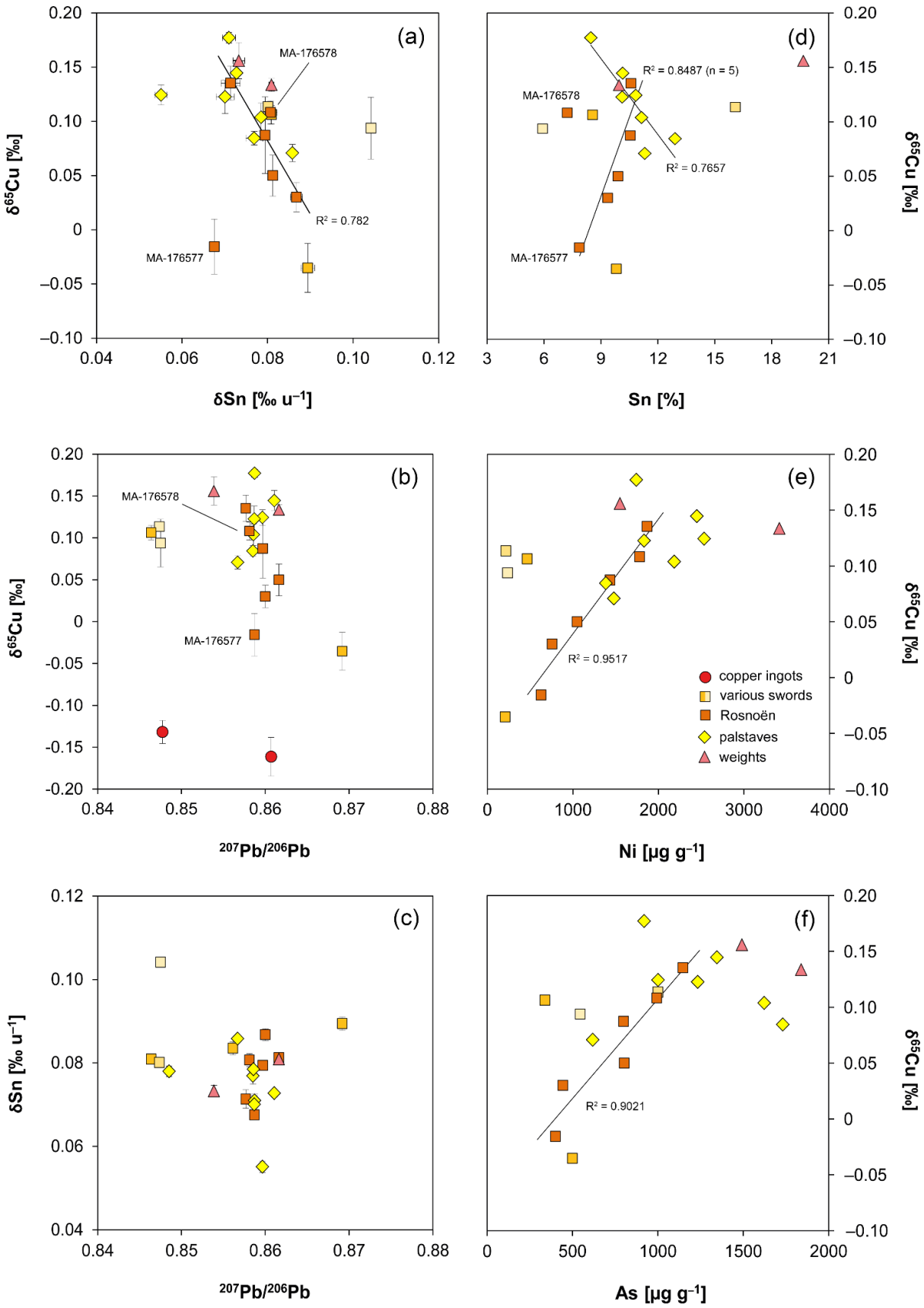
(a)
MA-176578
R² = 0.782
MA-176577
δ65Cu [‰]
δSn [‰ u−1]
(d)
R² = 0.8487 (n = 5)
MA-176578
R² = 0.7657
MA-176577
Sn [%]
(b)
MA-176578
MA-176577
207Pb/206Pb
(e)
R² = 0.9517
copper ingots
various swords
Rosnoën
palstaves
weights
Ni [µg g−1]
(c)
δSn [‰ u−1]
207Pb/206Pb
(f)
R² = 0.9021
As [µg g−1]

Fig. 13

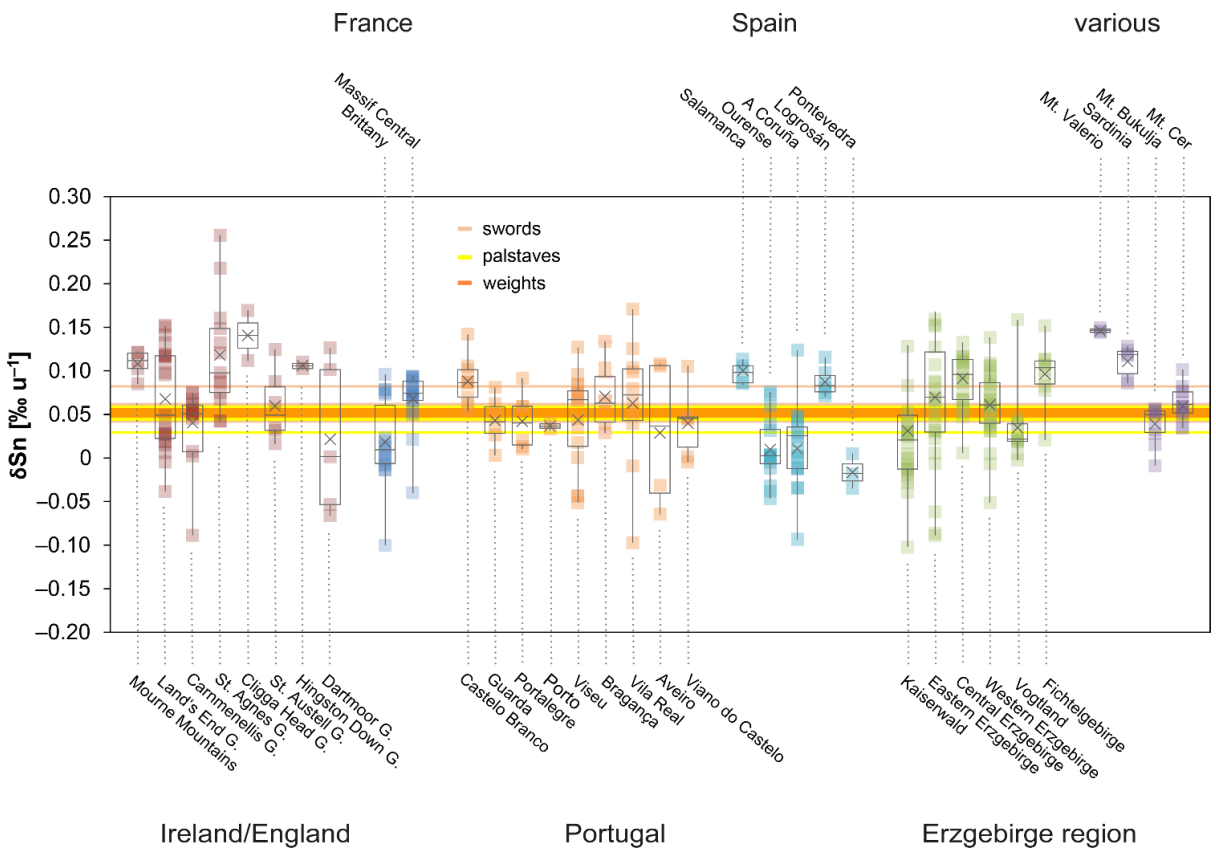

Fig. 14

All Supplementary Material is only available online from

https://doi.org/10.1016/j.jas.2022.105543